Report: S-67-7

NEW YORK UNIVERSITY
New York, N. Y.

DYNAMIC BEHAVIOR OF RECTANGULAR PLATES AND CYLINDRICAL SHELLS

by

Edward N. Wilson
Professor
Department of Civil Engineering

and

Are Tsirk
Research Assistant
Department of Civil Engineering

Prepared for the
Office of University Affairs
National Aeronautics and Space Administration
under Research Grant NGR-33-016-067

October 1967

TABLE OF CONTENTS

LIST OF FIGURES

ABSTRACT

A numerical procedure is presented for the determination of the dynamic response of rectangular plates and cylindrical shells subjected to stationary time dependent loads as well as to multiple loads moving with constant velocity along any path on the structure. The masses of the moving loads are included in the analysis.

Finite element models are adopted to reduce the continuous media of the plate and the cylindrical shell to systems having a finite number of degrees of freedom, with inertia forces concentrated at a finite number of nodes. Displacement functions are assumed for each of the constituent elements to obtain node forces equivalent to the applied loading. The displacement method of analysis is employed, considering three and six degrees of freedom at each node for the plate and shell model, respectively, to obtain a set of simultaneous differential equations describing the motion of the models. These equations are solved by a step-by-step numerical integration technique to find the displacements and the concentrated forces at the nodes of the models.

Numerical results are presented for plates and for circular cylindrical shells. The response of plates subjected to stationary impact load is investigated as well as the case of plates carrying single or multiple loads and masses moving with various velocities. Both square and rectangular plates, each with simply supported and clamped boundaries, are considered. Also continuous plates clamped at the periphery are investigated. The circular cylindrical shells considered in the numerical samples are subjected to stationary impact loads only.

This report includes most of the material in "Elastic Response of Rectangular Plates Subjected to Dynamic Loadings", Report S-67-4, which appeared in April, 1967. The scope of the latter report is extended herein to include additional topics discussed above.

INTRODUCTION

The availability of digital computers to solve large numbers of simultaneous algebraic equations has spurred the development of various finite element techniques for plane stress problems, for plates in flexure, for shells, and even for solids. In general, the finite element approach to a continuous medium reduces it to a system with a finite number of degrees of freedom, thereby facilitating the solution to problems of a mathematically complex nature.

The method of analysis of a static plate or shell problem by a finite element model is similar to the analysis of a framed structure. However, dynamic analysis of a plate or shell with moving forcing functions requires modifications to be discussed in the development.

As in the case of a framed structure with a large number of degrees of freedom, the normal mode method of analysis for moving masses acting on finite element models would be timewise prohibitive even when a large-scale computer is employed.

No solutions are known for plates or cylindrical shells with arbitrary restraints subjected to multiple moving forcing functions.

The method of analysis presented here is an extension of the procedure H. Allik[1] used to study the response of space frames to moving mass loadings.

---

[1]The superscripted numbers refer to References.

PURPOSE AND SCOPE

The purpose of this research is to develop an approximate method for determining the elastic dynamic response of isotropic rectangular plates and cylindrical shells. Stationary loads varying arbitrarily with time, as well as loads and load-masses moving with a constant velocity across the structures are considered. The loads and masses are assumed to remain in contact with the structure throughout the analysis.

The method of analysis is based on the theory of thin plates and shells with small deflections. The approach used is a numerical one. The continuous medium of the plate and the shell is each reduced to a system with a finite number of degrees of freedom by means of a finite element model. The distributed mass of the system is concentrated at a finite number of points or nodes of this model. For a load acting at an arbitrary point of the structure at any instant of time, a set of equivalent node forces is found by assuming displacement functions for each of the finite elements. The assumed displacement functions also permit the evaluation of a set of node forces equivalent to the inertia forces associated with a concentrated mass at an arbitrary point of the structure. Deformations and forces are obtained only at the nodes of the plate and the shell.

The set of simultaneous differential equations of motion obtained in each case is solved by the linear acceleration method, a step-by-step numerical integration technique in which the accelerations of the nodes are assumed to vary linearly over each time interval.

Numerical samples are presented to demonstrate the feasibility of the solution with a large scale digital computer.

The applicability of the procedure to plates of variable thickness, to orthotropic plates, to shells of arbitrary shape, and to other types of structures is discussed.

HISTORICAL REVIEW

Exact solutions of the partial differential equations governing the dynamic behavior of plates and shells are available for only relatively simple types of loading and special boundary conditions. Consequently, to obtain solutions to many problems of practical interest approximate methods of solution must be used. Such methods of analysis, which are numerical in nature, have become more popular in recent years because of the availability of electronic computers. In general, the approximate methods of solution are of two basic types. In one case the governing differential equation is solved by some approximate method. In the other case, rather than solve the actual differential equation, some fictitious discrete element system is substituted for the plate.

Of the approximate methods of analysis falling in the first category, the most popular and rewarding one is the finite difference technique in which the numerical solution of the governing differential equation is obtained at some specified finite number of points by approximation of the partial derivatives.

An alternate approach to the approximate analysis of plates and shells is by a discrete or finite element technique. These techniques can be divided into two basic categories. One of these categories included the methods in which the continuous medium is subdivided into a number of small elements, and these elements are used to obtain the solution. For the sake of clarity, this method of analysis will be herein referred to as the continuous finite element approach. The stiffness matrix relating the displacements of the nodes at the corners of the elements to the forces at these corners of the

element has then been obtained. Once this stiffness matrix is available, static problems can be solved by the conventional displacement method of structural analysis. Alternately, the force method of structural analysis has been employed with flexibility matrices.

A stiffness matrix for a rectangular plate element in bending has been obtained by R. J. Melosh[2] by assuming third-order polynomials for the displacements along the edges of the element. Numerical examples obtained were compared with known series solutions. It was demonstrated that as the number of elements used is increased convergence to the final solution is not always monotonic. In a later paper[3] Melosh provides a criterion to insure monotonic convergence using an element stiffness matrix obtained by assuming a more complicated function for the element displacements.

A different stiffness matrix for a rectangular plate element in bending has been derived by O. C. Zienkiewicz[4,5] and Y. K. Cheung[4] by assuming a fourth order twelve-term polynomial function for the displacements of an element.

Triangular plate elements have been used as well for flexure in the continuous finite element technique[6,7,8,9]. For example, R. W. Clough[8] has compared the numerical results obtained by assuming various displacement functions for an element to obtain the stiffness matrix. Clough indicated that, for the example considered, convergence was monotonic as the number of elements was increased. However, he also pointed out that convergence does not necessarily imply convergence to the correct solution.

It has been observed that by assuming a displacement function for an element, vertical displacement compatibility between adjacent elements for

a plate in flexure can be maintained all along the edges of the elements, but normal slope compatibility is in general violated.[5, 8, 10] T. H. H. Pian[10] indicates that normal slope compatibility could be maintained as well when the element stiffness matrix is derived by assumed stress distributions using the principle of minimum complementary energy.

On the other hand, as already mentioned, plates have also been analyzed by various discrete or finite element methods in which some fictitious system is substituted for the actual plate medium. It has been pointed out by S. Spierig[11] that the idea of representing a continuous medium by a framework was conceived by F. Klein[12] as early as 1903. Klein indicated the equivalence of the plane state of stress in a disk and in a grid framework. In 1906 K. Wieghardt[13] applied this analogy to engineering problems. However, at that time Wieghardt approximated the stresses in frameworks from the plane stress condition in a beam. In 1927, the ideas of Klein and Wieghardt were used by W. Riedel[14] who calculated stresses in a continuous medium by use of a grid of square elements consisting of bars. The analogy of plates in flexure to frameworks was originated by A. P. Hrennikoff in 1940[15, 16]. Hrennikoff[15] also derived frameworks analogous to a plane stress condition in a disk. In considering a plate in flexure, Hrennikoff subdivided the plate into small square elements, and then derived a framework element analogous to the plate element. For Poisson's ratio of 1/3, such a square framework element consisted of six bars, each possessing a flexural stiffness. For arbitrary values of Poisson's ratio, a more complicated framework model was used by Hrennikoff. More recently, S. Spierig[11, 17] has

extended Hrennikoff's ideas to devise framework element models for rectangular, triangular and trapezoidal plate elements as well. These models, however, are somewhat more complicated, and are all restricted to Poisson's ratio of 1/3.

In a paper published in 1965, A. L. Yettram and H. M. Husain[18] have derived a relatively simple rectangular framework model for a plate in bending for an arbitrary value of Poisson's ratio. This model (see Fig. 1) has six bars as does the Hrennikoff's model for Poisson's ratio of 1/3, but in addition torsional stiffnesses are prescribed for the peripheral beams.

For all of the framework element models described above, the model is not a physical one since the bar stiffnesses may take on negative values for certain elastic constants. This, however, places no limitations on the analogy.

With the framework element bar properties known, the framework element stiffness matrix has been calculated. From that point on the analysis by the framework analogy and by continuous finite element approach is identical. Deflections for a particular problem obtained by Husain[18] have been found to agree closely by J. L. Tocher[19].

In addition to the framework analogies described above, various other fictitious systems have been substituted for the plate in flexure to obtain approximate solutions. A. H. S. Ang and N. M. Newmark[20] have used a model for the plate consisting of rigid bars, elastic hinges and coil springs. M. Badir[21] has used a model with orthogonal beams and coil springs, while E. Lightfoot[22] has used one with orthogonal beams and torsion bars. A. L. Yettram and H. M. Husain[23] have used a model of only orthogonally connected beams, using iteration for Poisson's ratio other than zero.

For the analysis of static shell problems by a finite element approach, a stiffness matrix for a plate element in plane stress has generally been combined with one for a plate in flexure to include the membrane stresses of the shell in the analysis. In addition to the plane stress framework models used by Hrennikoff[15, 16] and Spierig[11, 17], which have already been mentioned, there are various other models available for this purpose. For example, Hrennikoff's plane stress framework model has been extended by C.W. McCormick[24], and A. L. Yettram and H. M. Husain[25]. The plane stress framework model of the latter two authors consists of six beams, as in the case of the framework model for out-of-plane bending by the same authors. The beams possess stiffnesses for in-plane movement of the model.

In the continuous finite element approach for plane stress, rectangular elements have been used, for example, by R.W. Clough[8, 26], and triangular elements have been used by J. L. Tocher and B. J. Hartz[27] and by others[8, 28].

Extension of finite element techniques to cylindrical shells by use of the framework analogies for plane stress and out-of-plane bending has been suggested by Hrennikoff[16] and McCormick[24]. Pestel[17], in fact, extended the procedure to cylindrical shells using Hrennikoff's models, but only for the limited case of Poisson's ratio of 1/3. Later, E. F. Benard[29] used another type of a framework model to study the static behavior of cylindrical shells. Zienkiewicz[5] has employed the continuous finite elements for plane stress and out-of-plane bending to obtain a stiffness matrix for a rectangular shell element, which can be used to analyze cylindrical shells. A. Hrennikoff

and S. S. Tezcan[30] have used yet another approach to study the static cylindrical shell behavior. These authors have combined the continuous finite element technique of Clough[26] for plane stress with Yettram and Husain's[18] framework element approach for out-of-plane bending to analyze cylindrical shells. A discrete element model consisting of rigid bars and deformable nodes has been used by B. Mohraz and W. C. Schnobrich[31] to study cylindrical as well as other types of shells.

The dynamic analysis of plates and shells has been limited to relatively simple cases. Special boundary conditions, simplified loadings, or both have been used in such analysis.

The natural frequencies of plates in flexure have been studied by E. C. Pestel[17, 32, 33, 34] and F. A. Leckie[32, 35] by employing the framework model of Hrennikoff[15, 16].

Exact solutions to the differential equations of motion governing the behavior of plates subjected to multiple moving mass loads have been obtained by A. P. Cappelli[36] in the form of triple infinite series. These solutions, however, are limited to plates with simply supported boundaries.

For cylindrical shells, mathematical solutions have been obtained by J. P. Jones and P. G. Bhuta[37] for moving loads. These solutions, however, are only for infinitely long cylinders subjected to symmetrical, ring loading moving at constant velocity.

The dynamic response of space frames to moving loads and masses was investigated by H. Allik[1] in 1966. Allik used a discrete mass model, considering six degrees of freedom at each node, to obtain the set of governing

differential equations. Allik then solved these equations numerically by several step-by-step numerical integration techniques. Of the methods used in his study, Allik found the linear acceleration method to be the most efficient technique time-wise for solving the differential equations by use of a computer.

Allik[1] has also pointed out that his procedure can be extended to study plates and shells subjected to moving mass loads.

METHOD OF ANALYSIS

A. Formulation of the Plate Problems

1. - Discrete Element Model

The response of rectangular plates to dynamic loadings can be described approximately by the displacements of the plate at a finite number of points. Since the method of analysis presented herein is based on the theory of thin plates with small deflections, only the deflection of the plate normal to its plane, and the rotations about the two axes lying in the middle plane of the plate will be considered. In Fig. 1 is shown a rectangular plate of dimensions L_X, L_Y and a constant thickness h with X and Y axes taken in the middle plane of the plate, and the Z axis taken normal to that plane and directed downwards, the plate is divided by an orthogonal grid into small plate elements with dimensions L and cL. The intersections of the grid lines, i. e. the corners of the small plate elements, will be referred to as the nodes. It is at these nodes that the displacements are to be described.

A typical small plate element is shown in Fig. 2 with its orientation to the XYZ coordinates of the plate. The displacements of the nodes of the plate element, and the generalized forces, i.e. the forces and moments, acting on the plate element at the nodes are shown in their positive directions in vector notation. Right hand screw rule is used for the signs of the rotation and moment vectors. Also shown in Fig. 2 are the element coordinates axes x and y which will be used later.

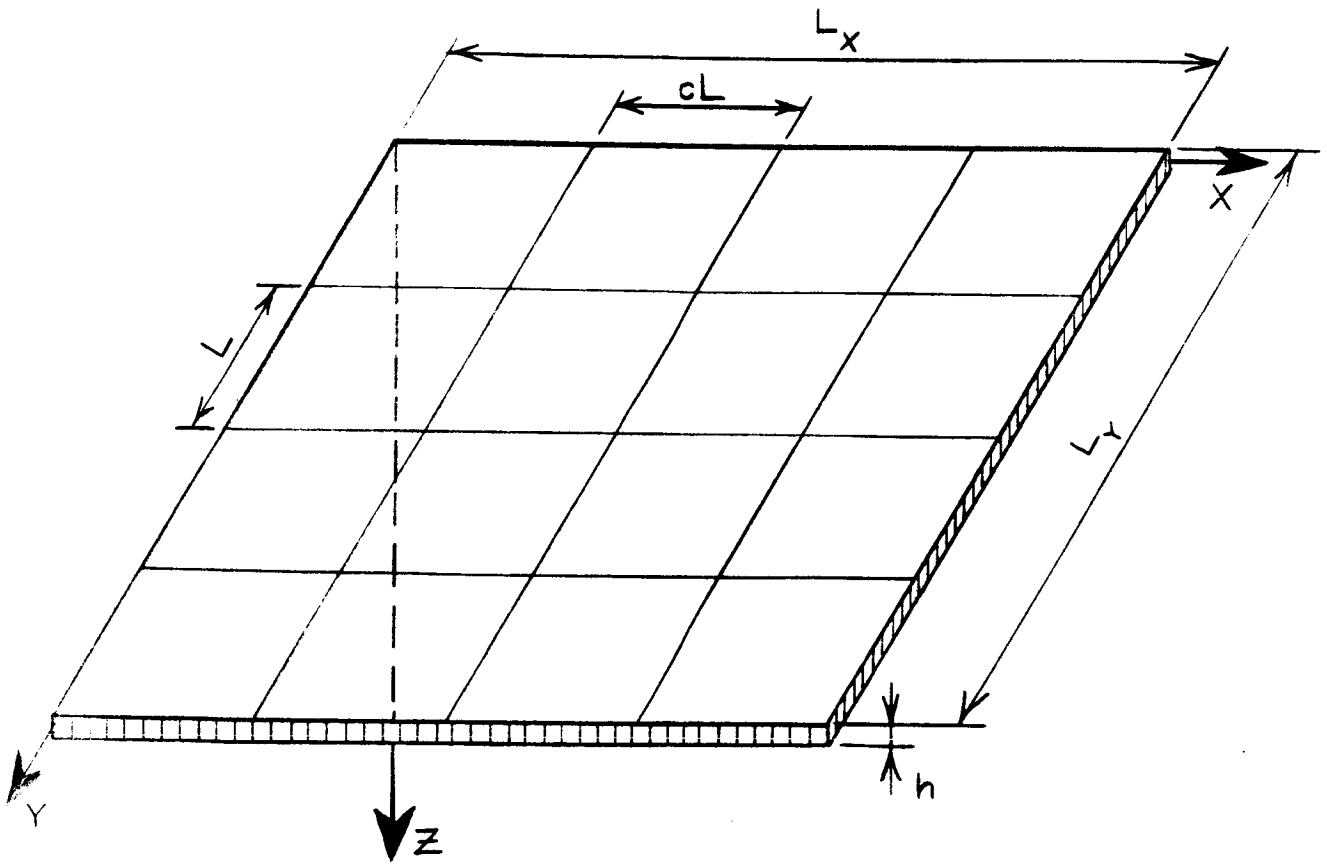

FIG. 1 – PLATE AND ITS COORDINATE SYSTEM

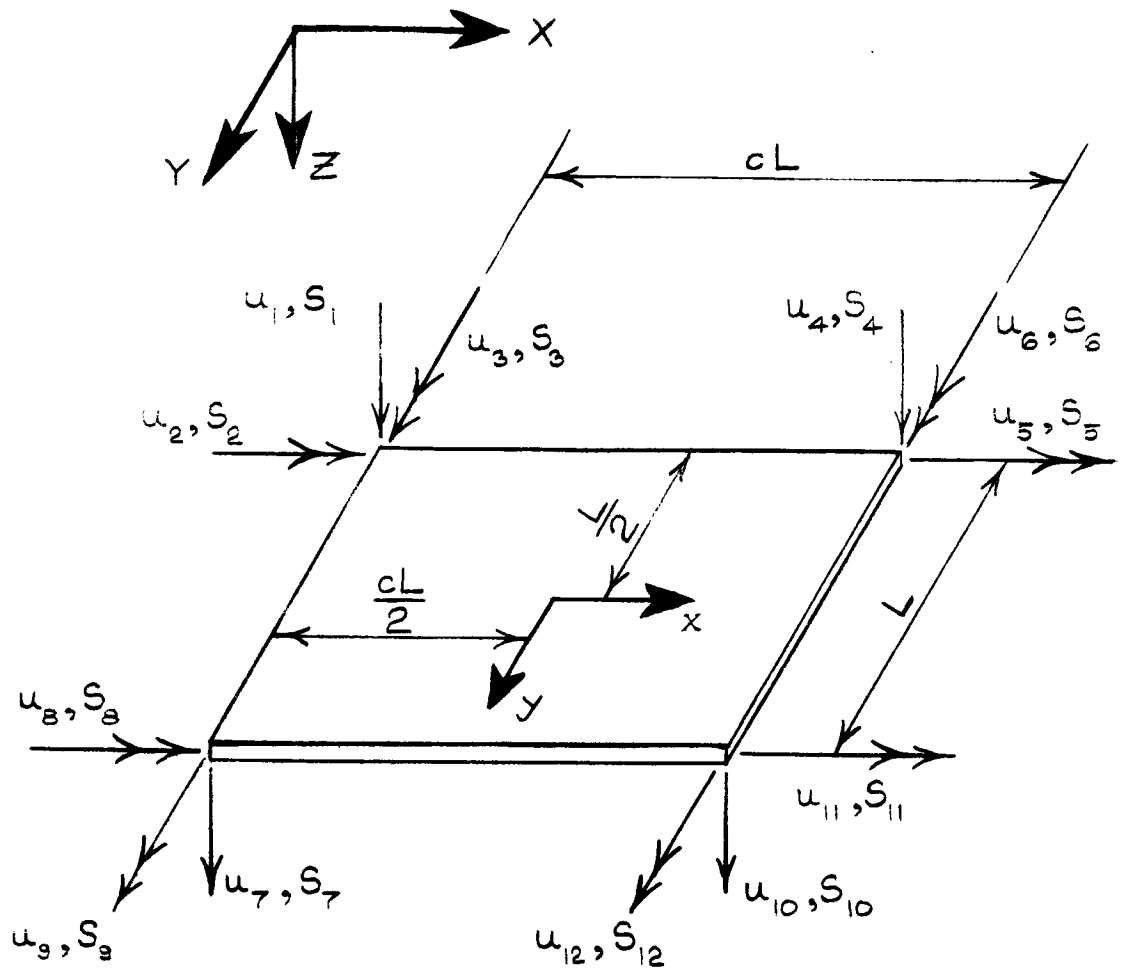

FIG. 2 – PLATE ELEMENT

The sign convention and orientation used for the displacements of the plate at the nodes and for the generalized forces acting on the plate at the nodes are identical to those of the displacements of a plate element and of the generalized forces acting on a plate element, as shown on Fig. 2. Therefore, with the sign conventions adopted, plate displacements and plate generalized forces can be transformed into displacements and generalized forces of the element, or vice versa, by summations without geometrical considerations.

It has been proved by A. L. Yettram and H. M. Husain [18] that an analogous framework element of six beams with flexural and torsional properties shown in Fig. 3 can be substituted for each of the small plate elements into which the plate was divided. The beams of the framework element are rigidly joined to the beams of the adjacent elements at the nodes only. Since in the resulting framework model for the plate there may be two parallel beams between two interior nodes, the beams are imagined to occupy the same physical space. Hence, strictly speaking, the resulting framework is considered here to be a fictitious rather than a physical model for the plate.

Basically, the beam constants for the framework element of Fig. 3 were derived by Yettram and Husain [18] by comparison of deformations of the plate element of Fig. 2 and the framework element of Fig. 3 when uniform moments and torques were in turn applied to the plate element and statically equivalent concentrated moments and torques were applied at the nodes of the framework element. Therefore inherent to this derivation is the assumption that the distribution of moments and torques in the plate is such that linear distributions of these results on a plate element. Thus the analogy of Yettram

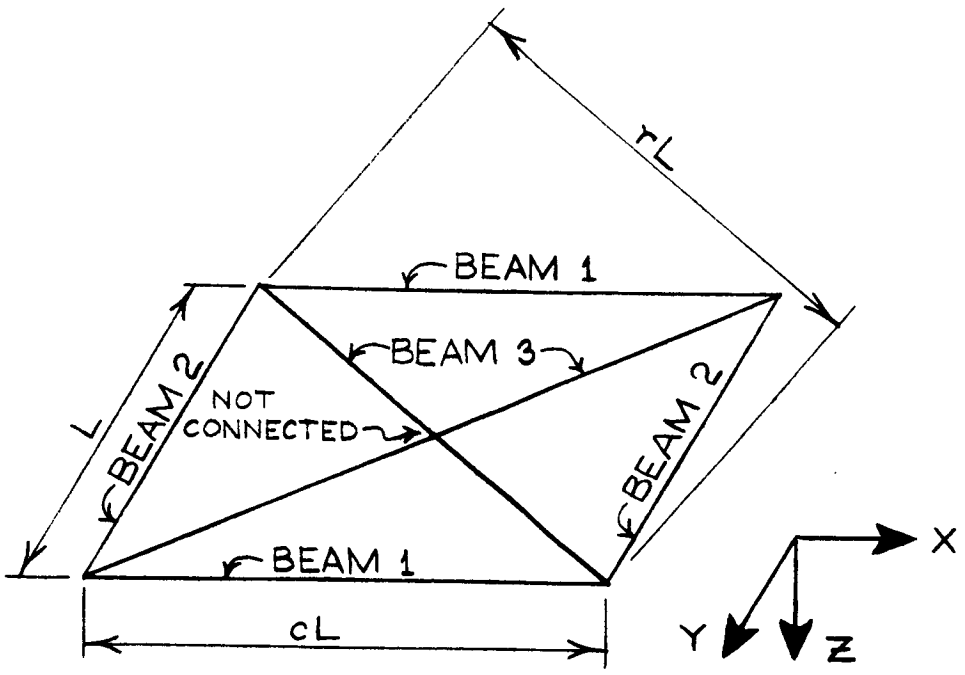

BEAM PROPERTIES:

$$I_1 = \frac{(1-c^2\nu)L}{2(1-\nu^2)} \cdot \frac{h^3}{12} \qquad \frac{GJ_1}{E} = \frac{(1-3\nu)L}{2(1-\nu^2)} \cdot \frac{h^3}{12}$$

$$I_2 = \frac{(c^2-\nu)L}{2c(1-\nu^2)} \cdot \frac{h^3}{12} \qquad \frac{GJ_2}{E} = \frac{c(1-3\nu)L}{2(1-\nu^2)} \cdot \frac{h^3}{12}$$

$$I_3 = \frac{\nu r^3 L}{2c(1-\nu^2)} \cdot \frac{h^3}{12} \qquad \frac{GJ_3}{E} = 0$$

where h = plate thickness
ν = Poisson's ratio for plate material
E = modulus of elasticity of plate material
I = beam moment of inertia for bending out of plane of plate
GJ = beam torsion constant

FIG. 3 – PLATE ELEMENT FRAMEWORK MODEL

and Husain [18] is theoretically correct only in the limit when the elements become infinitely small. However, elements of finite and relatively large size yield results of sufficient accuracy, as will be demonstrated by the numerical results presented subsequently.

2. - General Equations of Motion

Knowing the stiffness properties for each of the beams in the framework element of Fig. 3, the stiffness matrix of the plate element can be assembled to relate the node displacements to the node forces of the element by the following expression.

$$\left\{ S_i \right\} = \left[k_i \right] \left\{ u_i \right\} \tag{1}$$

where $\left\{ S_i \right\}$ is the vector of the 12 generalized internal forces acting at the nodes of element i. (See Fig. 2.)

$\left[k_i \right]$ is the 12x12 stiffness matrix of element i given in the Appendix.

$\left\{ u_i \right\}$ is the vector of the 12 displacements of the nodes of the element i. (See Fig. 2.)

The equilibrium of generalized forces at nodes yields

$$\left\{ R \right\} = \sum_{i=1}^{n} \left\{ S_i \right\} \tag{2}$$

where the summation extends over the n elements into which the plate was divided. $\left\{ R \right\}$, the vector of external forces acting at the nodes, consists of the following:

1.- External forces $\left\{ Q \right\}_n$ applied at the nodes.

2.- Equivalent node forces $\left\{ Q \right\}_e$ from external forces applied to the plate at points away from nodes.

$$\left\{ Q \right\}_e = \sum_{i=1}^{n} \left\{ F_i \right\}$$

where $\left\{ F_i \right\}$ is the vector of 12 generalized equivalent node forces associated with element i. These will be derived in a subsequent section.

3.- Inertia forces $\left\{ R \right\}_{in}$.

The inertia forces are found as follows. For an element i, by D'Alembert's principle

$$\left\{ R_i \right\}_{in} = - \left[m_i \right] \left\{ \ddot{u}_i \right\} \tag{3}$$

where $\left[m_i \right]$ is the diagonal 12x12 element mass matrix. The elements of this matrix, along with the assumptions used for its derivation, are given in the Appendix.

$\left\{ \ddot{u}_i \right\}$ is the vector of the 12 accelerations of the nodes of the element.

Summing the contributions from the inertia forces acting on all the elements, by Eq. (3)

$$\left\{ R \right\}_{in} = - \sum_{i=1}^{n} \left[m_i \right] \left\{ \ddot{u}_i \right\} \tag{4}$$

or

$$\left\{ R \right\}_{in} = - \left[m \right] \left\{ \ddot{u} \right\} \tag{5}$$

where n is the number of elements into which the plate was divided.

$\left[m \right] = \sum_{i=1}^{n} \left[m_i \right]$ is the mass matrix for the entire structure. It can be assembled by placing the elements of $\left[m_i \right]$ in the appropriate rows and columns of $\left[m \right]$ and adding the overlapping terms.

Substituting $\left\{ S_i \right\}$ from Eq. (1) into Eq. (2) results in

$$\left\{ R \right\} = \sum_{i=1}^{n} \left[k_i \right] \left\{ u_i \right\} \tag{6}$$

or

$$\left\{ R \right\} = \left[k \right] \left\{ u \right\} \tag{7}$$

where

$\left[k \right] = \sum_{i=1}^{n} \left[k_i \right]$ is the stiffness matrix for the entire structure, assembled in the same manner as the mass matrix $\left[m \right]$.

Substituting the components of $\left\{ R \right\}$ into Eq. (7) yields the equations of motion for the discrete element plate structure

$$\left[m \right] \left\{ \ddot{u} \right\} + \left[k \right] \left\{ u \right\} = \left\{ Q \right\} \tag{8}$$

where $\left\{ Q \right\} = \left\{ Q \right\}_n + \left\{ Q \right\}_e$. It should be noted that this vector may vary with time.

Eq. (8) represents a set of simultaneous, linear, second order differential equations equal in number to the number of degrees of freedom for the

discrete element plate structure. This equation was derived without making reference to the plate boundary conditions. To include these or any other restraints, after assembling the $\left[k \right]$ and $\left[m \right]$ matrices the rows and columns corresponding to the restrained displacement components should be removed. Accordingly, the same rows are to be removed from the vectors in Eqs. (5), (7) and (8).

Equation (8) was derived with rotary inertias included. When these are not included, the number of equations can be reduced to the number of degrees of freedom in deflection only, as shown in a subsequent section.

By use of the linear acceleration method, as shown later, node displacements can be found for any time. Then, the concentrated forces and moments acting at the nodes of element i can be found from

$$\left\{ S_i \right\} = \left[k_i \right] \left\{ u_i \right\} - \left\{ F_i \right\} \tag{9}$$

The internal plate forces and moments concentrated at a typical interior node can then be found by considering two adjacent elements at that node and summing the forces and moments acting at that node on these elements.

Alternately, the plate forces and moments at the nodes can be obtained from the transverse node deflections, using the well-known plate formulas.

3. - Forcing Functions

a. Moving Forces

In the analysis of the discrete element structure, it is necessary that external forces act only at the nodes. Since a moving load or a stationary

load varying with time may be acting at an arbitrary point on an element of the structure, a set of equivalent forces acting at the nodes of this element, which would cause the same displacements in the structure, must be determined. In the following derivation the load on the plate will be assumed to consist of only force components, and it will be assumed to remain in contact with the plate at all times.

Consider a moving force P acting in the Z-direction at an instant of time $t = t_1$ when it is located on an element at $x = a$ and $y = b$ of the element coordinates shown on Fig. 2. Applying virtual displacements δu_i at this instant of time at the nodes of this element, the deflection under the load caused by δu_i is assumed to be

$$w_o (x, y, t_1)\Big|_{\substack{x=a \\ y=b}} = \sum_{i=1}^{12} A_i (x, y)\, \delta u_i (t_1)\Big|_{\substack{x=a \\ y=b}} \qquad (10)$$

where $A_i (x, y)$ is the assumed deflection of the plate element due to a node displacement $u_i = 1$ and $u_j = o$ for $j \neq i$. $A_i (x, y)$ is given in the Appendix.

$\delta u_i (t_1)$ is the i-th virtual node displacement of the element in orientation and sign convention identical to u_i shown on Fig. 2.

For the dynamic system at time t_1, the virtual work done by the equivalent node forces F_i must equal the virtual work done by the force P.

Hence

$$\sum_{i=1}^{12} F_i \ \delta u_i (t_1) = P\, w_o (x, y, t_1)\Big|_{\substack{x=a \\ y=b}} \tag{11}$$

Substituting for $w_o (x, y, t_1)$ from Eq. (10), Eq. (11) yields

$$\sum_{i=1}^{12} F_i \ \delta u_i (t_1) = P \sum_{i=1}^{12} A_i (x, y) \ \delta u_i (t_1)\Big|_{\substack{x=a \\ y=b}} \tag{12}$$

from which the i-th equivalent node force is

$$F_i = P\, A_i (x, y)\Big|_{\substack{x=a \\ y=b}} \qquad (i=1, 2, \ldots, 12) \tag{13}$$

Equation (13) was derived for a single moving load. This equation obviously is also valid for a stationary time-varying load P applied at x = a and y = b. The equivalent node forces due to several stationary time-varying loads or due to multiple moving loads can be obtained by summing the equivalent node forces from Eq. (13) for each load applied.

b. - Moving Masses

To obtain the equivalent node forces resulting from a moving mass, the interaction force between the plate and the mass must be evaluated. In

this derivation, the moving mass on the plate will be assumed to remain in contact with the plate at all times, and the rotary inertia effect of this mass will be neglected.

It will be assumed that the deflection of a plate element under a moving mass at x, y on the element can be expressed by

$$w(x, y, t) = \sum_{j=1}^{12} A_j (x, y)\, u_j (t) \tag{14}$$

where $A_j (x, y)$ is the same as in Eq. (10) if i = j.

$u_j (t)$ is the j-th actual node displacement of the element nodes. (See Fig. 2.)

Since Eq. (14) represents the movement of the mass in the Z-direction while the mass itself is moving along the plate, the deflection w in Eq. (14) is

$$w (x, y, t) = w \left[x (t), y (t), t \right] \tag{15}$$

Denoting by V_x and V_y the x and y components of the velocity of the mass along the plate,

$$V_x = \frac{dx}{dt} \tag{16a}$$

$$V_y = \frac{dy}{dt} \tag{16b}$$

and hence, differentiating w twice with respect to time and using Eqs. (16),

$$\ddot{w}\left[x(t),\ y\ (t),t\right]= V_x^{\,2}\frac{\partial^2 w}{\partial x^2} + V_y^{\,2}\frac{\partial^2 w}{\partial y^2} + 2\,V_x\,V_y\frac{\partial^2 w}{\partial x\,\partial y}$$

$$+ 2\,V_x\frac{\partial^2 w}{\partial x\,\partial t} + 2V_y\frac{\partial^2 w}{\partial y\,\partial t} + \frac{\partial^2 w}{\partial t^2} \tag{17}$$

Substituting the derivatives of w obtained from Eq. (14) into Eq. (17) yields

$$\ddot{w}\left[x(t),\ y(t),\ t\right] = \sum_{j=1}^{12}\left(V_x^{\,2}A_{j,\,xx}\,u_j + V_y^{\,2}A_{j,\,yy}u_j + 2V_xV_yA_{j,\,xy}u_j\right.$$

$$\left. + 2V_xA_{j,x}\dot{u}_j + 2V_yA_{j,\,y}\dot{u}_j + A_j\ddot{u}_j\right) \tag{18}$$

where $A_{j,xx}$, etc., represents the second derivative of

A_j with respect to x, etc. (See Appendix.)

For a moving mass M located at x = a and y = b at time t_1, the associated inertia force is obtained from D'Alembert's principle as

$$-\,M\,\ddot{w}\left[\,x(t),\ y(t),\ t\,\right]\Big|_{\substack{x=a\\ y=b\\ t=t_1}} \tag{19}$$

where $\ddot{w}$ is given by Eq. (18). The i-th equivalent node force on an element at time t_1 is determined by substituting expression (19) for P in Eq. (13).

$$F_i = - M \sum_{j=1}^{12} (V_x^2 A_i A_{j,\,xx} u_j + V_y^2 A_i A_{j,\,yy} u_j$$

$$+ 2 V_x V_y A_i A_{j,\,xy} u_j + 2 V_x A_i A_{j,\,x} \dot{u}_j + 2 V_y A_i A_{j,\,y} \dot{u}_j$$

$$+ A_i A_j \ddot{u}_j) \Big|_{\substack{x = a \\ y = b \\ t = t_1}} \qquad (i=1, 2, \ldots, 12) \qquad (20)$$

This equation can be written as

$$F_i = - \sum_{j=1}^{12} (k_{ij}^* u_j + d_{ij}^* \dot{u}_j + m_{ij}^* \ddot{u}_j) \Big|_{\substack{x=a \\ y=b \\ t=t_1}} \qquad (21)$$

where $$k_{ij}^* = M A_i (V_x^2 A_{j,\,xx} + V_y^2 A_{j,\,yy} + 2 V_x V_y A_{j,\,xy}) \Big|_{\substack{x=a \\ y=b}}$$

$$d_{ij}^* = 2 M A_i (V_x A_{j,\,x} + V_y A_{j,\,y}) \Big|_{\substack{x=a \\ y=b}}$$

$$m_{ij}^* = (M A_i A_j) \Big|_{\substack{x=a \\ y=b}}$$

The vector of 12 equivalent node forces associated with element r is then

$$- \left\{ F_r \right\} = \left[k_r^* \right] \left\{ u_r \right\} + \left[d_r^* \right] \left\{ \dot{u}_r \right\} + \left[m_r^* \right] \left\{ \ddot{u}_r \right\} \qquad (22)$$

where the 12x12 matrix $\left[k_r^* \right]$ is assembled by placing each k_{ij}^* in the i-th row and j-th column of the matrix. The matrices $\left[d_r^* \right]$ and $\left[m_r^* \right]$ are obtained similarly. Adding the contributions from all the moving masses on all the elements of the plate yields

$$-\left\{ Q \right\}_e = \left[k^* \right] \left\{ u \right\} + \left[d^* \right] \left\{ \dot{u} \right\} + \left[m^* \right] \left\{ \ddot{u} \right\} \tag{23}$$

where $\left[k^* \right] = \sum_{r=1}^{n} \left[k_r^* \right]$

$$\left[d^* \right] = \sum_{r=1}^{n} \left[d_r^* \right]$$

$$\left[m^* \right] = \sum_{r=1}^{n} \left[m_r^* \right]$$

where the summation is to n, the number of elements of the structure.

Adding Eq. (23) to the node forces in Eq. (8) gives the equations of motion for the discrete-element plate with moving masses

$$\left[M \right] \left\{ \ddot{u} \right\} + \left[D \right] \left\{ \dot{u} \right\} + \left[K \right] \left\{ u \right\} = \left\{ Q \right\} \tag{24}$$

where $\left[M \right] = \left[m \right] + \left[m^* \right]$ (24a)

$\left[D \right] = \left[d^* \right]$ (24b)

$\left[K \right] = \left[k \right] + \left[k^* \right]$ (24c)

and where $\left\{ Q \right\}$ includes the node forces from all forces, static and moving, on the plate except those caused by the masses. Eq. (24)

represents a set of simultaneous, linear, second order differential equations where the coefficient matrices vary with time.

As shown later, Eq. (24) can be solved for node displacements, velocities and accelerations at a given time. Then the concentrated forces and moments acting at the nodes of element r can be found from

$$\left\{S_r\right\} = \left[K_r\right]\left\{u_r\right\} + \left[m_r^*\right]\left\{\ddot{u}_r\right\} + \left[d_r^*\right]\left\{\dot{u}_r\right\} - \left\{F_r\right\} \qquad (25)$$

Alternately, as before, the plate forces and moments at the nodes can be obtained from the transverse node deflections, using the plate equations from elasticity.

Eq. (24) was derived with rotary inertias of the plate included. In such a case the number of simultaneous equations in the set of Eqs. (24) is equal to the number of degrees of freedom of the plate model considered. When the rotary inertia of the plate is neglected, the number of equations can be reduced as explained in a subsequent section.

B. Formulation of the Cylindrical Shell Problems

1. General Remarks

The analysis of cylindrical shells and the analyses of rectangular plates is similar when finite elements are used for both structures. Due to the presence of membrane stresses in a cylindrical shell, a finite element model for the latter must, in general, possess six degrees of freedom for each node, while a finite element model for a plate in flexure only has three degrees of freedom at each node. Therefore, the stiffness matrix for a shell element must be a 24 by 24 matrix. Moreover, because of the

curvature of the shell, the coordinate systems of the overall structure and its elements do not coincide. Therefore geometric transformation matrices must be used to relate the displacements and forces from one coordinate system to the other. Also, in addition to the influence function A_i (x, y) used for the plate, another influence function must be considered for the shell because of the additional degrees of freedom present. Aside from the differences outlined above, the method of analysis for a rectangular plate and a cylindrical shell is the same.

2. Discrete Element Model

A right-handed cylindrical coordinate system XYZ, as indicated on Fig. 4, is adopted for the overall shell structure. The X-axis is in the middle surface of the shell and parallel to the axis of the shell. The Z-axis is normal to the surface of the shell and directed inwards. This set of coordinates is henceforth referred to as the system coordinates.

The rectangular finite elements for the shell, to be used subsequently, are obtained by subdividing the shell by an orthogonal grid parallel to X and Y axes. The intersections of such grid lines will henceforth be referred to as the nodes of the shell. Each of the small shell segments obtained by such a subdivision is then replaced by a flat plate. It is clear that such a substitute structure of flat plate segments approaches the physical structure of the actual shell only in the limit as the grid size becomes infinitely small. For any finite sizes of the plate segments, the actual cylindrical shell structure can only be approximated.

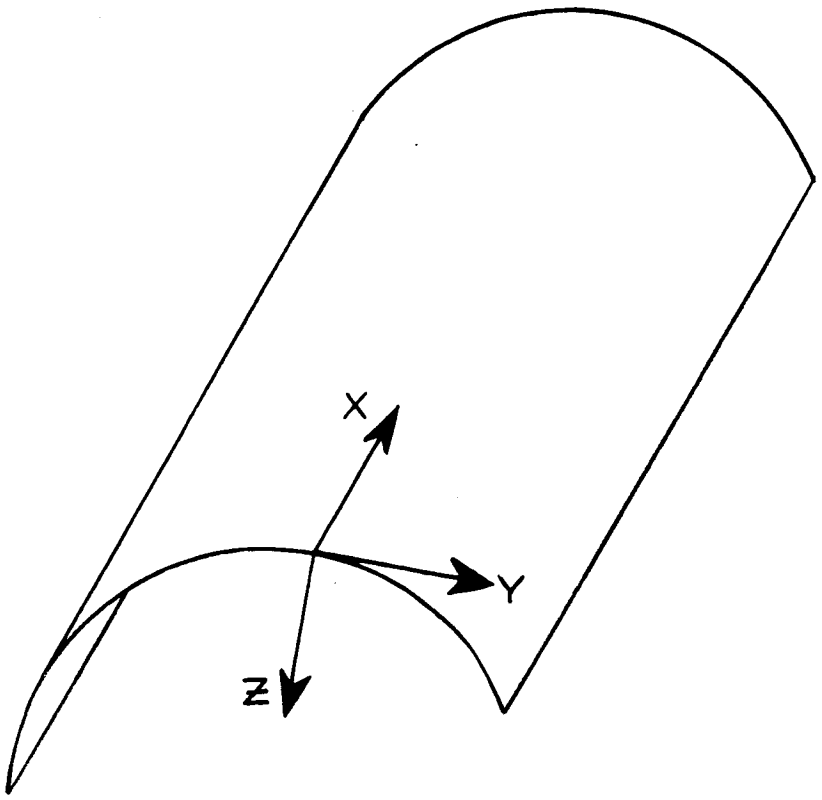

FIG. 4 - SYSTEM COORDINATES OF A CYLINDRICAL SHELL

On Fig. 5 is shown a typical shell element, i.e. a small rectangular plate that was substituted for a small shell segment as described above. The corners of such an element coincide with the nodes of the shell. It is at these corners, or nodes, that displacements and concentrated plate forces are to be considered. The right-handed element coordinate system shown on Fig. 5 is oriented so that the x-axis is parallel to the X-axis of the system coordinates, and the z-axis is normal to the element and directed toward the center of curvature of the shell. The node displacements u_i and the generalized node forces S_i, which always refer to the element coordinate system, are shown on Fig. 5 in their positive directions. Vector notation with right-hand screw rule is used for moments and displacements on the figure.

The sign convention and orientation used for the node displacements q_i and node forces Q_i, which always refer to the system coordinates, is shown on Fig. 6. Again a right-hand screw rule is used for the moment and displacement vectors.

It is to be noted that the numbering of displacements and forces on both Fig. 5 and 6 refers only to a relative sequence adopted in conjunction with matrices to be developed subsequently.

The orientation of the system coordinates YZ with respect to the element coordinates yz is indicated on Fig. 7. For a circular cylindrical shell the angles a_L and a_R are equal.

In the subsequent analysis of the cylindrical shell, the framework analogy for plane stress developed by Yettram and Husain[25] is combined with the framework analogy for plates in flexure by the same authors which was already discussed.

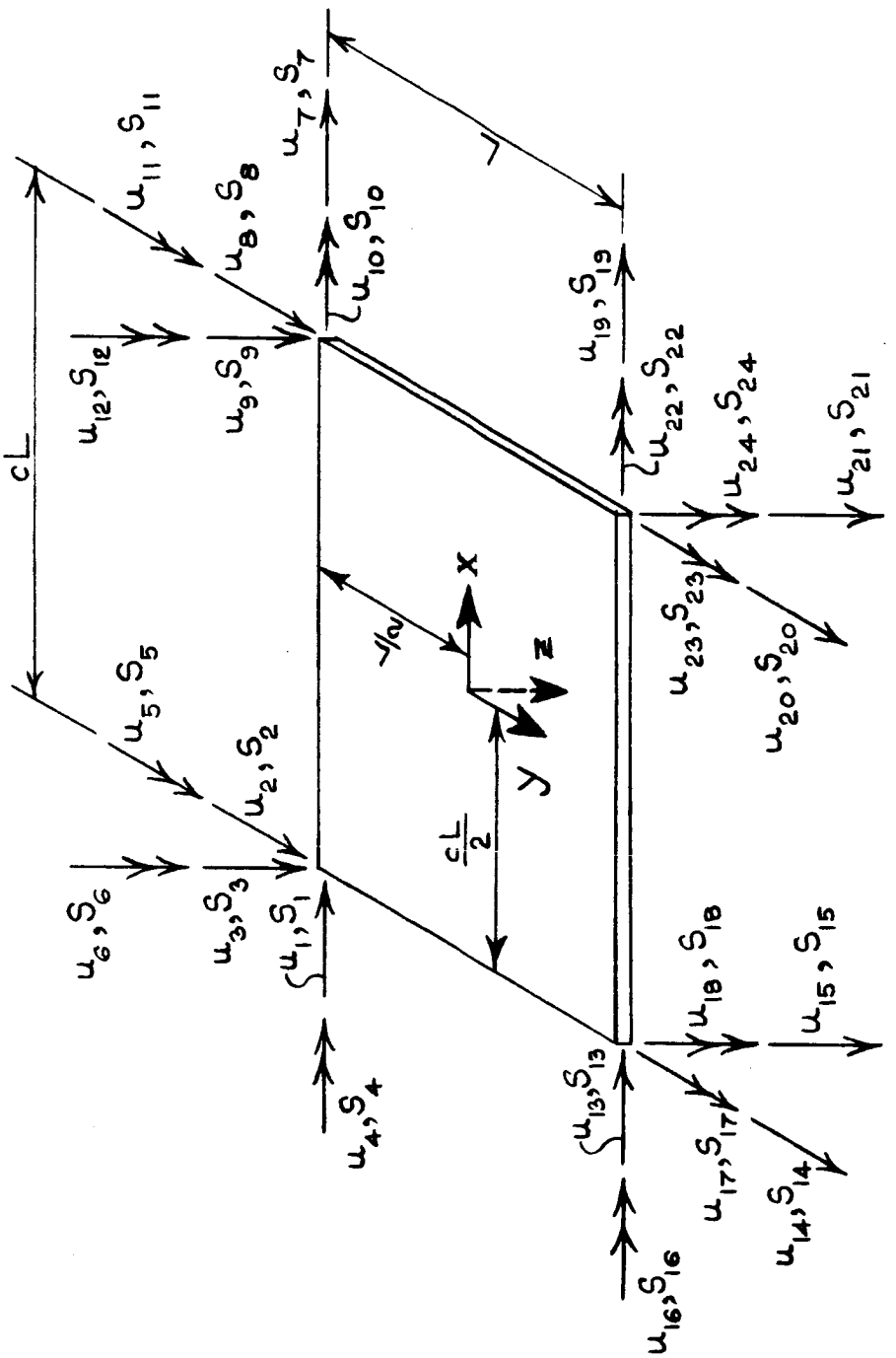

FIG. 5 – SHELL ELEMENT

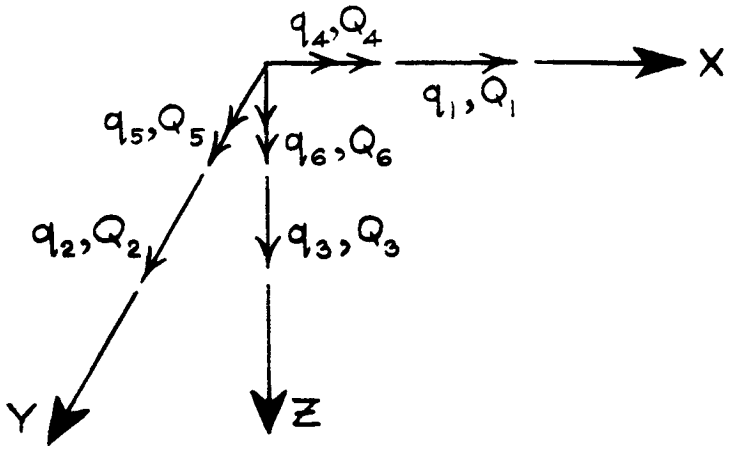

FIG. 6 – NODE DISPLACEMENTS AND FORCES IN SYSTEM COORDINATES

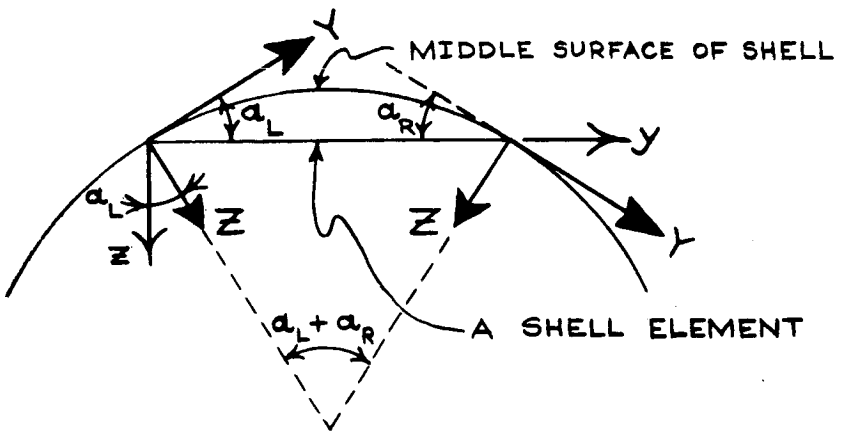

FIG. 7 – SYSTEM AND ELEMENT COORDINATES

As for plates in flexure, Yettram and Husain[25] have also shown that for a plate in plane stress an analogous framework of beams can be substituted to approximate the displacements and stresses in the plate. For each rectangular plate element six fictitious beams are substituted. The arrangement of the beams in this analogous framework element is identical to that of the framework element for a plate in flexure shown on Fig. 3. However, for the framework element for plane stress all of the beams possess extensional stiffnesses, and the four peripheral beams also have flexural stiffnesses for in-plane bending. The derivation of the above beam constants is quite similar to the derivation of beam constants for the framework analogous to a plate in flexure. Thus, the assumption used for the plate in plane stress is that the direct stresses and shears are constant along the edges of an element. The implications of such an assumption are analogous to those for a plate in flexure.

Since in the subsequent analysis linear theory is used, with changes in geometry not being considered, the beam properties for plane stress and those for out-of-plane bending may be combined to obtain a framework model analogous to a shell element, as to the one on Fig. 5. Such a framework model for a shell element with the appropriate beam constants is shown on Fig. 8.

3. General Equations of Motion

With the beam constants of a framework model shown on Fig. 8, the stiffness matrix of the shell element can be assembled. If all the elements of the shell are of the same size, then the element stiffness matrix is

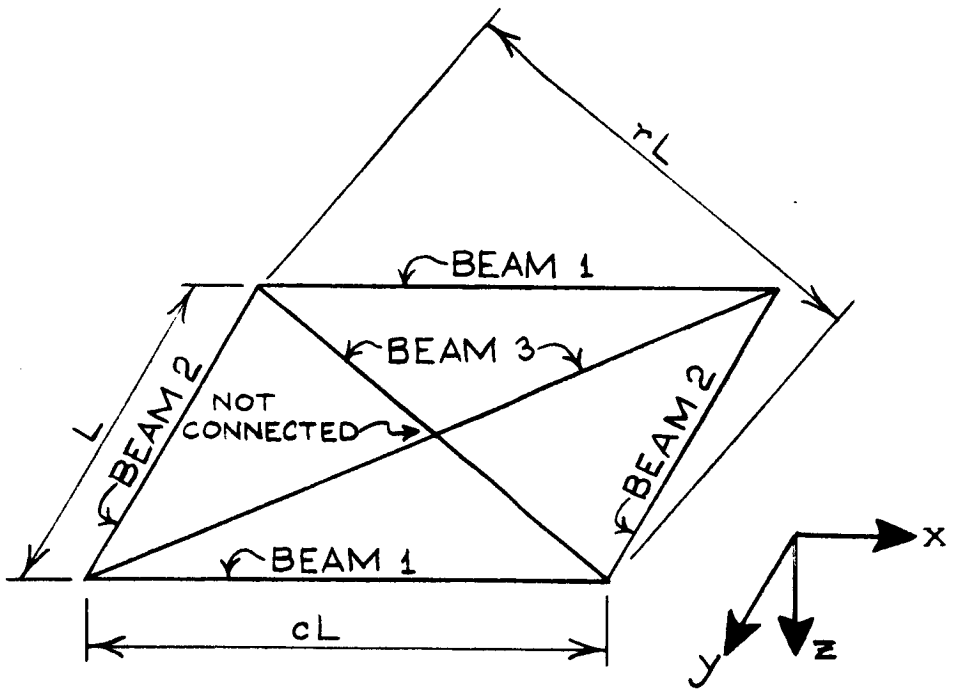

BEAM PROPERTIES FOR PLANE STRESS:

$$A_1 = \frac{(1-c^2\nu)L}{2(1-\nu^2)} \cdot h \qquad I'_1 = \frac{(1-3\nu)L^3c^2}{2(1-\nu^2)} \cdot \frac{h}{12}$$

$$A_2 = \frac{(c^2-\nu)L}{2c(1-\nu^2)} \cdot h \qquad I'_2 = \frac{(1-3\nu)L^3c}{2(1-\nu^2)} \cdot \frac{h}{12}$$

$$A_3 = \frac{\nu r^3 L}{2c(1-\nu^2)} \cdot h \qquad I'_3 = 0$$

where A = cross-sectional area of beam
I' = beam moment of inertia for in-plane bending of element

NOTE: Beam properties for out-of-plane bending are same as those on Fig. 3.

FIG. 8 - SHELL ELEMENT FRAMEWORK MODEL

identical for all of the shell elements. However, for a cylindrical shell that is not circular, it may be convenient to vary the element length in the y direction for different elements. The node displacements are related to the node forces for an element i by

$$\left\{ S_i \right\} = \left[k_i \right] \left\{ u_i \right\} \tag{26}$$

where $\left\{ S_i \right\}$ is the vector of the 24 generalized internal forces, expressed in the element coordinates xyz, acting at the nodes of shell element i. (See Fig. 5.)

$\left[k_i \right]$ is the 24 x 24 stiffness matrix of shell element i discussed in the Appendix.

$\left\{ u_i \right\}$ is the vector of the 24 displacements of the nodes of shell element i, expressed in the element coordinates xyz. (See Fig. 5.)

Node displacement in system coordinates are transformed into those in element coordinates by

$$\left\{ u_i \right\} = \left[C_i \right] \left\{ q_i \right\} \tag{27}$$

where $\left\{ q_i \right\}$ is the vector of the 24 displacements of the nodes of shell element i, expressed in system coordinates.

$\left[C_i \right]$ is the 24 x 24 geometric transformation matrix for shell element i, given in the Appendix.

From Eqs. (26) and (27), the node forces of element i resulting from node displacements $\left\{ q_i \right\}$ are

$$\left\{ S_i \right\} = \left[k_i \right] \left[C_i \right] \left\{ q_i \right\} \tag{28}$$

The equilibrium of generalized forces at nodes requires that

$$\left\{ R \right\} = \sum_{i=1}^{n} \left[C_i \right]^T \left\{ S_i \right\} \tag{29}$$

where the summation extends over all the n elements of the shell, and where $\left\{ R \right\}$ is the vector of resultant node forces, to be explained subsequently. Substituting Eq. (28) into (29) yields

$$\left\{ R \right\} = \sum_{i=1}^{n} \left[C_i \right]^T \left[k_i \right] \left[C_i \right] \left\{ q_i \right\} \tag{30}$$

This equation, which relates the node displacements in system coordinates to the resultant node forces, can be rewritten as

$$\left\{ R \right\} = \left[k \right] \left\{ q \right\} \tag{31}$$

where $\left[k \right] = \sum_{i=1}^{n} \left[C_i \right]^T \left[k_i \right] \left[C_i \right]$ is the stiffness matrix for the entire shell structure. It is assembled by first transforming each of the element stiffness matrices as indicated, and then placing the elements of each of these transformed matrices in the appropriate rows and columns of $\left[k \right]$, adding the overlapping terms.

$\left\{ R \right\}$, the vector of resultant node forces, consists of the following:

1. - External forces $\left\{ Q \right\}_n$ applied at the nodes, expressed in system coordinates XYZ.

2. Equivalent node forces $\left\{ Q \right\}_e$, expressed in system coordinates, from forces acting on the shell away from the nodes:

$$\left\{ Q \right\}_e = \sum_{i=1}^{n} \left[C_i \right]^T \left\{ F_i \right\} \tag{32}$$

where $\left\{ F_i \right\}$ is the vector of the generalized equivalent node forces associated with shell element i. These will be derived in a subsequent section.

3. Inertia forces $\left\{ R \right\}_{in}$ associated with the inertia of the structure. These forces, expressed in system coordinates, are found as follows. Node accelerations $\left\{ \ddot{q}_i \right\}$ in system coordinates transform into node accelerations $\left\{ \ddot{u}_i \right\}$ in element coordinates by

$$\left\{ \ddot{u}_i \right\} = \left[C_i \right] \left\{ \ddot{q}_i \right\} \tag{33}$$

From D'Alembert's principle, the inertia forces associated with the nodes of shell element i are

$$- \left[m_i \right] \left[C_i \right] \left\{ \ddot{q}_i \right\} \tag{34}$$

where $\left[m_i \right]$ is the 24x24 shell element mass matrix. The elements of this matrix, along with the assumptions used for its derivation, are given in the Appendix.

Transforming the forces of expression (34) into system coordinates and summing over all the n elements of the shell structure yields

$$\left\{ R \right\}_{in} = - \sum_{i=1}^{n} \left[C_i \right]^T \left[m_i \right] \left[C_i \right] \left\{ \ddot{q}_i \right\} \tag{35}$$

or

$$\left\{ R \right\}_{in} = - \left[m \right] \left\{ \ddot{q} \right\} \tag{36}$$

where $\left[m \right] = \sum_{i=1}^{n} \left[C_i \right]^T \left[m_i \right] \left[C_i \right]$ is the mass matrix for the entire shell structure, assembled in the same manner as the structure stiffness matrix $\left[k \right]$. (See Appendix.)

Substituting the components of $\left\{ R \right\}$ into Eq. (31) yields

$$\left[m \right] \left\{ \ddot{q} \right\} + \left[k \right] \left\{ q \right\} = \left\{ Q \right\} \tag{37}$$

where $\left\{ Q \right\} = \left\{ Q \right\}_n + \left\{ Q \right\}_e$ is a vector which varies with time in general.

Eq. (37) is completely analogous to Eq. (8) obtained for the plate. Thus, the number of equations represented by expression (37) is equal to the number of degrees of freedom of the finite element shell structure. However, in contrast to Eq. (8), Eq. (37) is associated only with the system coordinates. Boundary conditions or other restraints for the shell structure are introduced in the same manner as for plates.

The method of solution used for Eq. (37) to find node displacements, which appears in a later section, is the same as that for Eq. (8). Once the node displacements are knows for any instant of time, the concentrated forces and moments acting at the nodes of element i can be found from

Eq. (9), where $\{u_i\}$ is obtained from Eq. (27). Alternately, the plate forces and moments can be found from the node deflections using the equations from elasticity.

4. Forcing Functions

a. General

It is recalled that before a framework was substituted for the cylindrical shell, each of a finite number of curved small shell elements had to be replaced by a small flat plate segment. Since in the following development it is necessary to know the components of velocity of the moving load-mass along such a flat plate element, it can be assumed that the position of a load, which at any instant of time acts at an arbitrary point of a curved shell element, is at a point on a flat plate element which is on the line from the point of application on the curved shell element normal to the corresponding flat plate element. Although there will be apparent abrupt changes in the direction of motion of the load as it moves from one flat element to the next, these abrupt changes may be discarded since they do not exist on the actual curved shell. Since the X-coordinate of the system coordinates is always parallel to the x-coordinate of the element coordinates, the corresponding components of velocity of the moving load are equal on a curved shell element and on its corresponding flat plate element. This, however, is not the case with the Y and y components of velocity of the moving load, referring to system and element coordinates, respectively. Obviously, if a sufficiently large number of

finite elements is used in the Y-direction so that the arc length of the curved shell element is approximately equal to the length in y-direction of the flat plate element, then the corresponding components of velocity may be considered to be equal. To obtain the y-component of velocity more exactly, however, the Y-component of velocity should be multiplied by the ratio of the length of the flat element in y-direction to the arc length of the corresponding curved shell element. The theoretically exact relation between these velocity components could, of course, be calculated from geometry, even for a non-circular cylindrical shell, but for practical purposes this is not justified.

As mentioned earlier, the subsequent development is for loads and masses moving with a constant speed along the cylindrical shell.

The derivation of the equivalent node forces for the cylindrical shell requires the assumption of certain displacement functions for a flat plate element. Such functions are assumed since no exact functions are available. In this derivation, the moving loads will be assumed to consist of forces but not of moments.

b. Moving Forces

As in the analysis of plates, also in the analysis of cylindrical shells by the finite element technique it is necessary that all forces act at the nodes. Thus for a moving load, which may act at an arbitrary point of the shell at a given instant of time, it is necessary to find a set of equivalent node forces at that instant of time that would cause the same displacements in the structure.

In the subsequent development it will be assumed that the load or mass, as it moves along the shell, remains in contact with the shell at all times.

Consider a moving force P at an instant of time $t = t_1$, acting in an arbitrary direction, when it is located on a flat element at $x = a$ and $y = b$ of element coordinates. The force P is divided into its components P_x, P_y and P_z. The first two components cause plane stress in the element, while P_z causes out-of-plane bending of the element. The two cases are considered separately.

The equivalent node forces from P_z are the same as those obtained for a plate element in the analysis of plates, given by Eq. (13). Only the subscripts i have to be modified in that equation, in order that the numbering of the components of the equivalent node forces corresponds to that indicated in Fig. 5 for a flat shell element. Therefore in the subsequent analysis only components P_x and P_y need to be considered.

In the analysis by a finite element approach, after the structure stiffness matrix has been assembled, the procedure is identical regardless of whether a framework analogy or some continuous finite element technique is being used. This justifies the derivation of equivalent node forces independently from the particular finite element technique adopted for the rest of the analysis, without any inconsistencies resulting.

With the Yettram and Husain[25] framework model for plane stress, twelve possible node forces are associated with any one element. However, with some other continuous finite element techniques for plane stress,

only eight such forces would be considered. But in the analysis of an "angular" shell structure, corresponding to each of the above alternatives there would still be the same number of equilibrium equations in the system coordinates. Therefore, in the following derivation, the calculation of only eight equivalent node forces for the plane stress condition implies no inconsistencies.

Consider P_x, the x-component of the moving force P, at an instant of time $t=t_1$ located on an element at x=a and y=b. Applying virtual displacements δu_i (i=1, 2, 7, 8, 13, 14, 19, 20) at this instant of time at the nodes of this element, the translational displacement of the point (a, b) in the x-direction, due to virtual displacements δu_i, is assumed to be

$$w_x(x, y, t_1)\Big|_{\substack{x=a \\ y=b}} = \sum_i B_i(x, y)\ \delta u_i(t_1)\Big|_{\substack{x=a \\ y=b}} \tag{38}$$

where $i = 1, 7, 13, 19$

$B_i(x, y)$ is the assumed displacement of the element in x-direction due to a node displacement $u_i = 1$ and $u_j = 0$ for $j \neq i$, when i=1, 7, 13, 19. (See Appendix.)

$\delta u_i(t_1)$ is the i-th virtual node displacement of the element, in orientation and sign convention identical to u_i shown in Fig. 5.

As in the plate analysis (See Eqs. (10) to (13).), this leads to the expression for the i-th equivalent node force

$$F_i = P_x B_i (x, y) \Big|_{\substack{x=a \\ y=b}} \qquad (i=1, 7, 13, 19) \tag{39}$$

Similarly, from the y-component of the moving force P

$$F_i = P_y B_i (x, y) \Big|_{\substack{x=a \\ y=b}} \qquad (i=2, 8, 14, 20) \tag{40}$$

In this equation $B_i (x, y)$ is defined as in Eq. (38) except that here it refers to the assumed displacement in the y-direction, for i=2, 8, 14, 20. (See Appendix.)

Although it appears from the foregoing development that four equivalent node forces for each of P_x and P_y are determined independently, this is seen not to be the case when reference is made to the Appendix. It is seen from the Appendix that the displacement functions $B_i (x, y)$ for i=1, 7, 13, 19 are related to $B_i (x, y)$ for i=2, 8, 14, 20 by some common constants. Therefore, the equivalent node forces due to P_x and those due to P_y are in fact related, and can not be determined independently.

The comments made in the plate analysis for stationary time-varying loads and for multiple moving loads also hold here.

c. Moving Masses

As in the plate analysis, the interaction force between the shell element and the mass is evaluated in order to obtain a set of equivalent node forces resulting from a moving mass. Again, the rotary inertia effect of the mass is neglected.

The interaction force between the shell element and the mass can be divided into components along the x, y, and z directions. The z-component of the interaction force has already been determined in the development of the plate analysis. Thus, the equivalent node forces due to this force are given by Eqs. (20) and (21). However, the subscripts i and j have to be modified in that expression so that their numbering corresponds to the numbering of node forces and displacements indicated on Fig. 5.

The determination of the x and y components of the interaction force is similar to that for the z-component, except that here the displacement function $B_i(x, y)$ is used. This function and its appropriate subscripts are those used in the previous section when equivalent node forces due to a moving load were determined. Thus it suffices but to write down the expression, analogous to Eq. (20), for the equivalent node forces associated with the x and y components of the interaction force. That is, for a mass M at time $t=t_1$ located at x=a and y=b of an element,

$$F_i = - M \sum_j B_i (V_x^2 B_{j,xx} u_j + V_y^2 B_{j,yy} u_j + 2V_x V_y B_{j,xy} u_j + 2V_x B_{j,x} \dot{u}_j + 2V_y B_{j,y} \dot{u}_j + B_j \ddot{u}_j) \Big|_{\substack{x=a \\ y=b \\ t=t_1}} \tag{41}$$

where i and j each = 1, 2, 7, 8, 13, 14, 19, 20

B_i is defined in Eq.(38) and given in the Appendix.

B_j is defined as B_i, with j substituted for i.

Eqs. (41) and (21) can be together written as

$$F_i = -\sum_j \left(k_{ij}^* u_j + d_{ij}^* \dot{u}_j + m_{ij}^* \ddot{u}_j\right) \Bigg|_{\substack{x=a \\ y=b \\ t=t_1}} \tag{42}$$

where i and j each take on all values from

1 to 24 except 6, 12, 18, 24.

and where, for i and j each = 3, 4, 5, 9, 10, 11, 15, 16, 17, 21, 22, 23,

$$k_{ij}^* = M A_i \left(V_x^2 A_{j,xx} + V_y^2 A_{j,yy} + 2 V_x V_y A_{j,xy}\right) \Bigg|_{\substack{x=a \\ y=b}} \tag{42a}$$

$$d_{ij}^* = 2MA_i\left(V_x A_{j,x} + V_y A_{j,y}\right) \Bigg|_{\substack{x=a \\ y=b}} \tag{42b}$$

$$m_{ij}^* = MA_i A_j \Bigg|_{\substack{x=a \\ y=b}} \tag{42c}$$

and where, for i and j each = 1, 2, 7, 8, 13, 14, 19, 20,

$$k_{ij}^* = M B_i \left(V_x^2 B_{j,xx} + V_y^2 B_{j,yy} + 2 V_x V_y B_{j,xy}\right) \Bigg|_{\substack{x=a \\ y=b}} \tag{42d}$$

$$d^*_{ij} = 2\ MB_i\ (V_x B_{j,x} + V_y B_{j,y}) \Big|_{\substack{x=a \\ y=b}} \tag{42e}$$

$$m^*_{ij} = MB_i B_j \Big|_{\substack{x=a \\ y=b}} \tag{42f}$$

Eqs. (42a, b, c) are associated with out-of-plane bending of the element, and Eqs. (42d, e, f) are associated with plane stress condition of the element. All k^*_{ij}, d^*_{ij}, and m^*_{ij} not specifically defined by Eqs. (42a) through (42f) are zero.

Eq. (42) was derived for a single moving mass on an element. For several moving masses on the same element, the equivalent node forces are obtained by adding those caused by each mass, using Eq. (42). Thus the vector of all equivalent node forces, caused by moving masses, that are associated with element r is defined by

$$-\left\{F_r\right\} = \left[k^*_r\right]\left\{u_r\right\} + \left[d^*_r\right]\left\{\dot{u}_r\right\} + \left[m^*_r\right]\left\{\ddot{u}_r\right\} \tag{43}$$

For convenience, Eq. (43) is written with the vectors each having 24 rows, although the rows 6, 12, 18 and 24 are zero. Similar statement holds for the 24x24 matrices in this equation. The 24x24 matrices $\left[k^*_r\right]$, $\left[d^*_r\right]$ and $\left[m^*_r\right]$ are assembled by placing each k^*_{ij}, d^*_{ij}, and m^*_{ij} in the i-th row and j-th column of the respective matrix.

Transforming Eq. (43) to system coordinates, and adding the contributions from all the moving masses on all the elements of the structure yields

$$-\left\{Q\right\}_e = \left[k^*\right]\left\{q\right\} + \left[d^*\right]\left\{\dot{q}\right\} + \left[m^*\right]\left\{\ddot{q}\right\} \tag{44}$$

where $$\left\{Q\right\}_e = \sum_{i=1}^{n} \left[C_i\right]^T \left\{F_i\right\} \tag{44a}$$

$$\left[k^*\right] = \sum_{i=1}^{n} \left[C_i\right]^T \left[k_i^*\right] \left[C_i\right] \tag{44b}$$

$$\left[d^*\right] = \sum_{i=1}^{n} \left[C_i\right]^T \left[k_i^*\right] \left[C_i\right] \tag{44c}$$

$$\left[m^*\right] = \sum_{i=1}^{n} \left[C_i\right]^T \left[m_i^*\right] \left[C_i\right] \tag{44d}$$

where the summation extends to n, the number of elements used for the shell. Although for only a few moving masses on the shell structure most of the rows and columns of the matrices (44b, c, d) would consist of zeros, for reasons that will become apparent later, it is more convenient to arrange the matrices as shown.

Adding Eq. (44) to the node forces in Eq. (37) yields the following equations of motion for the finite element shell structure subjected to moving masses

$$\left[M\right]\left\{\ddot{q}\right\} + \left[D\right]\left\{\dot{q}\right\} + \left[K\right]\left\{q\right\} = \left\{Q\right\} \tag{45}$$

where $\left[M \right] = \left[m^* \right] + \left[m \right]$ (45a)

$$\left[D \right] = \left[d^* \right] \tag{45b}$$

$$\left[K \right] = \left[k^* \right] + \left[k \right] \tag{45c}$$

and where $\left\{ Q \right\}$ includes the node forces from all forces on the shell, static and moving, except those caused by the moving masses.

Eqs. (45) are analogous to the corresponding Eqs. (24) derived for the plate. Thus the remarks made in reference to Eqs. (24) in regard to a plate also hold here in regard to the cylindrical shell. Therefore, rather than solve Eqs. (24) and (45) separately for the plate and the shell, respectively, these sets of equations will be treated together in the subsequent sections.

C. Solution of Equations of Motion

1. General Case

For the solution of equations of motion in the general case it is assumed that all the inertia effects of the structure, including those of rotary inertia, are included. As mentioned previously, since the equations of motion for the plate structure are analogous to the equations of motion for the cylindrical shell structure, the two cases will be treated together. Henceforth reference will be made only to the equations of motion for the plate structure. However, all the discussions, the development and the solutions are equally valid for the equations of motion for the shell structure when q is substituted for u.

In the equations of motion (8) the vector $\{Q\}$ may vary arbitrarily with time. Moreover, when moving masses are considered, the coefficient matrices in the equations of motion may be time-dependent, as seen from Eq. (24). Hence only numerical solutions to the equations of motion are generally possible. Of the various numerical techniques available, Allik[1] has studied the linear acceleration method, Runga-Kutta method due to Gill, Milne's 4-th order method and Houbolt's method. Of these methods, Allik[1] has found the linear acceleration method to be the most efficient one in computer time. Hence this method, as used by Allik[1], will be adopted here. It should be noted, however, that other methods are applicable here as well.

The accuracy of the solution of an initial value problem by a step-by-step numerical integration method depends on the size of the time interval h chosen. Since it is not possible in general to determine the required size of the time increment h beforehand, a solution for a given h can be considered acceptable when it agrees sufficiently well with a solution obtained for a smaller time increment.

In the linear acceleration method the accelerations of the nodes of the plate are assumed to vary linearly for a small time increment h. Hence the acceleration in the interval between times n and n + 1 is given by

$$\ddot{u} = \ddot{u}_n + \frac{1}{h} (\ddot{u}_{n+1} - \ddot{u}_n) (t - t_n) \tag{46}$$

The expressions for the displacements and velocities used in the linear acceleration method, which have been derived previously from the assumption of Eq. (46)[38], are as follows

$$\left\{ u \right\}_{n+1} = \left\{ u \right\}_n + h \left\{ \dot{u} \right\}_n + \frac{h^2}{3} \left\{ \ddot{u} \right\}_n + \frac{h^2}{6} \left\{ \ddot{u} \right\}_{n+1} \tag{47}$$

$$\left\{ \dot{u} \right\}_{n+1} = \left\{ \dot{u} \right\}_n + \frac{h}{2} \left\{ \ddot{u} \right\}_n + \frac{h}{2} \left\{ \ddot{u} \right\}_{n+1} \tag{48}$$

a. Problem with Moving Forces

The equations of motion (8) for the end of a time interval can be written as

$$\left[m \right] \left\{ \ddot{u} \right\}_{n+1} = - \left[k \right] \left\{ u \right\}_{n+1} + \left\{ Q \right\}_{n+1} \tag{49}$$

Substituting for $\left\{ u \right\}_{n+1}$ from Eq. (47) and rearranging yields

$$\left(\left[m \right] + \frac{h^2}{6} \left[k \right] \right) \left\{ \ddot{u} \right\}_{n+1} = \left\{ Q \right\}_{n+1} - \left[k \right] \left(\left\{ u \right\}_n + h \left\{ \dot{u} \right\}_n + \frac{h^2}{3} \left\{ \ddot{u} \right\}_n \right) \tag{50}$$

which can be written as

$$\left[E \right] \left\{ \ddot{u} \right\}_{n+1} = \left\{ G \right\} \tag{51}$$

where $\left[E \right] = \left[m \right] + \frac{h^2}{6} \left[k \right]$ (51a)

$\left\{ G \right\}$ = right side of Eq. (50) (51b)

Since $\left[E \right]$ depends only on the properties of the discrete element plate, the node accelerations at the end of the time interval can be calculated from Eq. (51) as

$$\left\{ \ddot{u} \right\}_{n+1} = \left[E \right]^{-1} \left\{ G \right\} \tag{52}$$

Hence the displacements and the velocities at the end of the time interval can be calculated from Eqs. (47) and (48). It should be noted that the vector $\{ G \}$ in Eq. (52) depends on the displacements, velocities, and accelerations at the beginning of the time increment. Therefore $\{ G \}$ must be evaluated for each time interval.

The linear acceleration method is self-starting. With the initial conditions of zero displacements and zero velocities at each node, the initial accelerations are found from Eq. (49).

It should be noted that since the equations of motion (8) are valid for moving loads as well as for stationary time-varying loads, the foregoing solution also holds for the latter case.

b. Problem with Moving Masses

The equations of motion (24) for the case with moving masses can be solved as follows. Equation (24) for the end of the time interval n+1 can be written as

$$[M]\{\ddot{u}\}_{n+1} + [D]\{\dot{u}\}_{n+1} + [K]\{u\}_{n+1} = \{Q\}_{n+1} \tag{53}$$

Substituting for $\{u\}_{n+1}$ and $\{\dot{u}\}_{n+1}$ from Eqs. (47) and (48) gives

$$\left([M] + \frac{h}{2}[D] + \frac{h^2}{6}[K]\right)\{\ddot{u}\}_{n+1} = \{Q\}_{n+1} - [D]\left(\{\dot{u}\}_n + \frac{h}{2}\{\ddot{u}\}_n\right) - [K]\left(\{u\}_n + h\{\dot{u}\}_n + \frac{h^2}{3}\{\ddot{u}\}_n\right) \tag{54}$$

which can be written as

$$[E]\{\ddot{u}\}_{n+1} = \{G\} \tag{55}$$

where $\left[E \right] = \left[M \right] + \frac{h}{2}\left[D \right] + \frac{h^2}{6}\left[K \right]$ (55a)

$\left\{ G \right\}$ = Right hand side of Eq. (54) (55b)

In Eq. (55) $\left[E \right]$ as well as $\left\{ G \right\}$ must be re-evaluated for each time interval. At the end of the time increment, the node accelerations, displacements, and velocities can be evaluated from Eqs. (55), (47), and (48), respectively.

2. Case when Rotary Inertia Neglected

a. Problem with Moving Forces

As previously mentioned, when the rotary inertia of the structure is neglected, the number of equations of motion for a plate subjected to moving loads or to stationary time-varying loads, as given by Eqs. (8), may be reduced. In such a case, the equations of motion (8) can be partitioned as

$$\left[m \right]_{11} \left\{ \ddot{u} \right\}_1 + \begin{bmatrix} \left[k \right]_{11} & \left[k \right]_{12} \\ \left[k \right]_{21} & \left[k \right]_{22} \end{bmatrix} \begin{Bmatrix} \left\{ u \right\}_1 \\ \left\{ u \right\}_2 \end{Bmatrix} = \begin{Bmatrix} \left\{ Q \right\}_1 \\ \left\{ Q \right\}_2 \end{Bmatrix} \tag{56}$$

where $\left\{ u \right\}_1$ is the vector of node deflections associated with inertia forces.

$\left\{ u \right\}_2$ is the vector of node rotations not associated with inertia forces.

From Eq. (56) it follows that

$$\left[m \right]_{11} \left\{ \ddot{u} \right\}_1 + \left[k \right]_{11} \left\{ u \right\}_1 + \left[k \right]_{12} \left\{ u \right\}_2 = \left\{ Q \right\}_1 \tag{57}$$

and

$$[k]_{21}\{u\}_1 + [k]_{22}\{u\}_2 = \{Q\}_2 \tag{58}$$

From Eq. (58)

$$\{u\}_2 = -[k]_{22}^{-1}[k]_{21}\{u\}_1 + [k]_{22}^{-1}\{Q\}_2 \tag{59}$$

Substituting Eq. (59) for $\{u\}_2$ in Eq. (57) yields the equations of motion in terms of $\{u\}_1$ only:

$$[m]_{11}\{\ddot{u}\}_1 + [K]\{u\}_1 = \{Q\}_1 - [k]_{12}[k]_{22}^{-1}\{Q\}_2 \tag{60}$$

where $[K] = [k]_{11} - [k]_{12}[k]_{22}^{-1}[k]_{21}$ (60a)

Using the linear acceleration method of numerical integration on Eq. (60) yields

$$\{\ddot{u}_1\}_{n+1} = [E]^{-1}\{G\} \tag{61}$$

where $\{\ddot{u}_1\}_{n+1} = \{\ddot{u}\}_1$ at the end of the time increment considered.

$[E] = [m]_{11} + \frac{h^2}{6}[K]$, where $[K]$ is defined by Eq. (60a).

and where

$$\{G\} = \{Q_1\}_{n+1} - [k]_{12}[k]_{22}^{-1}\{Q_2\}_{n+1}$$

$$-[K]\left(\{u_1\}_n + h\{\dot{u}_1\}_n + \frac{h^2}{3}\{\ddot{u}_1\}_n\right)$$

In the latter expression the subscripts of Q, u and its derivatives have been moved inside the brackets only for clarity.

Once the node accelerations at the end of a time increment have been determined by Eq. (61), the displacements and velocities for the end of the time interval can be found from expressions analogous to Eqs. (47) and (48), and from Eq. (53).

b. Problem with Moving Masses

The number of equations of motion for a plate subjected to moving masses, as given by Eqs. (24), may be reduced when the rotary inertia of the structure is neglected. However, in this case, the reduced number of equations will not be equal to the number of degrees of freedom in deflection for the structure. The reduced number of equations, as shown subsequently, changes in general whenever a moving mass crosses from one element to another.

The equations of motion (24) can be written as

$$\left[m \right] \left\{ \ddot{u} \right\} + \left[m^{*} \right] \left\{ \ddot{u} \right\} + \left[d^{*} \right] \left\{ \dot{u} \right\} + \left[k \right] \left\{ u \right\} + \left[k^{*} \right] \left\{ u \right\} = \left\{ Q \right\} \quad (62)$$

As previously mentioned, the number of equations constituting the set of equations (62) is equal to the number of degrees of freedom of the plate structure. Define

N_S = number of degrees of freedom of the structure.

D_S = number of degrees of freedon of the structure in deflection.

and, for a given instant of time, define

M_S = number of equivalent node moments from all of the moving masses at the instant of time considered.

When the rotary inertia effects of the structure are neglected, at any given instant of time, Eq. (62) can be partitioned as

$$\begin{aligned}
&[m]_{11}\{\ddot{u}\}_1 + \begin{bmatrix}[m^*]_{11} & [m^*]_{12}\\ [m^*]_{21} & [m^*]_{22}\end{bmatrix}\begin{Bmatrix}\{\ddot{u}\}_1\\ \{\ddot{u}\}_2\end{Bmatrix} + \begin{bmatrix}[d^*]_{11} & [d^*]_{12}\\ [d^*]_{21} & [d^*]_{22}\end{bmatrix}\begin{Bmatrix}\{\dot{u}\}_1\\ \{\dot{u}\}_2\end{Bmatrix}\\
&+\begin{bmatrix}[k]_{11} & [k]_{12}\\ [k]_{21} & [k]_{22}\end{bmatrix}\begin{Bmatrix}\{u\}_1\\ \{u\}_2\end{Bmatrix} + \begin{bmatrix}[k^*]_{11} & [k^*]_{12}\\ [k^*]_{21} & [k^*]_{22}\end{bmatrix}\begin{Bmatrix}\{u\}_1\\ \{u\}_2\end{Bmatrix} = \begin{Bmatrix}\{Q\}_1\\ \{Q\}_2\end{Bmatrix}
\end{aligned} \tag{63}$$

where $\{u\}_1$ is the vector of D_s node translational displacements associated with inertia forces and M_s node rotations for which there correspond equivalent node moments from moving masses. The vector consists of $(D_s + M_s)$ rows.

$\{u\}_2$ is the vector of those node rotations for which no corresponding equivalent node moments exist from moving masses. This vector consists of $(N_s - D_s - M_s)$ rows.

and where other vectors and submatrices are defined in accordance with $\{u\}_1$ and $\{u\}_2$. From this definition it follows that

$$[m^*]_{mn} = [d^*]_{mn} = [k^*]_{mn} = [0] \text{ except when } m=n=1 \tag{64}$$

With Eq. (64), Eq. (63) yields

$$\left([m]_{11} + [m^*]_{11}\right)\{\ddot{u}\}_1 + [d^*]_{11}\{\dot{u}\}_1 + \left([k]_{11} + [k^*]_{11}\right)\{u\}_1 + [k]_{12}\{u\}_2 = \{Q\}_1 \tag{65}$$

and

$$[k]_{21}\{u\}_1 + [k]_{22}\{u\}_2 = \{Q\}_2 \tag{66}$$

From the latter equation

$$\{u\}_2 = [k]_{22}^{-1}\left(\{Q\}_2 - [k]_{21}\{u\}_1\right) \tag{67}$$

Substitution of Eq. (67) into Eq. (65) gives

$$[M]_{11}\{\ddot{u}\}_1 + [D]_{11}\{\dot{u}\}_1 + [K']_{11}\{u\}_1 = \{Q'\}_1 \tag{68}$$

where $[M]_{11} = [m^*]_{11} + [m]_{11}$ (68a)

$$[D]_{11} = [d^*]_{11} \tag{68b}$$

$$[K']_{11} = [k^*]_{11} + [k]_{11} - [k]_{12}[k]_{22}^{-1}[k]_{21} \tag{68c}$$

$$\{Q'\}_1 = \{Q\}_1 - [k]_{12}[k]_{22}^{-1}\{Q\}_2 \tag{68d}$$

Thus the set of equations of motion (24) has been reduced in number to $(D_s + M_s)$, as given by Eq. (68), where M_s may vary with time.

Consider first a time interval between times t_n and t_{n+1} such that none of the moving masses on the structure crosses from one element to another during this interval. Hence, for such an interval,

the solution of Eqs. (68) proceeds in the same manner as that for Eqs. (24). Thus it follows that

$$\left[E\right]\left\{\ddot{u}_1\right\}_{n+1} = \left\{G\right\} \tag{69}$$

where $\left[E\right] = \left[M\right]_{11} + \frac{h}{2}\left[D\right]_{11} + \frac{h^2}{6}\left[K'\right]_{11}$ (69a)

$$\left\{G\right\} = \left\{Q_1'\right\}_{n+1} - \left[D\right]_{11}\left(\left\{\dot{u}_1\right\}_n + \frac{h}{2}\left\{\ddot{u}_1\right\}_n \right)$$

$$- \left[K'\right]_{11}\left(\left\{u_1\right\}_n + h\left\{\dot{u}_1\right\}_n + \frac{h^2}{3}\left\{\ddot{u}_1\right\}_n \right) \tag{69b}$$

In Eqs. (69), (69a) and (69b), the subscripts of Q', u and its derivatives have been moved inside the brackets only for clarity. The node accelerations at the end of the time interval considered are found from Eq. (69), and the corresponding displacements and velocities are determined as in previous cases.

Consider next a time interval between times t_n and t_{n+1} such that one or more of the moving masses on the structure does cross from one element to another during this interval. For such a time interval the numerical integration technique must proceed somewhat differently from the previous case because $\left\{u\right\}_1$ with its derivatives at time t_n and $\left\{u\right\}_1$ with its derivatives at time t_{n+1} do not refer to the same degrees of freedom. However, this poses no difficulties since the displacements, velocities, and accelerations corresponding to all possible degrees of freedom can be determined for time t_n, the beginning of the time interval, before proceeding to solve for node

accelerations at time t_{n+1}. Knowing all the node displacements, along with the node velocities $\{ \dot{u} \}_1$ and the node accelerations $\{ \ddot{u} \}_1$ at time t_n, the remaining node velocities and accelerations at time t_n can be found by differentiating Eq. (67). It should be noted that since the equivalent node forces have been assumed to remain constant over any one time interval,

$$\{ \ddot{Q}_2 \}_n = \{ 0 \} \tag{70}$$

and

$$\{ \dot{Q}_2 \}_n = \frac{1}{h} \left(\{ Q_2 \}_{n+1} - \{ Q_2 \}_n \right) \tag{71}$$

Since all the node displacements, velocities and accelerations are thus determined for time t_n, the right side of Eq. (69b) is known. Hence the numerical integration can proceed to time t_{n+1} to find the node accelerations by Eq. (69), and the corresponding displacements and velocities as previously described.

When the reduced number of equations represented by expression (68) is solved by the linear acceleration method, matrix $[E]$ must be inverted at each time interval. Moreover, the structure stiffness matrix must be partitioned anew for each time interval during which a moving mass crosses over from one element to another. For such a time interval the matrix $[k]_{22}$ as well as the matrix $[E]$ must be inverted.

NUMERICAL RESULTS

Numerical problems have been solved for plates and cylindrical shells subjected to dynamic loadings in order to demonstrate the feasibility of the analytical procedure. It was not intended to make a general study of the effects of the various parameters on the behavior of plates and cylindrical shells. All numerical results presented have been obtained through use of the CDC 6600 digital computer located at New York University.

A. Plate

1. General

Numerical results are presented here for square and rectangular plates, either with simply supported or clamped boundaries. The loads considered include impact, moving force, and moving mass loads. Also, two problems have been solved for continuous plates with a moving load. In all cases, the plate material has been assumed to weigh 495 lbs./cu. ft., and to have a modulus of elasticity of 30,000 ksi and a Poisson's ratio of 0.30. The weight of the plate has been neglected except for calculation of the mass parameters.

Because of the availability of only a very limited number of numerical results for static plate solutions using the Yettram and Husain[18] framework analogy, the results of some studies are presented in what follows to illustrate the accuracy of the use of a finite element approach to obtain static plate deflections. A simply supported 60.0" square plate of 0.25" thickness

was subjected to a 1.0^{K} central load. In Table 1, deflections obtained by Navier[39] solution are compared with those obtained by using Yettram and Husain[18] framework analogy with various grid sizes. Deflections are compared for the center of the plate, and for a point equidistant from the center and the corner of the plate, referred to as the quarter point. In Table 2, similar comparisons are made for a clamped plate of the same dimensions and with the same load. Here, however, the comparison is made with Timoshenko's solution by superposition as extended by Young[40]. From the comparison in Table 1, it is seen that Yettram and Husain's method with a 6x6 grid yields a center deflection for the simply supported plate which differs only 1.1% from the Navier solution. For the clamped plate, the corresponding deviation from Timoshenko-Young solution is even less.

It will be seen subsequently that also under dynamic loadings, in general, the improvement in the accuracy obtained for plate deflections is small as the grid size is made finer, thereby justifying the use of a relatively coarse grid. However, it should be noted that in case the plate forces and stresses are to be calculated, a relatively finer grid may have to be adopted.

In all subsequent problems for plates subjected to impact loads or to moving forces, as well as in the calculation of natural frequencies, the rotary inertia effects of the structure have been neglected. In calculating the response of plates to moving masses, however, these effects have been

TABLE 1

Deflections of a Simply Supported Plate (in.)

	Deflection at Center	Deflection at Quarter Point
6x6 Grid	0.9750	-
8x8 Grid	0.9741	0.4004
10x10 Grid	0.9737	-
12x12 Grid	0.9735	0.4000
14x14 Grid	0.9733	-
Navier	0.9644	0.3998

TABLE 2

Deflections of a Clamped Plate (in.)

	Deflection at Center	Deflection at Quarter Point
6x6 Grid	0.4738	-
8x8 Grid	0.4721	0.1033
10x10 Grid	0.4715	-
12x12 Grid	0.4712	0.1029
14x14 Grid	0.4711	-
Timoshenko-Young	0.469	0.103

included. For all problems, the mass matrix has been calculated by the direct lumping procedure explained in the Appendix.

2. Impact Loads

The simply supported plate shown on Fig. 9 was subjected at its center to the impact load indicated on that figure, applied normal to the plate. At first, a 6x6 grid was used, resulting in a total of 36 square elements for the plate. For such a finite element structure, the fundamental natural period is 0.0120 seconds, and the smallest natural period is 0.833×10^{-3} seconds. The response curves for the center deflection, along with the static deflection curve, are shown on Fig. 9 for two time intervals h. The time interval of 0.25×10^{-3} seconds corresponds to $0.30\ T_s$, where T_s is the shortest natural period, while the time interval of 0.10×10^{-2} seconds corresponds to $1.2\ T_s$. The response curve for a time interval of 0.10×10^{-3} seconds is almost identical to the one for 0.25×10^{-3} seconds on Fig. 9. Because of graphical difficulties, this curve is not shown on the figure. The response curves for the deflections at all other nodes indicated a smaller variation with the three time intervals used than did the center node.

For the same plate and loading, on Fig. 10 is shown a comparison of the response curves for the center deflection with two grid sizes, with a time interval of 0.25×10^{-3} seconds being used for both curves. It is seen that for practical purposes, the maximum deflections for a 12x12 grid are the same as those for a 6x6 grid, although the two curves are out of phase at times.

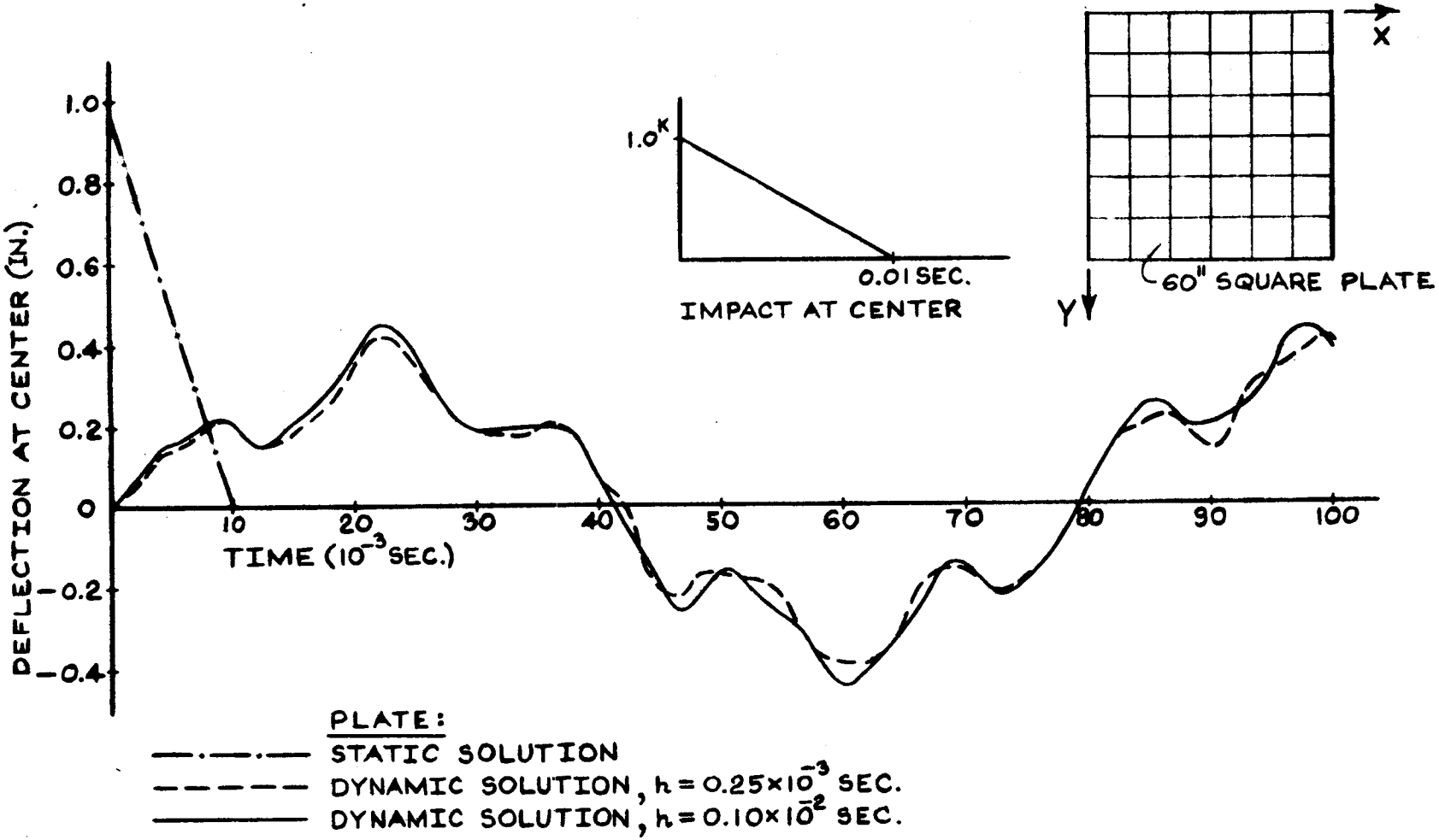

FIG. 9 – DEFLECTION OF CENTER NODE DUE TO IMPACT AT CENTER FOR TWO TIME INTERVALS OF INTEGRATION

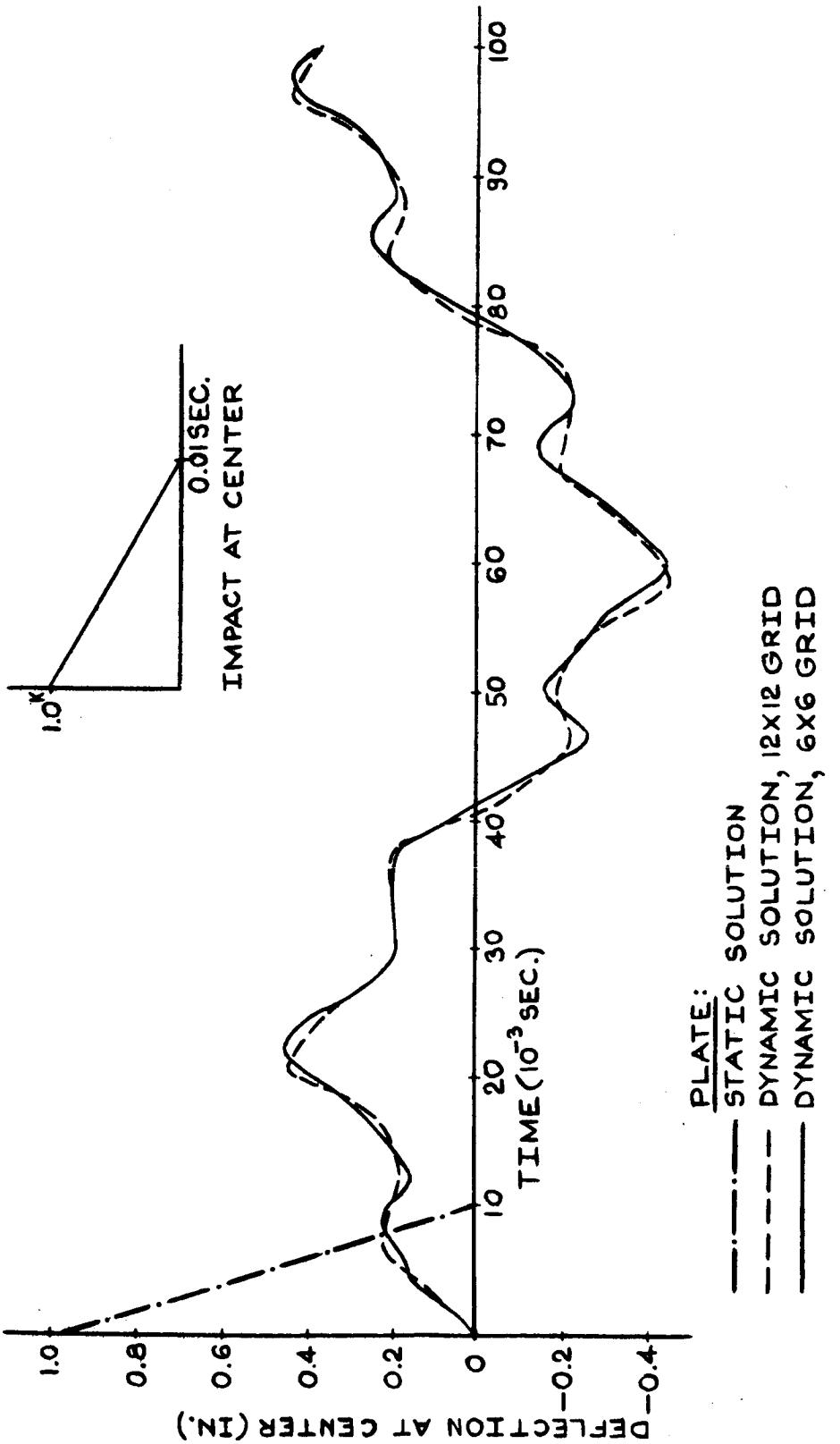

FIG. 10 – DEFLECTION OF CENTER NODE DUE TO IMPACT AT CENTER FOR TWO GRID SIZES

3. Moving Forces

The response of a square and a rectangular plate subjected to one or more loads, moving with various velocities and along different paths on the plate, has been investigated. Both simply supported and clamped boundaries have been used for these plates. The dimensions of the two plates are shown on Fig. 11. Unless otherwise noted, a 6x6 grid was used in the analysis of each of these plates, as indicated on Fig. 11. The smallest and largest natural periods for the resulting finite element structures are given on the figure.

The response curves for node deflections of the plates of Fig. 11, subjected to various moving loads, are shown on Figs. 12 through 21. The loading conditions, as well as the response curve for the deflection of the center, i.e. node 25 (See Fig. 11.), are presented on the figures. For one case, an additional response curve for the deflection of node 9 (See Fig. 11.) is given. In each case, a static deflection curve is shown for comparison. It is of interest to note that the static deflection curve shown on Fig. 13, obtained by the finite element solution, coincides with the corresponding curve obtained by the more exact Navier solution[39].

Fig. 12 shows the response curves of the deflection of node 25 for a single load moving along the centerline of the simply supported square plate at velocities of 200, 400 and 600 in./sec. For velocity of 600 in./sec., the problem was solved by using time intervals, h, of $0.25\text{x}10^{-3}$, $0.50\text{x}10^{-3}$, and $1.00\text{x}10^{-3}$ seconds. For all of these time intervals, the response curves coincide and are thus shown as a single curve on Fig. 12. Since a

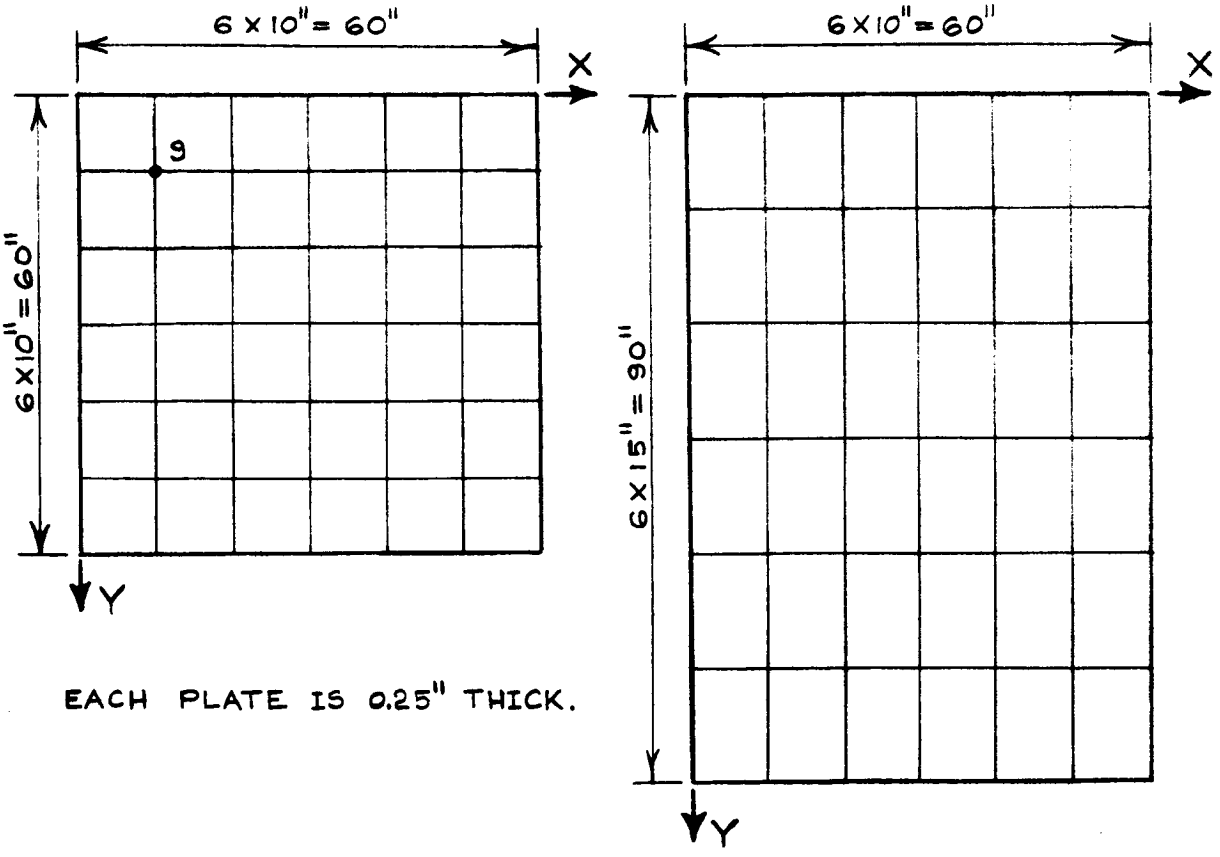

EACH PLATE IS 0.25" THICK.

	GREATEST PERIOD	SMALLEST PERIOD
SQUARE PLATE:		
SIMPLY SUPPORTED	0.120×10^{-1} SEC.	0.833×10^{-3} SEC.
CLAMPED	0.661×10^{-2} SEC.	0.826×10^{-3} SEC.
RECTANGULAR PLATE:		
SIMPLY SUPPORTED	0.166×10^{-1} SEC.	0.106×10^{-2} SEC.
CLAMPED	0.880×10^{-2} SEC.	0.102×10^{-2} SEC.

FIG. 11 - A SQUARE AND A RECTANGULAR PLATE

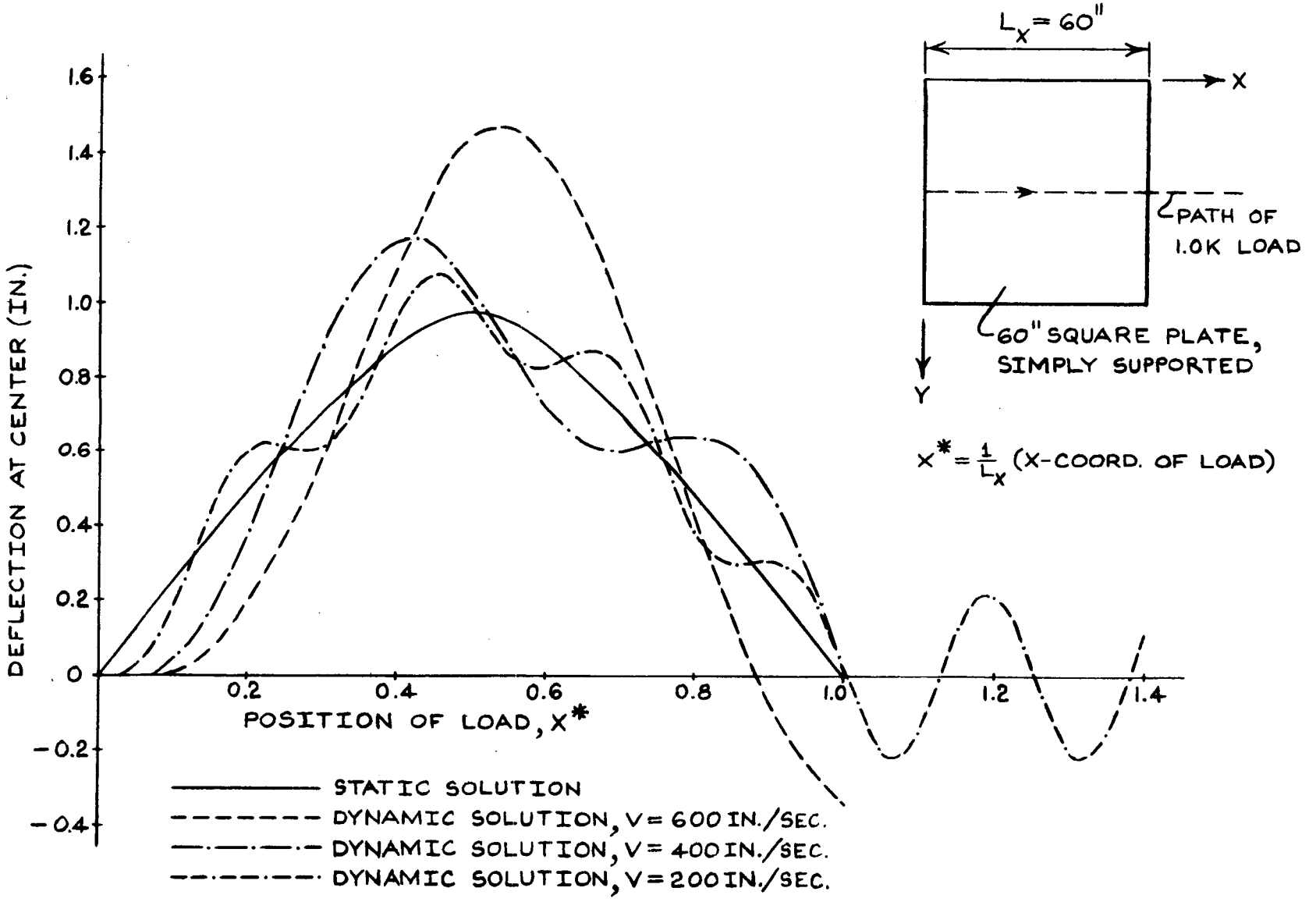

FIG. 12 – DEFLECTION OF CENTER NODE OF A SIMPLY SUPPORTED SQUARE PLATE DUE TO A SINGLE LOAD MOVING WITH VARIOUS VELOCITIES ALONG THE CENTERLINE

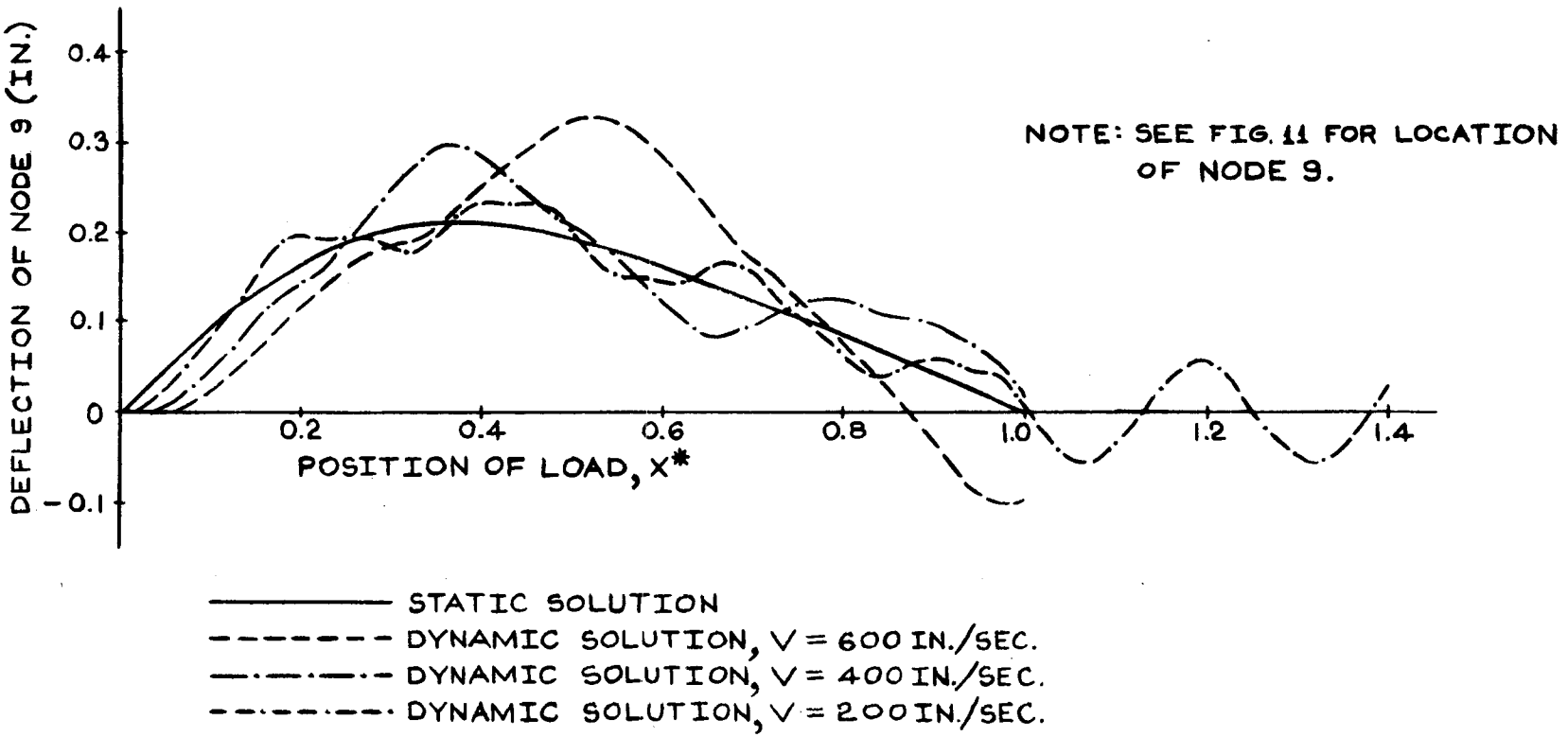

FIG. 13 - DEFLECTION OF NODE 9 OF A SIMPLY SUPPORTED SQUARE PLATE DUE TO A SINGLE LOAD MOVING WITH VARIOUS VELOCITIES ALONG THE CENTERLINE

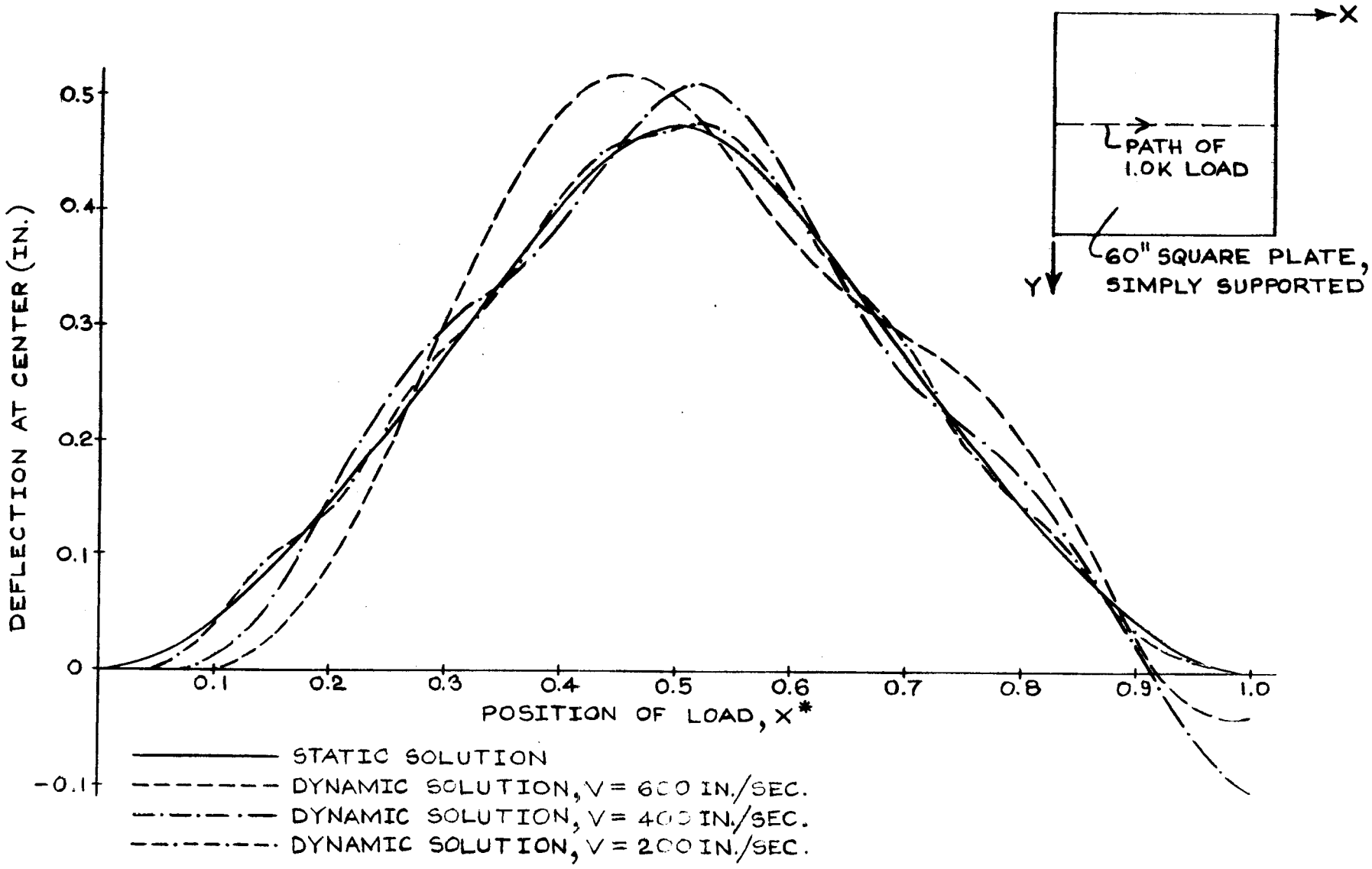

FIG. 14 - DEFLECTION OF CENTER NODE OF A CLAMPED SQUARE PLATE DUE TO A SINGLE LOAD MOVING WITH VARIOUS VELOCITIES ALONG THE CENTERLINE

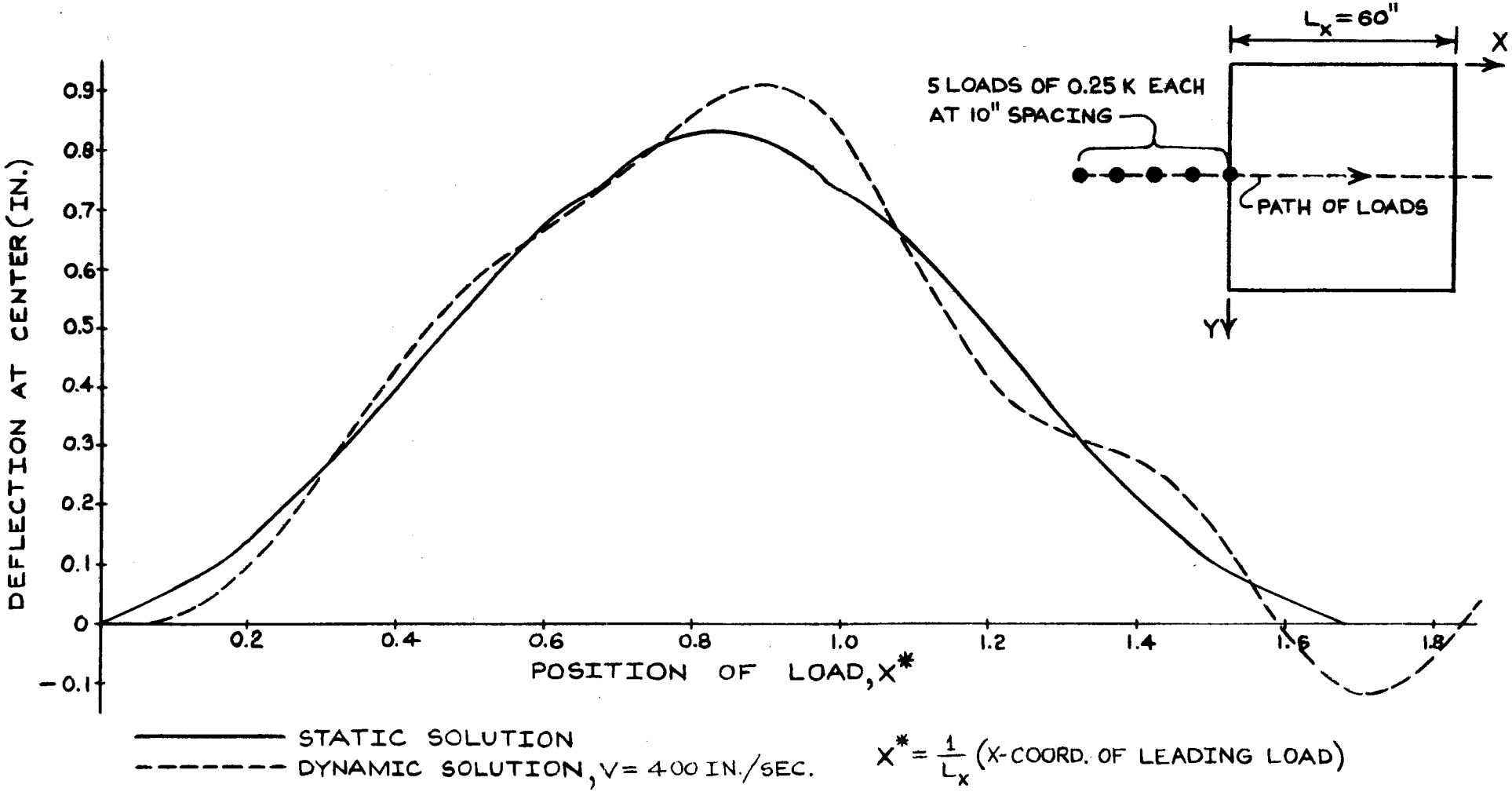

FIG. 15 - DEFLECTION OF CENTER NODE OF A SIMPLY SUPPORTED SQUARE PLATE DUE TO FIVE LOADS MOVING ALONG THE CENTERLINE

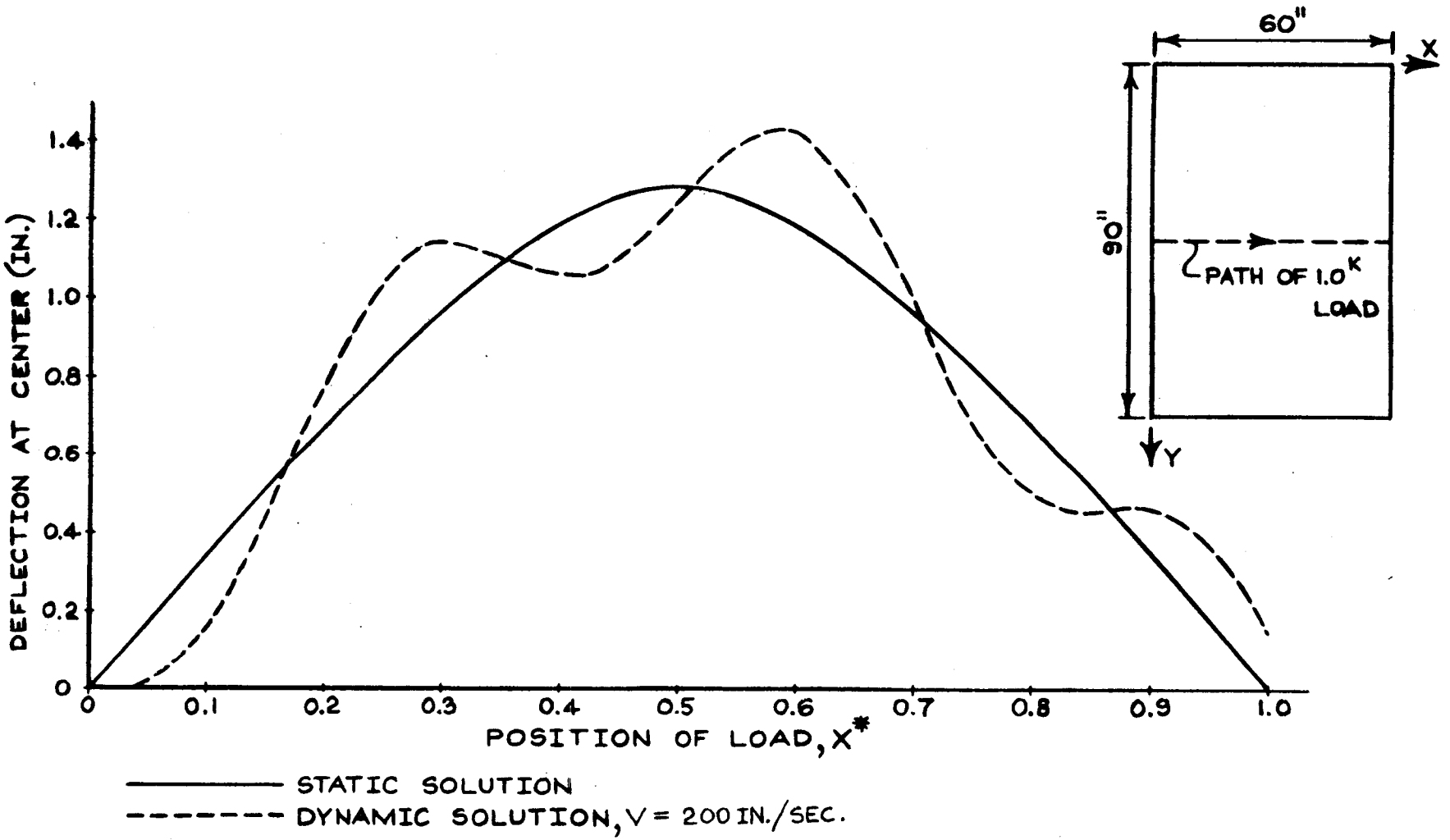

FIG. 16- DEFLECTION OF CENTER NODE OF A SIMPLY SUPPORTED RECTANGULAR PLATE DUE TO A LOAD MOVING ALONG A CENTERLINE

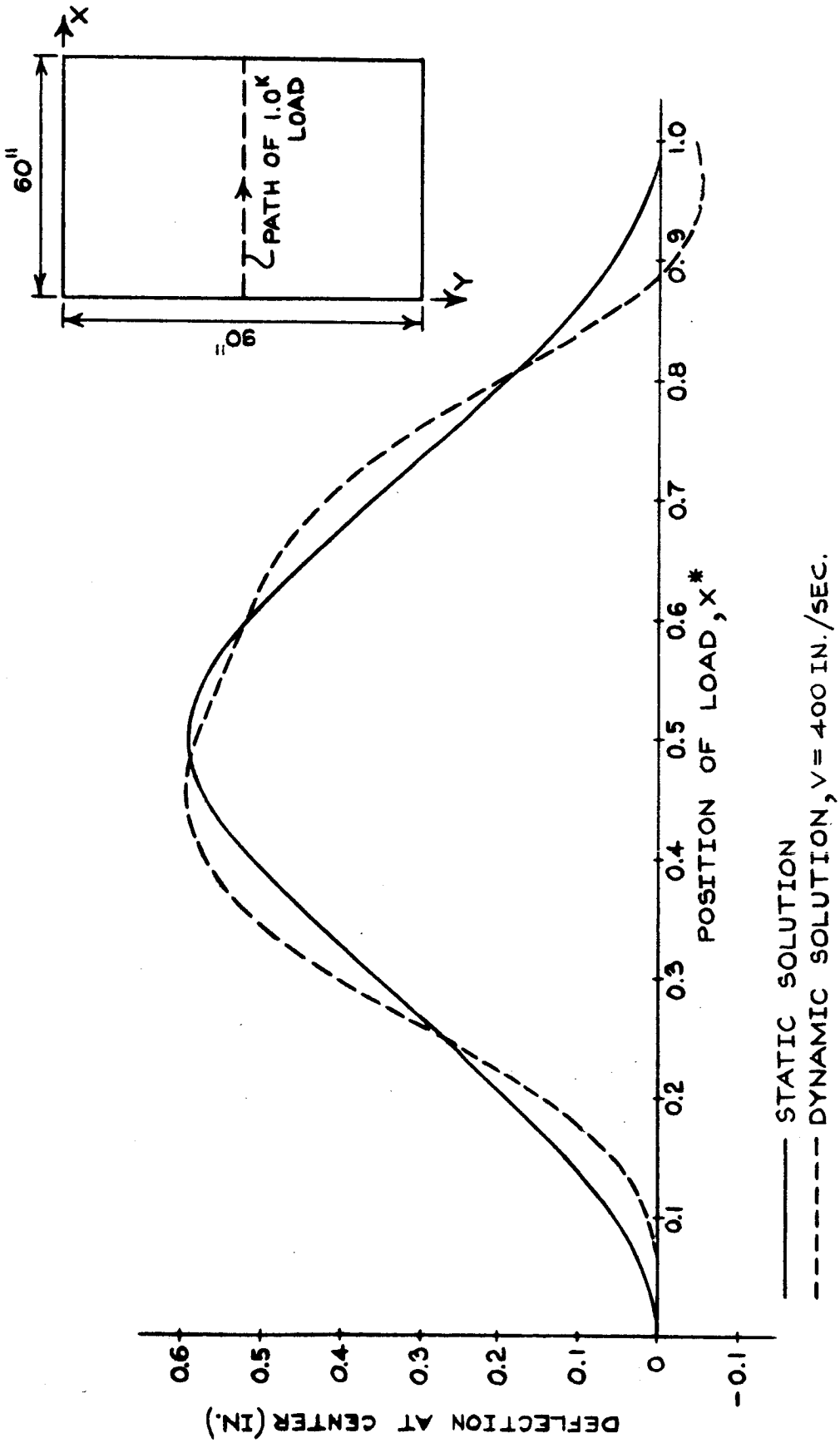

FIG. 17 - DEFLECTION OF CENTER NODE OF A CLAMPED RECTANGULAR PLATE DUE TO A LOAD MOVING ALONG A CENTERLINE

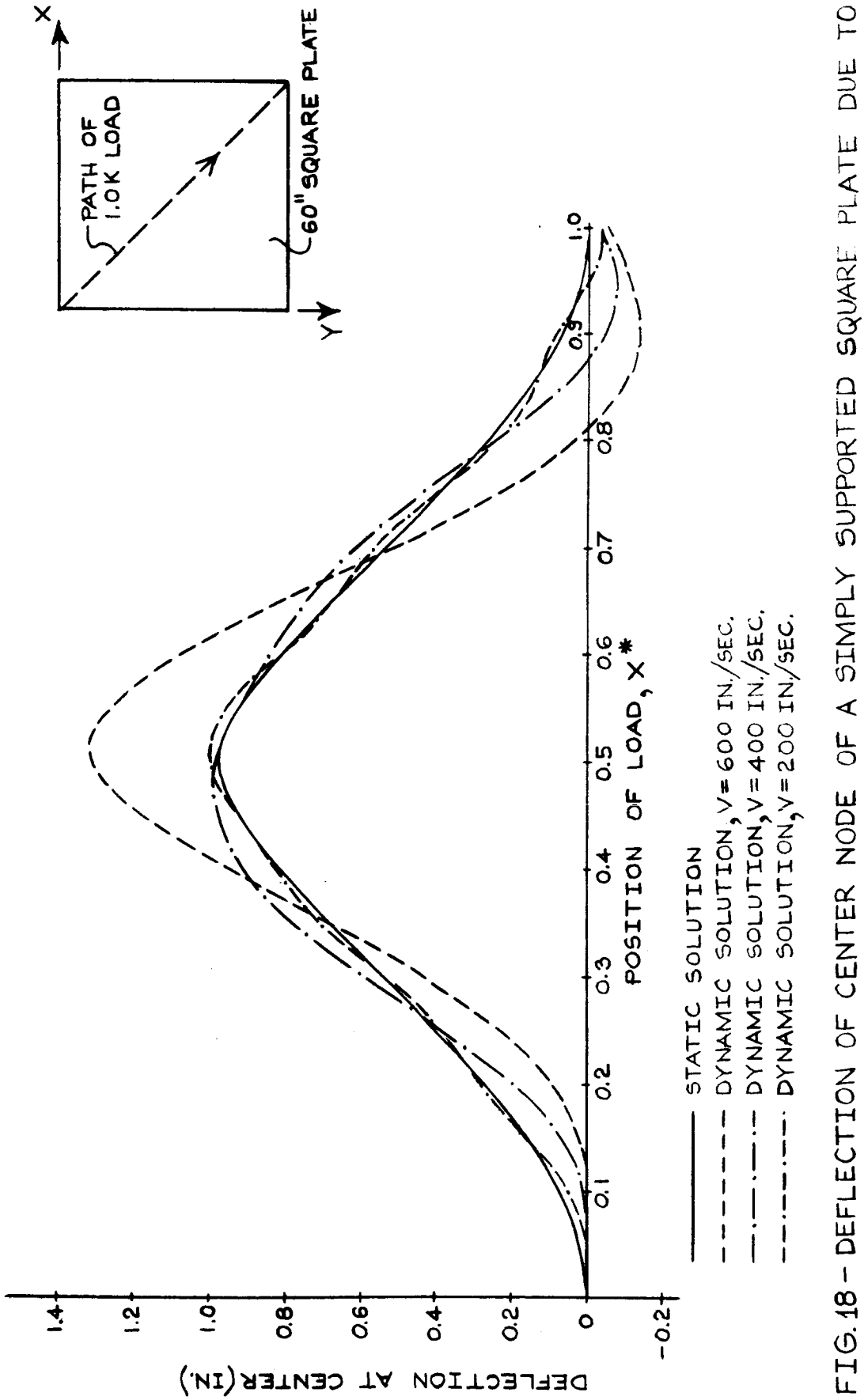

FIG. 18 - DEFLECTION OF CENTER NODE OF A SIMPLY SUPPORTED SQUARE PLATE DUE TO A LOAD TRAVERSING THE PLATE DIAGONALLY

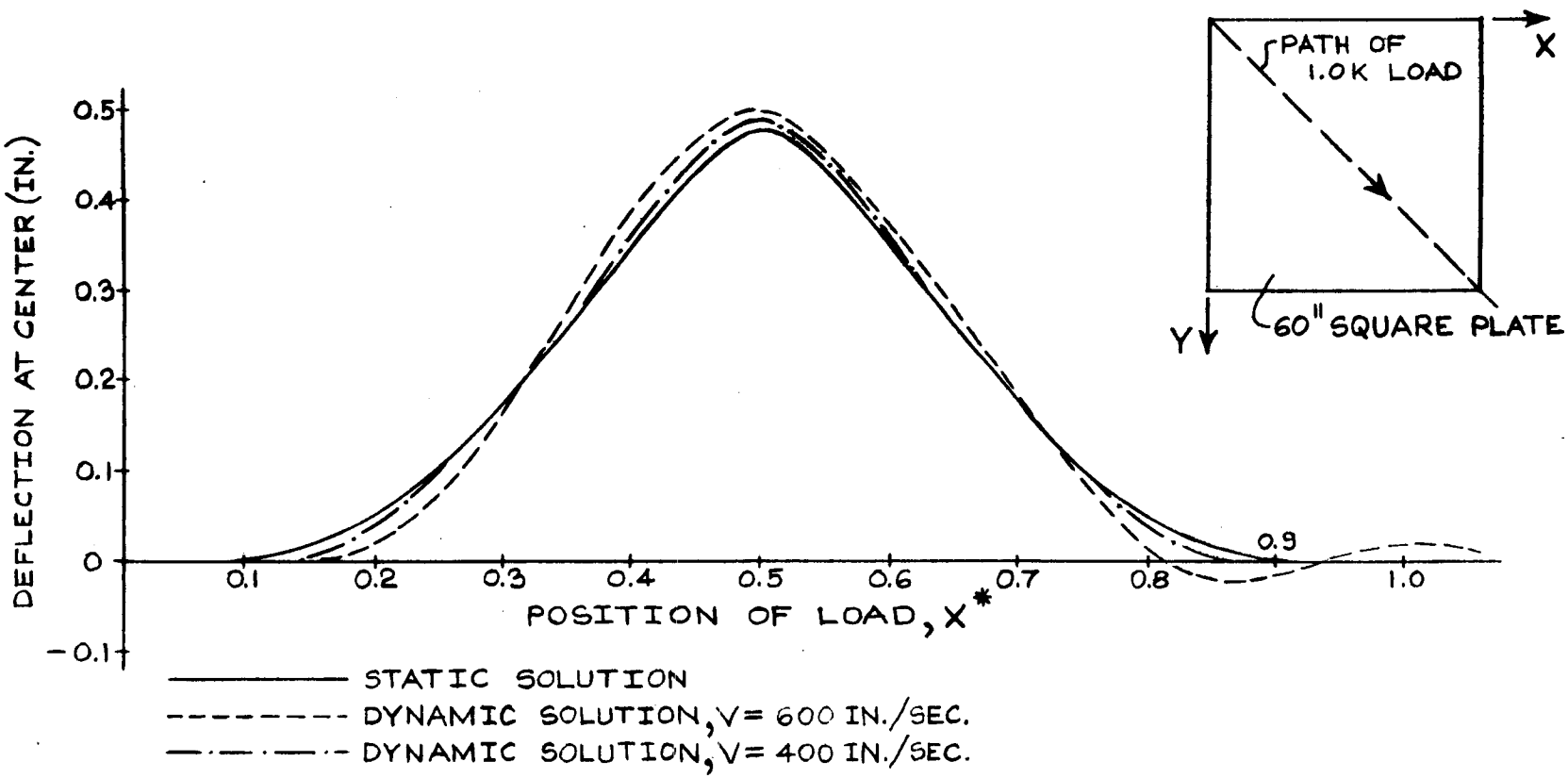

FIG. 19 - DEFLECTION OF CENTER NODE OF A CLAMPED SQUARE PLATE DUE TO A LOAD TRAVERSING THE PLATE DIAGONALLY

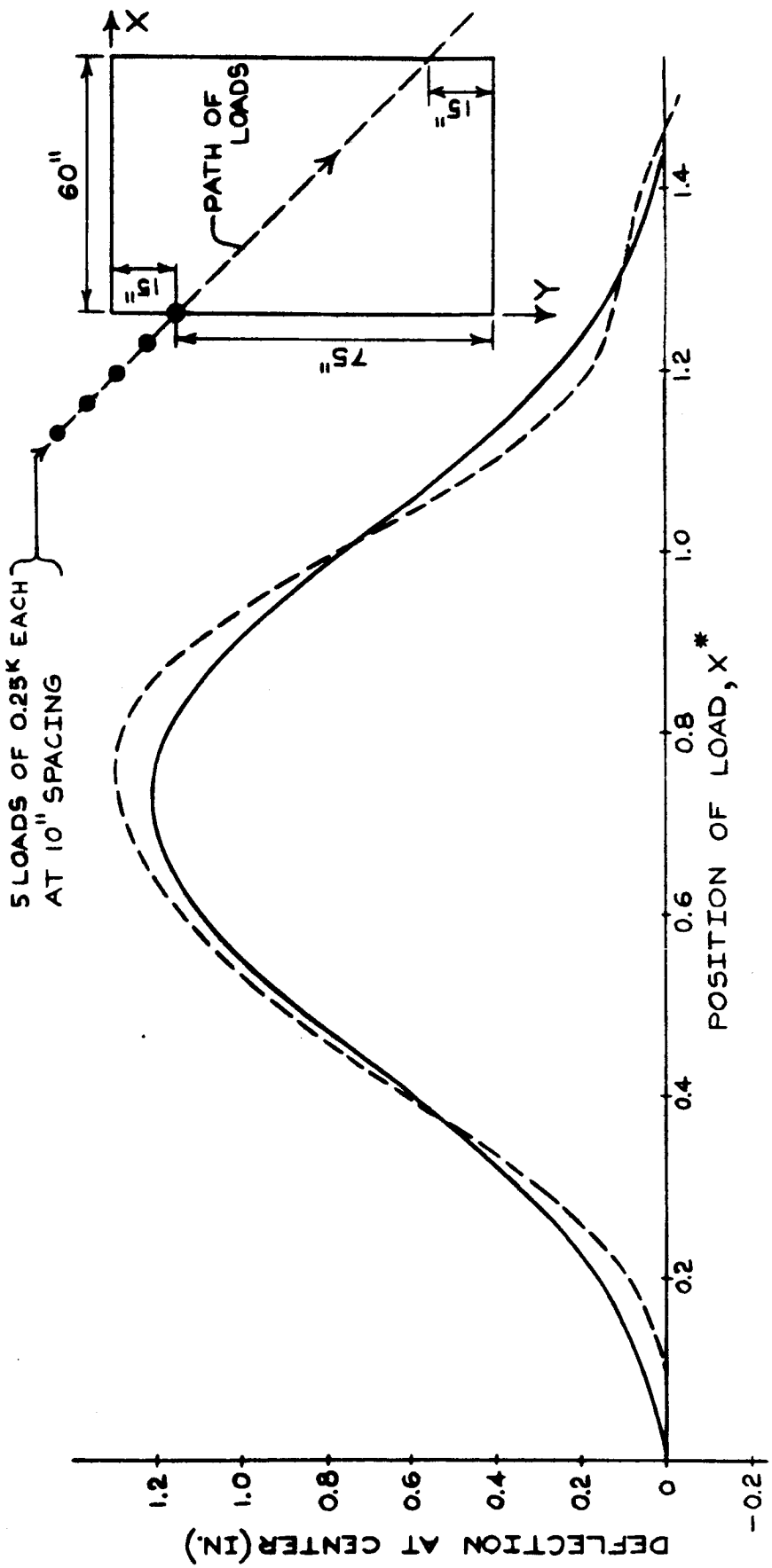

FIG. 20 – DEFLECTION OF CENTER NODE OF A SIMPLY SUPPORTED RECTANGULAR PLATE DUE TO FIVE LOADS TRAVERSING THE PLATE AT AN OBLIQUE ANGLE

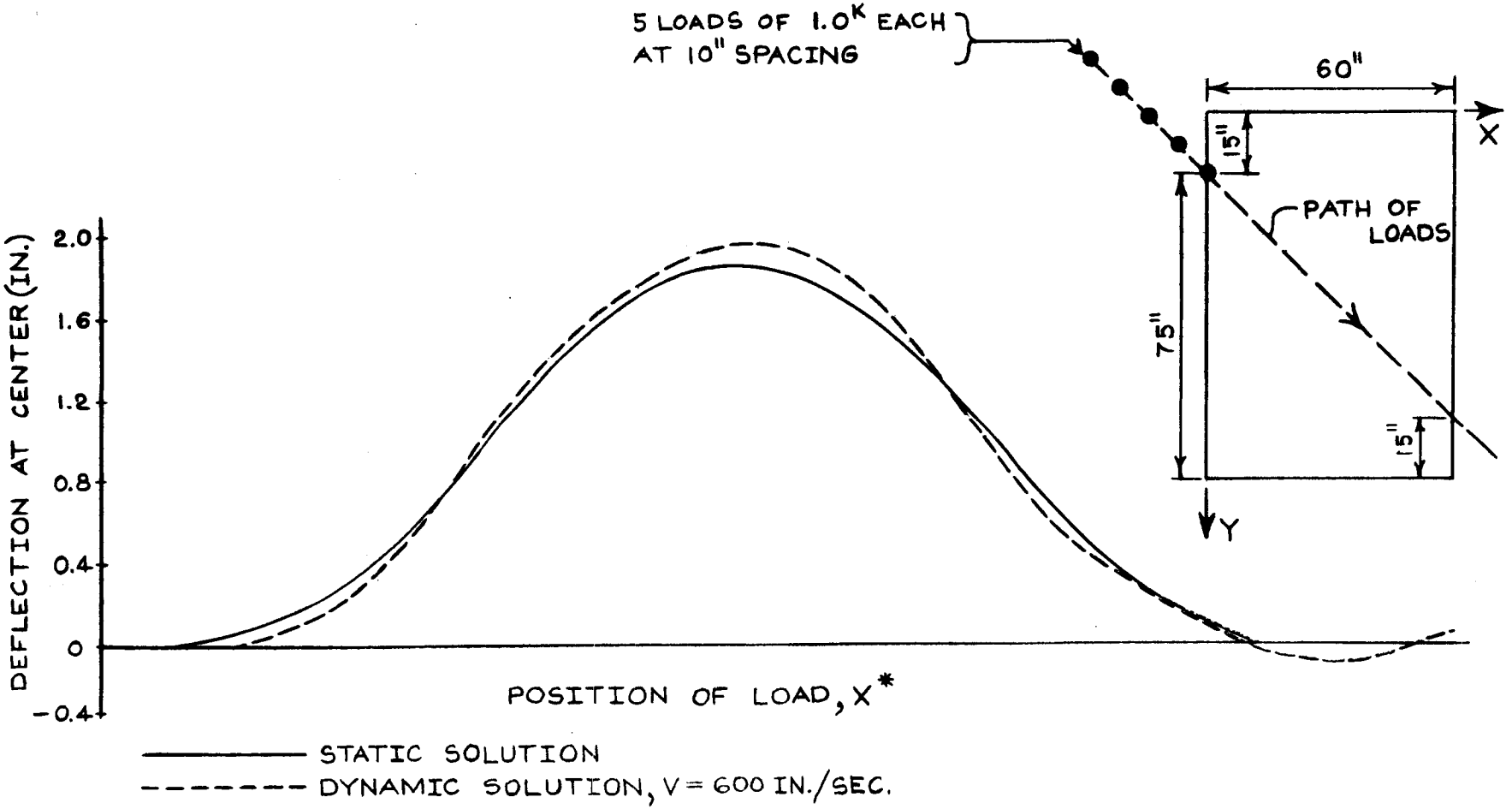

FIG. 21 - DEFLECTION OF CENTER NODE OF A CLAMPED RECTANGULAR PLATE DUE TO FIVE LOADS TRAVERSING THE PLATE AT AN OBLIQUE ANGLE

time interval of 1.00×10^{-3} seconds yields the same results as the smaller time interval, it may be concluded that a time interval even larger than this could be used to obtain approximations to the response curve in question. In subsequent problems, rather than find empirically the maximum time interval permissible for sufficient accuracy in each case, a time interval is used that is sufficiently small to avoid divergence. Thus in subsequent problems in this section, for convenience a time interval of 0.50×10^{-3} seconds is adopted for the simply supported plates, and 0.25×10^{-3} seconds is used for the stiffer, clamped plates.

From Fig. 12 it is seen that the maximum dynamic deflection occurs for the highest velocity, 600 in./sec. This is also true for node 9, for which the response curves are shown on Fig. 13, as well as for all other nodes, for which the response curves are not presented here. Inspection of Figs. 14, 18 and 19 indicates that in all cases, the maximum dynamic deflection occurs when the load is moving with the highest velocity. However, it would not be correct to conclude that the maximum dynamic deflection is always greater with higher velocities of the moving load, although this is usually the case. For example, on Fig. 18, the maximum dynamic deflection for velocity of 200 in./sec. is slightly greater than for velocity of 400 in./sec. However, from the response curves of Figs. 12, 13, 14, 18 and 19, it is seen that the amplitudes of the oscillations of a dynamic curve about the static curve, measured from the latter curve, are in general greater for greater velocities for a particular plate.

It is of interest to note from Fig. 12 that, for velocity of 200 in./sec., after the load leaves the plate the center node keeps vibrating at approximately the same frequency with which it vibrated about the static position when the load was on the plate.

Fig. 14 shows the response curves for the center deflection of the square plate with clamped boundaries and with the loadings used for the simply supported plate of Fig. 12. Comparison of the response curves of Figs. 12 and 14 indicates that for a given velocity the dynamic deflections deviate from the static deflections much less for the stiffer structure, i.e., for the fixed plate.

The fixed plate shown on Fig. 14 was also analysed for the case of a single load moving at velocity of 200 in./sec., along the path indicated on the figure, and using a 12x12 grid. The response curve for the deflection of the center node of the plate in this case coincides identically with the case when a 6x6 grid was used. Thus the response curve for velocity of 200 in./sec. shown on Fig. 14 is identical for the two grid sizes used, justifying the validity of the coarser grid.

On Fig. 15 is shown the response curve for the center deflection of the simply supported square plate subjected to five loads of 0.25^{K} each moving along the centerline of the plate at equal velocities at 400 in./sec., as shown on the figure. It is seen from this figure that the maximum dynamic deflection occurs shortly after the center load has crossed the center of the plate. It is also interesting to note from this figure that the difference

between the dynamic and static deflections are appreciably greater when the loads are leaving the plate than they are when the loads are entering the plate. That is, the greatest differences in these curves occur at times after the maximum static deflection has been attained. This does not happen in the case of a single load of 1.0^K moving at the same velocity, as seen from Fig. 12.

On Figs. 16 and 17 are shown the response curves for the center deflection of a simply supported and a clamped rectangular plate, subjected to a single 1.0^K load moving along the centerline x = 45'' at velocities of 200 and 400 in./sec., respectively. Comparing the response curves for velocity of 200 in./sec. for the simply supported rectangular plate, as shown on Fig. 16, and for the same velocity for the square plate, as shown on Fig. 12, it is seen that the ratio of the maximum dynamic deflection to the maximum static deflection is almost identical in each case. This, however, is not the case for a velocity of 400 in./sec. for the corresponding clamped plate, as seen from Figs. 14 and 17.

It is of interest to note from Figs. 12 through 17 that the ratio of the average period of oscillation of the dynamic curve about the static curve to the fundamental period of the particular finite element plate structure does not vary greatly. This is not apparent at first glance from the response curves with the coordinate axes used. However, if the abscissa-axis is converted to time, it is seen that the ratio in question, for each of the curves on Figs. 12 through 17, is between approximately 6.2 and 6.9.

For a load moving across a plate in an arbitrary direction, however, this is not the case. For example, from the response curves on Figs. 18 and 19, for a load moving diagonally across the simply supported and clamped plates, respectively, the ratio referred to above may be seen to vary greatly for different velocities.

Comparing the response curves of Figs. 18 and 19 with the ones of Figs. 12 and 14, it is seen that for any particular velocity the maximum dynamic deflection is smaller for the case when the load moves diagonally across a plate than it is when the load crosses the plate along its centerline.

On Figs. 20 and 21 are shown the response curves for the center deflections of simply supported and clamped plates, respectively, subjected each to five loads traversing the plates at an arbitrary direction. In order to draw any general conclusions for plates subjected to an arbitrary number of loads moving along an arbitrary direction, as for the cases shown on Figs. 20 and 21, additional numerical studies would have to be made.

To illustrate the flexibility of the method presented in this report, two continuous plates, as shown on Figs. 22 and 24, are analyzed, each for a single load moving at a velocity of 400 in./sec. along the centerline of the plate across the two spans. By considering symmetry, the 12x6 grid used for the half-plate of Fig. 22 results in 176 degrees of freedom for the half of the structure considered. The central processing time used by the computer for this problem was 265.5 seconds. Using similarly a 12x3 grid for the half-plate of Fig. 24 results in 83 degrees of freedom for the

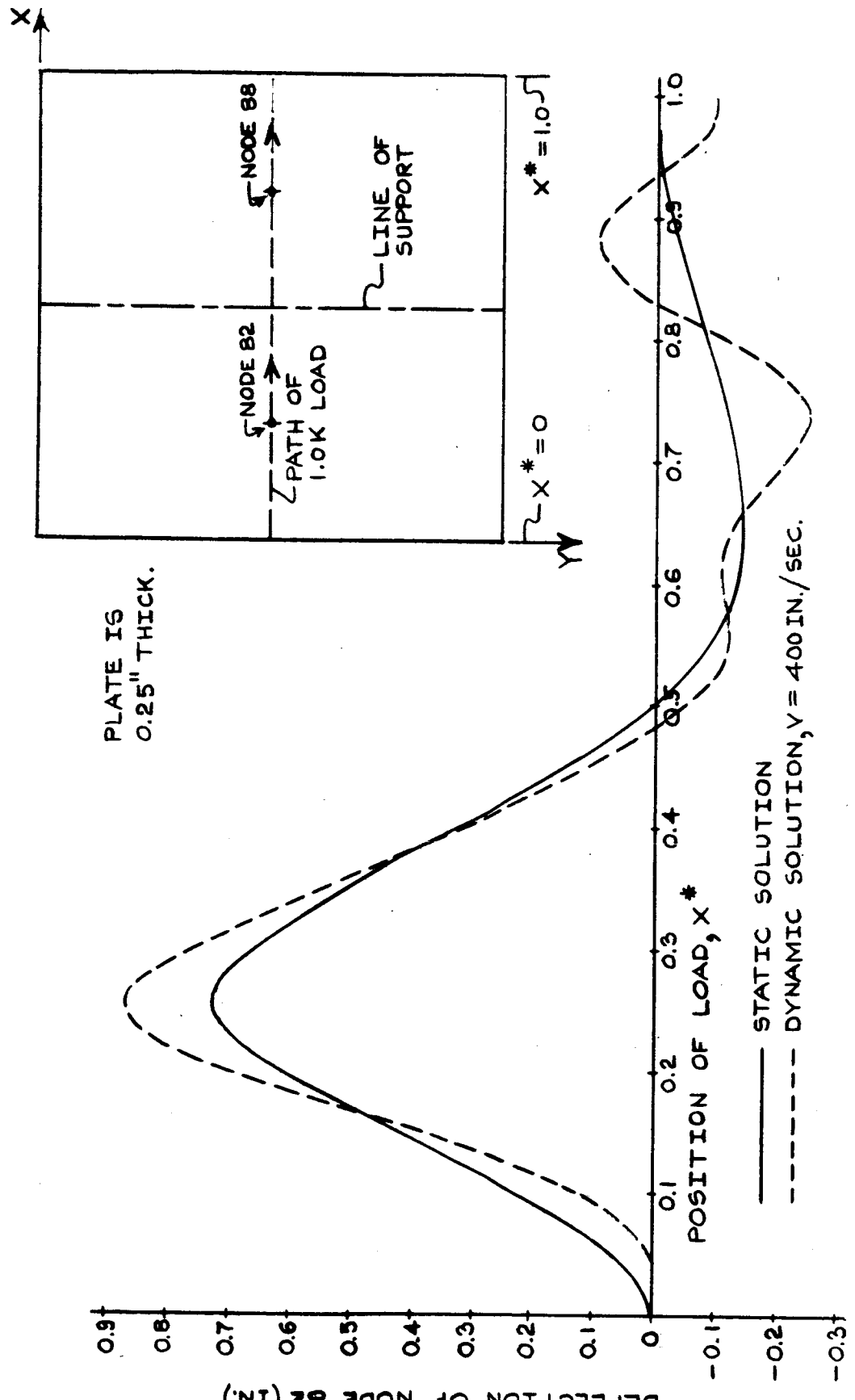

FIG. 22 – DEFLECTION OF NODE 82 OF CLAMPED CONTINUOUS PLATE OF 120"×120" OVERALL DIMENSIONS DUE TO A LOAD MOVING ALONG THE CENTERLINE

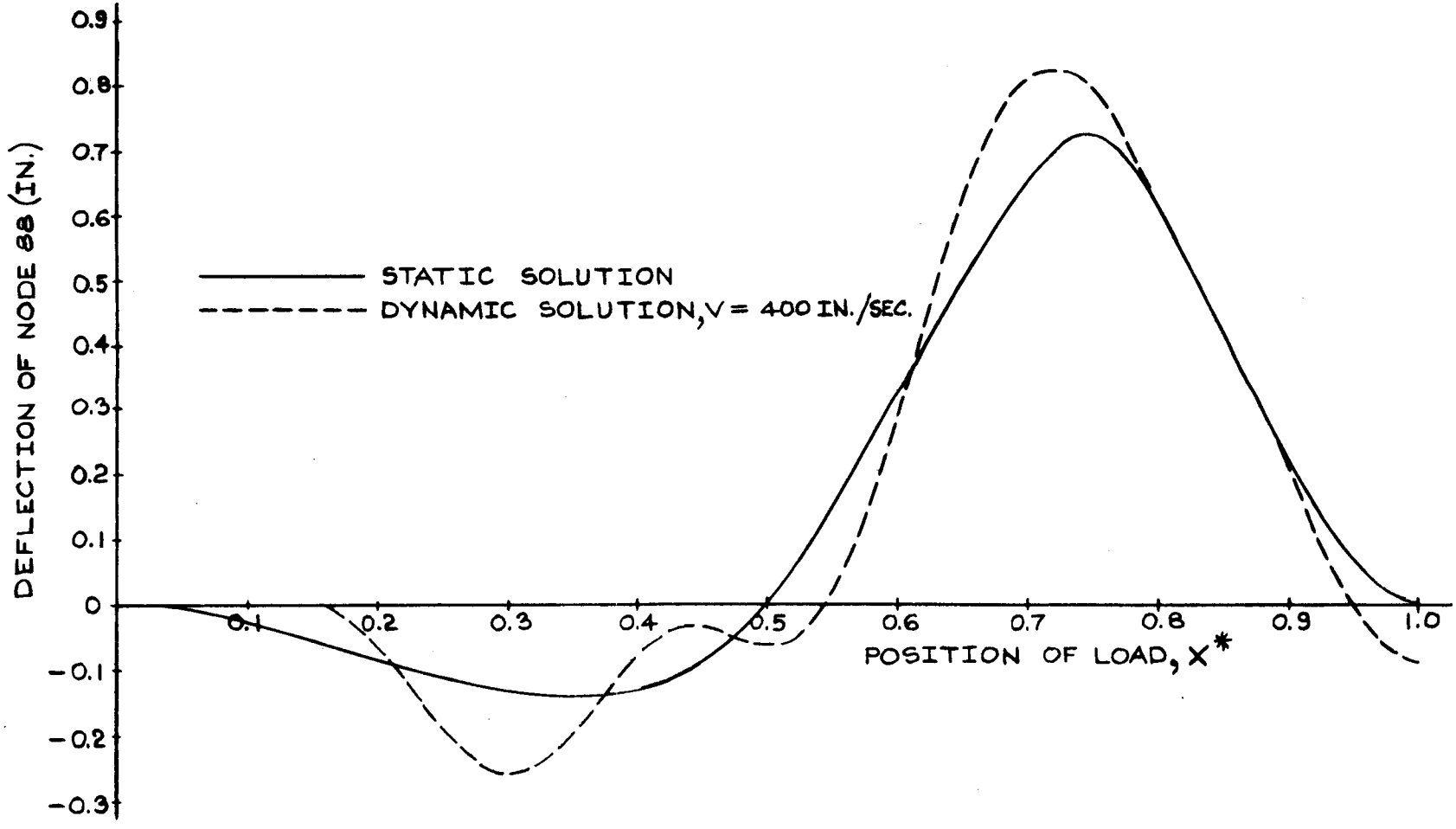

FIG. 23 – DEFLECTION OF NODE 88 OF CLAMPED CONTINUOUS PLATE OF 120"x120" OVERALL DIMENSIONS DUE TO A LOAD MOVING ALONG THE CENTERLINE

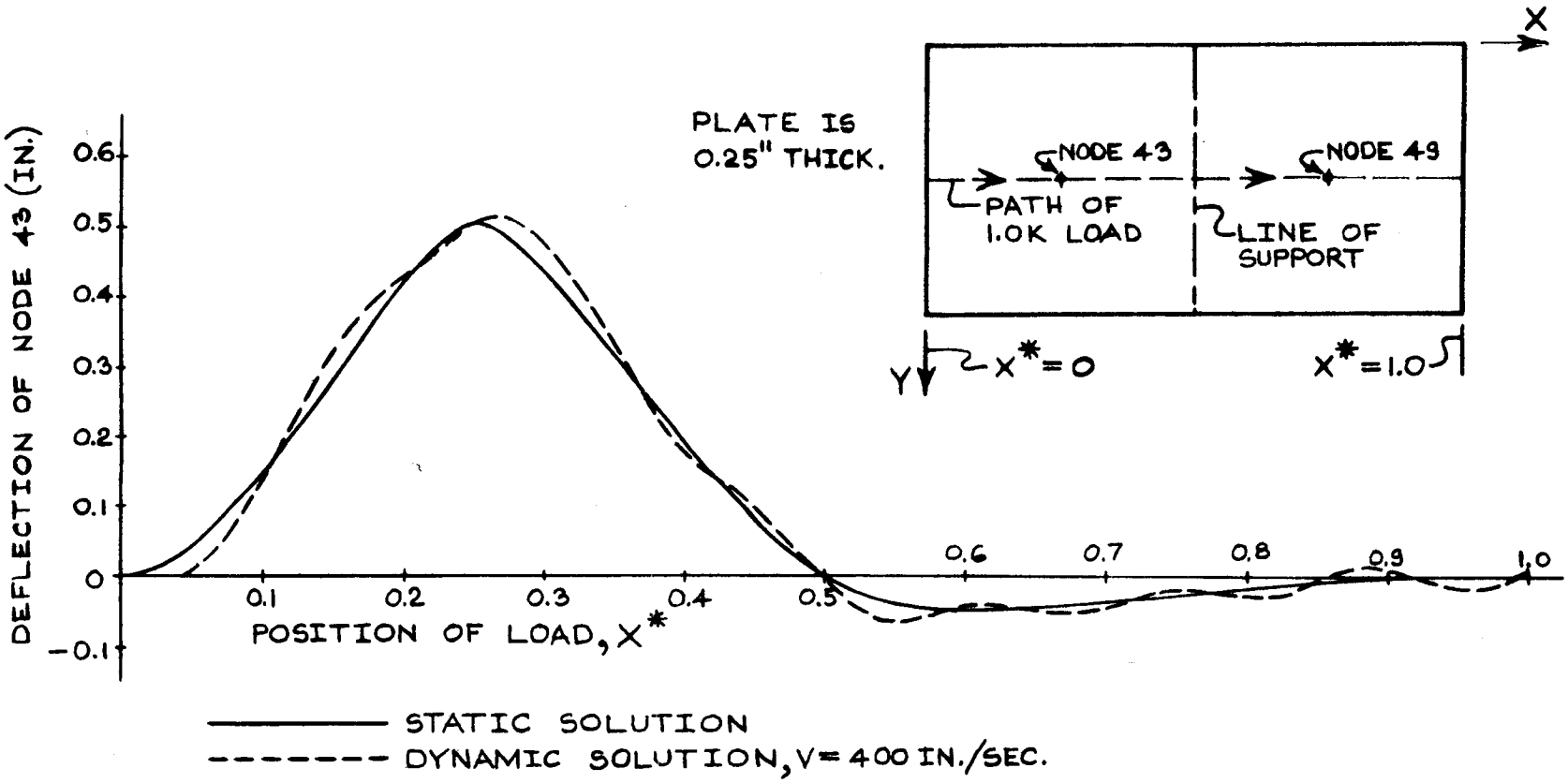

FIG. 24 - DEFLECTION OF NODE 43 OF CLAMPED CONTINUOUS PLATE OF 120"x60" OVERALL DIMENSIONS DUE TO A LOAD MOVING ALONG THE CENTERLINE

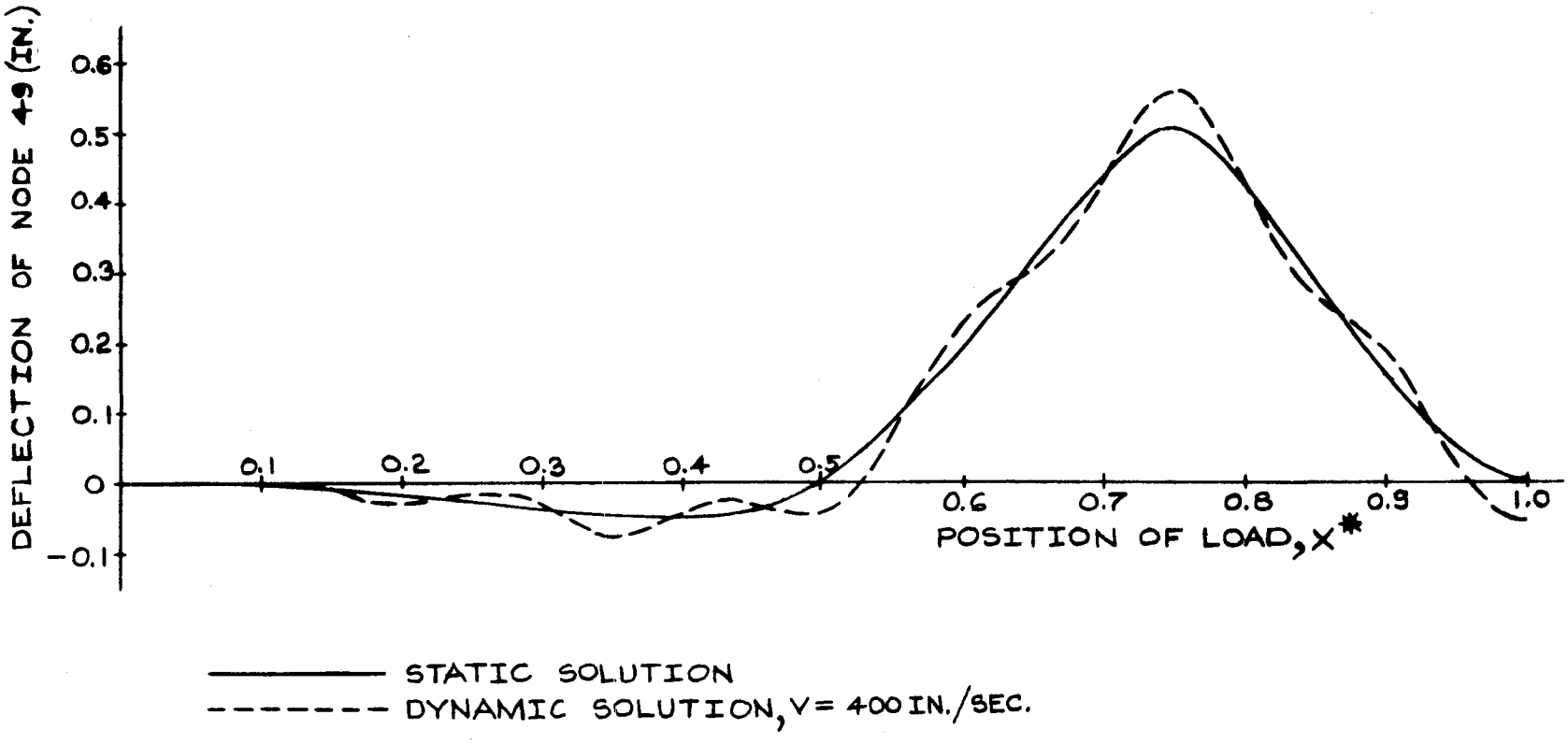

FIG. 25 - DEFLECTION OF NODE 49 OF CLAMPED CONTINUOUS PLATE OF 120"X 60" OVERALL DIMENSIONS DUE TO A LOAD MOVING ALONG THE CENTERLINE

half of that structure. In this case the central processing time used was 72.1 seconds. The computer times used by these two problems are by far the greatest for any of the problems considered thus far.

On Figs. 22 through 25 are presented the response curves for the deflection of the center node of each span of the two continuous plates. It can be seen from the response curves on Figs. 22 and 23 that the maximum dynamic deflection is greater for the center of the left-hand span than for the center of the other span, while, on the other hand, the reverse is true for the continuous plate of Fig. 24, as seen from the response curves on Figs. 24 and 25. This is perhaps explained by the fact that in the first case the vibration induced is of such frequency that the maximum dynamic deflection in the left-hand span occurs at almost the same instant as does the maximum static displacement in that span, while for the other continuous plate, as seen from Fig. 25, the frequency of vibration induced is such that the maximum dynamic and static deflections occur at almost the same instant for the right-hand span.

4. Moving Masses

The numerical results presented in this section are for a clamped square plate subjected to a single load-mass moving along the centerline of the plate, as shown on Fig. 26, and for a clamped rectangular plate subjected to three load-masses traversing the plate at an angle chosen arbitrarily, as shown on Fig. 27. For each plate, a 6x6 grid with a time interval of integration h of 0.50×10^{-3} sec. was used, unless otherwise

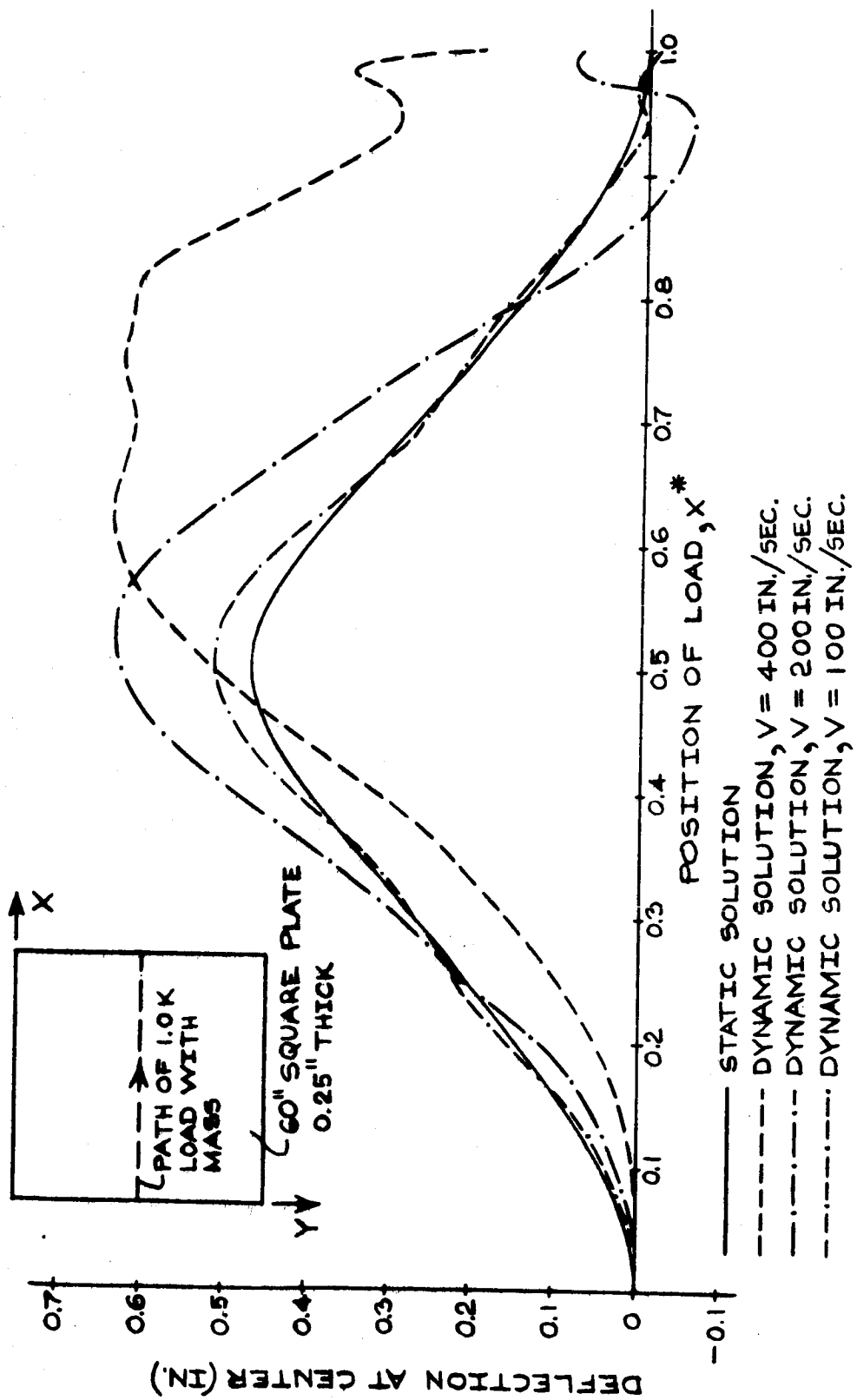

FIG. 26 – DEFLECTION OF CENTER NODE OF A CLAMPED SQUARE PLATE DUE TO A LOAD-MASS MOVING ALONG THE CENTERLINE

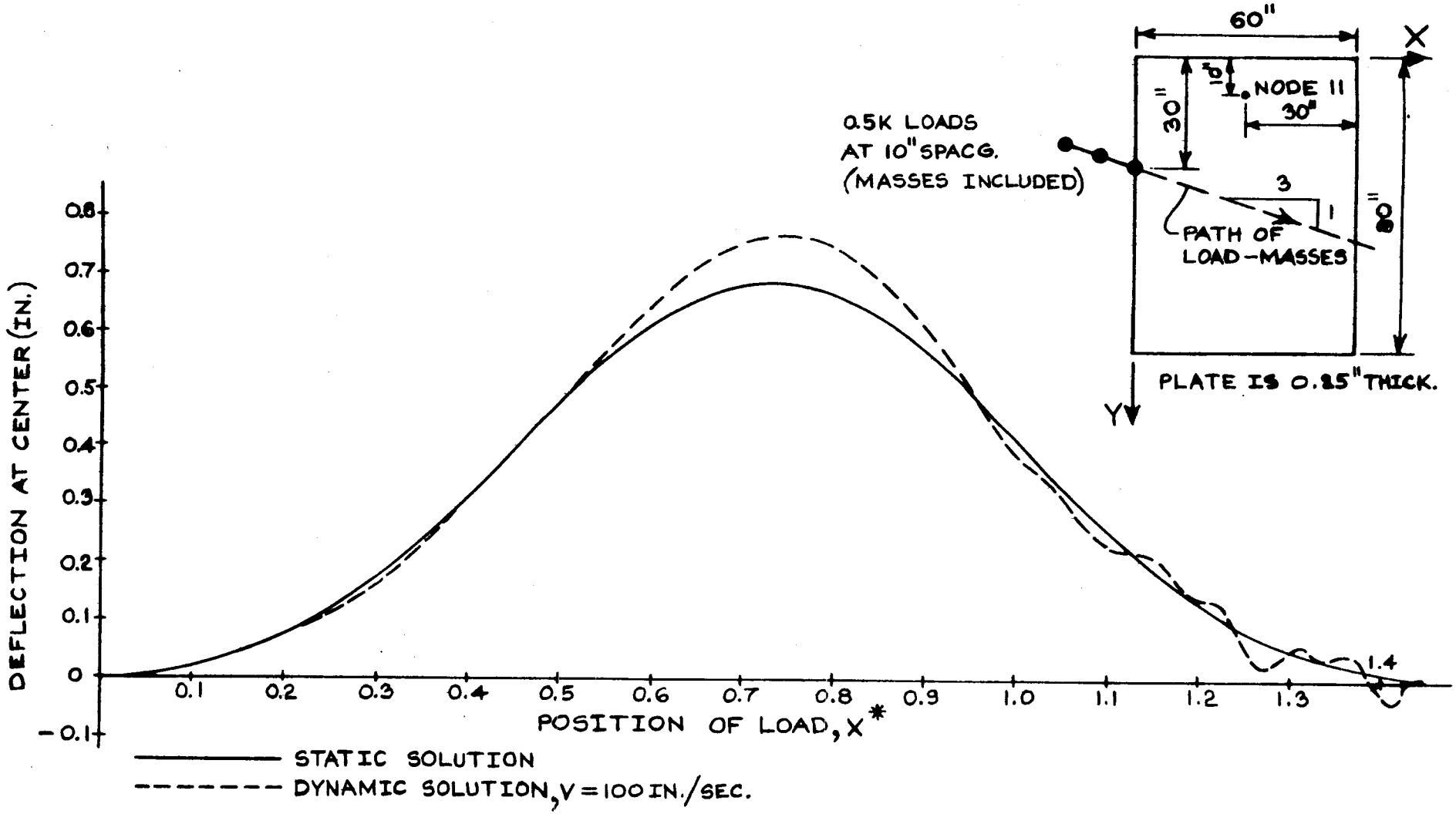

FIG. 27 – DEFLECTION OF CENTER NODE OF A CLAMPED RECTANGULAR PLATE DUE TO THREE LOAD-MASSES TRAVERSING THE PLATE AT AN OBLIQUE ANGLE

mentioned. The masses of the moving loads used in the solution were those due to a gravitational acceleration of 32.2 ft./sec.^{2}.

For the square plate, on Fig. 26 are shown the response curves for the center node deflection for velocities of 100, 200, and 400 in./sec. for the load-mass. The static deflection curve for the load is also shown. For the case of the load-mass moving with a velocity of 400 in./sec., a time interval h of $0.25\text{x}10^{-3}$ sec., as well as one of $0.50\text{x}10^{-3}$ sec. was used. The response curves for deflection were found to coincide for these two time intervals. Thus the same response curve shown on Fig. 26 for velocity of 400 in./sec. was obtained when each of these time intervals was used. For all other response curves referred to in this section, only a time interval of $0.50\text{x}10^{-3}$ sec. has been used.

Upon comparison of the response curves for velocities of 200 and 400 in./sec. shown on Fig. 26 with the response curves for the same velocities on Fig. 14, it is seen that the inclusion of the inertia of the moving load has a considerable effect on the solution. It is seen that the maximum dynamic deflection is greater, for each of the two velocities, when the effects of the mass of the load are included in the analysis.

For the solution of the square plate of Fig. 26, symmetry was used for each of the cases considered. With a time interval of $0.50\text{x}10^{-3}$ seconds, the central processing times used by the computer for the velocities of 100, 200 and 400 in./sec. were 291.2, 148.8, and 80.3 seconds, respectively. When a time interval of $0.25\text{x}10^{-3}$ seconds was used for the velocity of 400 in./sec., the time required was 153.0 seconds.

On Fig. 27 is shown a clamped rectangular plate subjected to three moving loads of 0.5 Kips each, with their masses included. The path of the moving load-masses indicated on the figure was chosen arbitrarily. The response curve for the center node deflection, along with the static deflection curve, has been plotted on this figure for the load-mass moving at 100 in./sec. For the same problem the dynamic response curve for node number 11 (See Fig. 27) is compared with the corresponding static deflection curve on Fig. 28. It is of interest to note from Figs. 27 and 28 that as the load-masses are leaving the plate, rather radical changes are occurring in the periods of vibration of the system. Such changes did not, in general, occur for the cases when the mass of the load or loads was not included in the analysis.

For the latter problem discussed above, for which 75 degrees of freedom were used, the computer required 34 min. 7 sec. for central processing time.

B. Cylindrical Shell

1. General

Numerical results are presented here for a circular cylindrical shell subjected to impact loads. The loads considered are applied in such a manner as to permit the use of double symmetry.

Since the framework analogy adopted here has not been previously used for the static analysis of cylindrical shells, a cylindrical shell subjected to static loads is considered to illustrate the accuracy of this framework analogy for a particular problem.

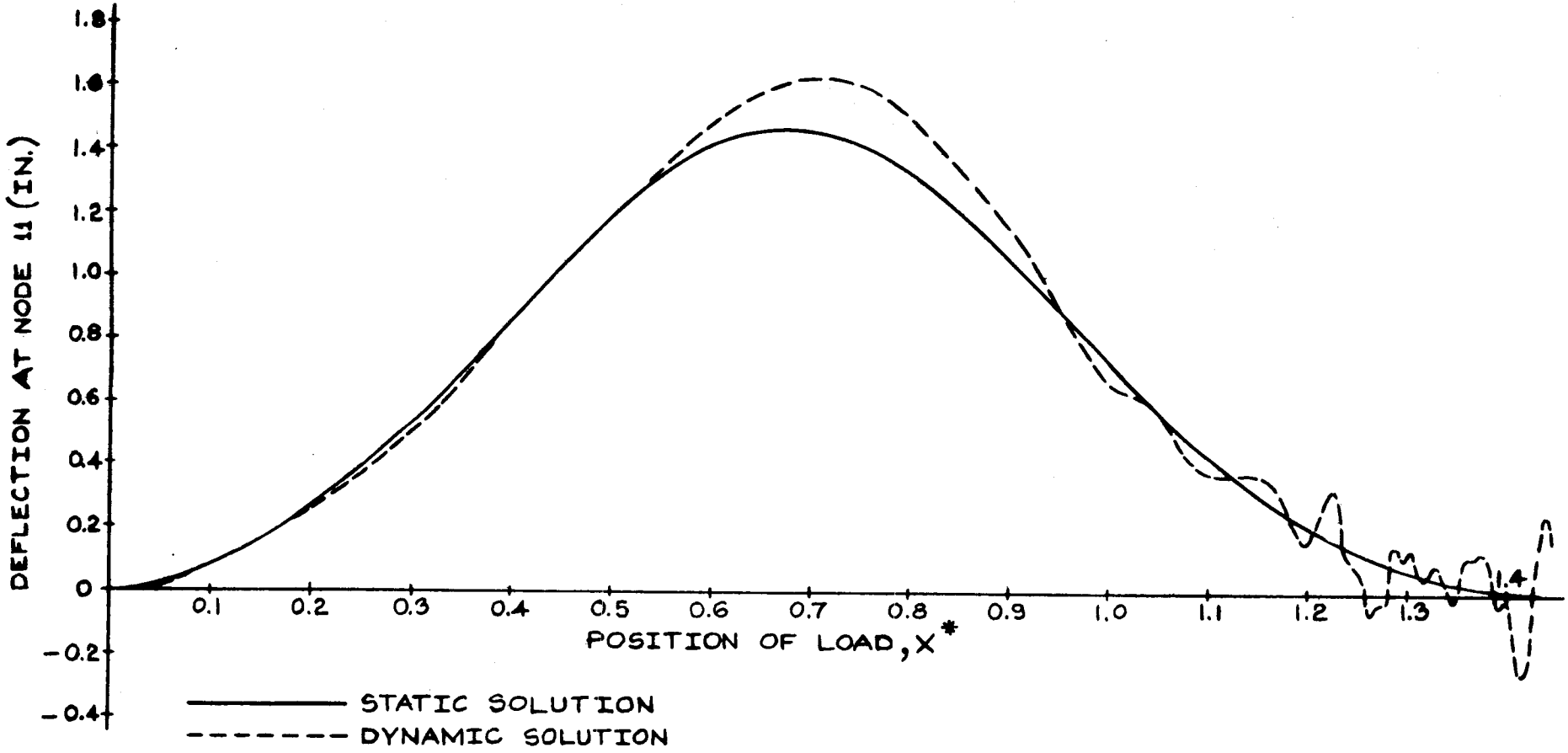

FIG. 28 - DEFLECTION OF NODE 11 OF CLAMPED RECTANGULAR PLATE DUE TO THREE LOAD-MASSES TRAVERSING THE PLATE AT AN OBLIQUE ANGLE

The static problem considered here has been used by Mohraz and Schnobrich[31] to compare their solution to a Fourier series solution of the differential equation. The circular cylindrical shell is subjected along its longitudinal edges to a sinusoidal load as indicated on Fig. 29. The transverse edges of the shell are supported by diaphragms and the longitudinal edges are free. The dimensions of the shell, along with the shell material properties, are shown on Fig. 29. In Table 3 are compared the radial center node deflections for various grid sizes for a shell quadrant. Also shown in the table is the result obtained by Mohraz and Schnobrich[31] and the one obtained from a Fourier series solution[31]. It is seen that 6x6 and 7x7 quadrant grids yield answers that differ from the Fourier series solution by 9.7% and 7.2%, respectively.

2. Impact Loads

Numerical results presented are for a constant and a triangular impact load. For both cases, the rotary inertia effect of the structure has been neglected, and the mass matrix has been obtained by the direct lumping of mass parameters as described in the Appendix.

The circular cylindrical shells used for the two problems in this section, together with their loadings, are shown on Figs. 30 and 31. Double symmetry, with a 6x6 grid for a quadrant, is used for both problems. The loads shown on the figures are applied radially at the nodes. The shell material has a modulus of elasticity of 30,000 ksi and a Poisson's ratio of 0.30. Fig. 32 shows the response curve for the radial deflection of the center node.

TABLE 3

Deflections of a Cylindrical Shell (in.)

	Radial Deflection at Center
3x3 Quadrant Grid	0.6508
4x4 Quadrant Grid	0.7580
5x5 Quadrant Grid	0.8198
6x6 Quadrant Grid	0.8575
7x7 Quadrant Grid	0.8819
Mohraz and Schnobrich	0.888
Fourier Series	0.95

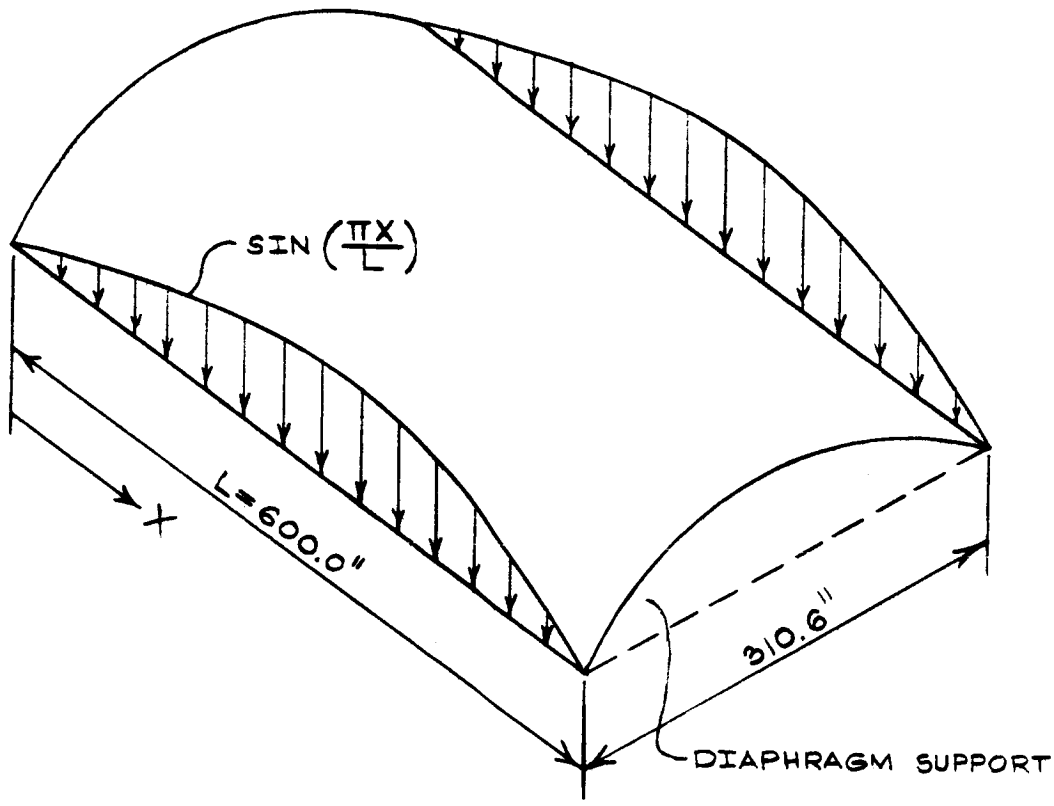

E = 30,000 ksi
ν = 0.15

RADIUS = 600.0"
THICKNESS = 6.0"

FIG. 29 - CYLINDRICAL SHELL USED FOR COMPARISON OF STATIC SOLUTION

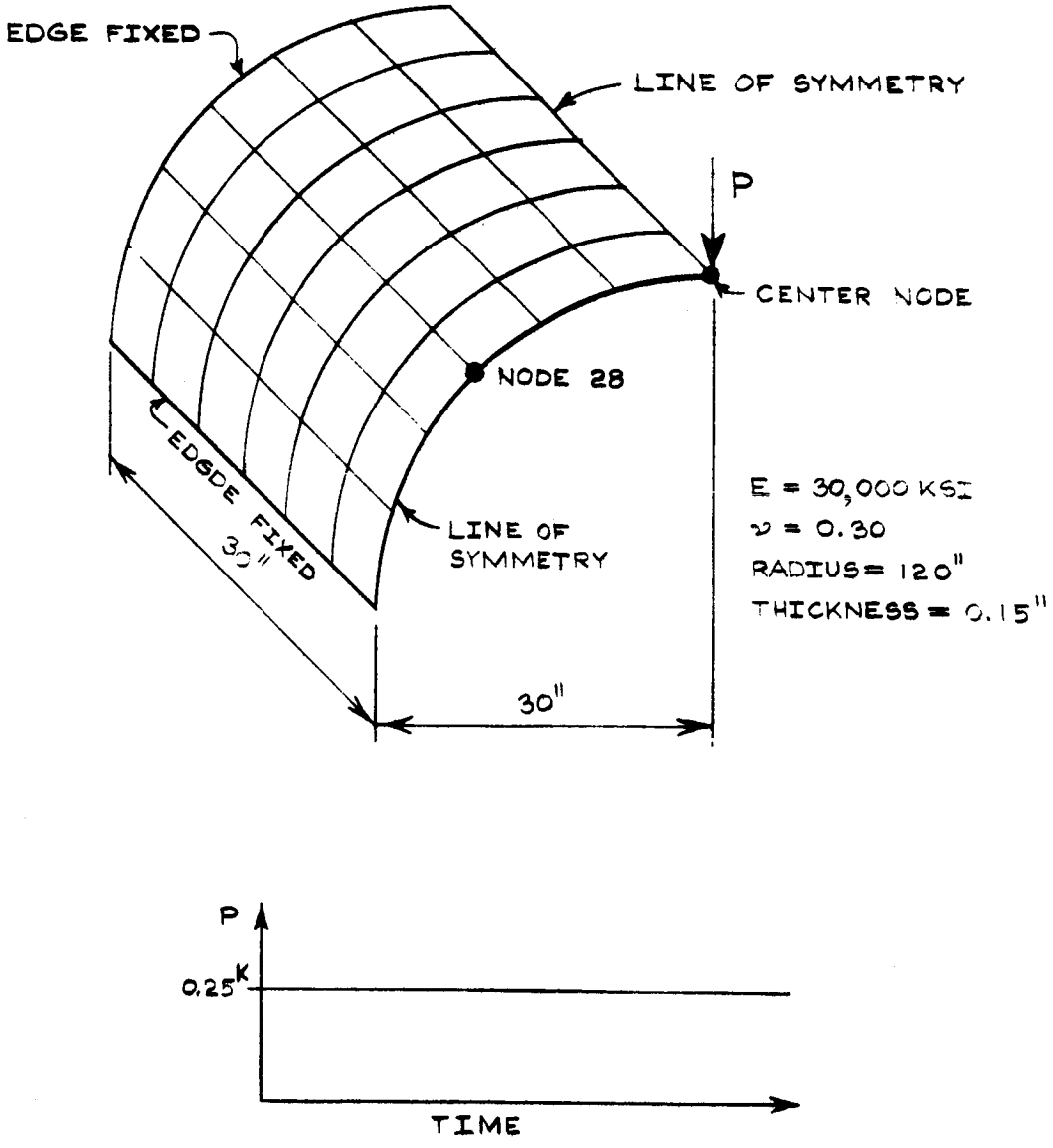

FIG. 30 – FIXED CYLINDRICAL SHELL AND ITS IMPACT LOADING

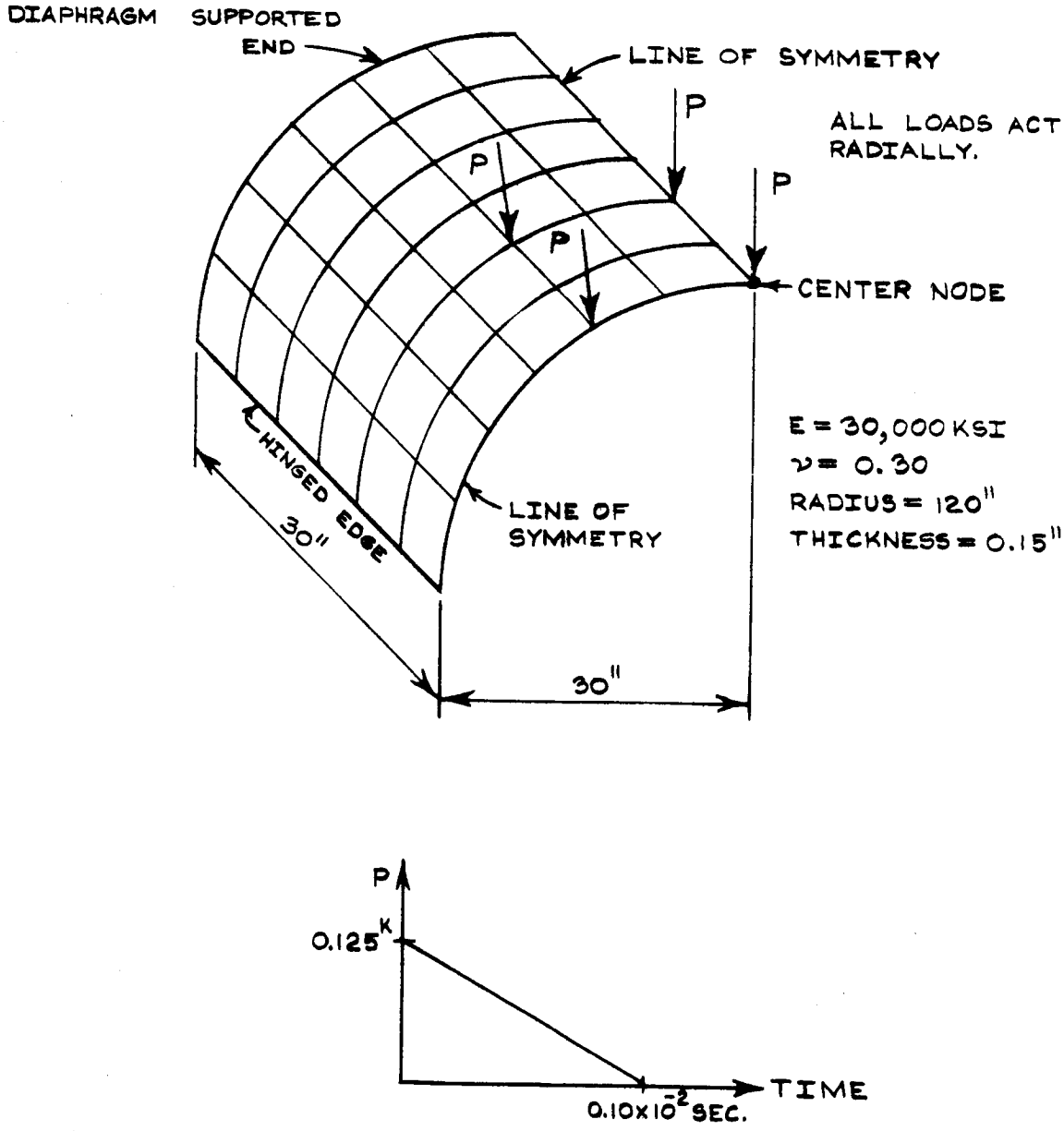

FIG. 31 - CYLINDRICAL SHELL WITH HINGED LONGITUDINAL EDGES AND DIAPHRAGM SUPPORTED TRANSVERSE ENDS, AND ITS IMPACT LOADING

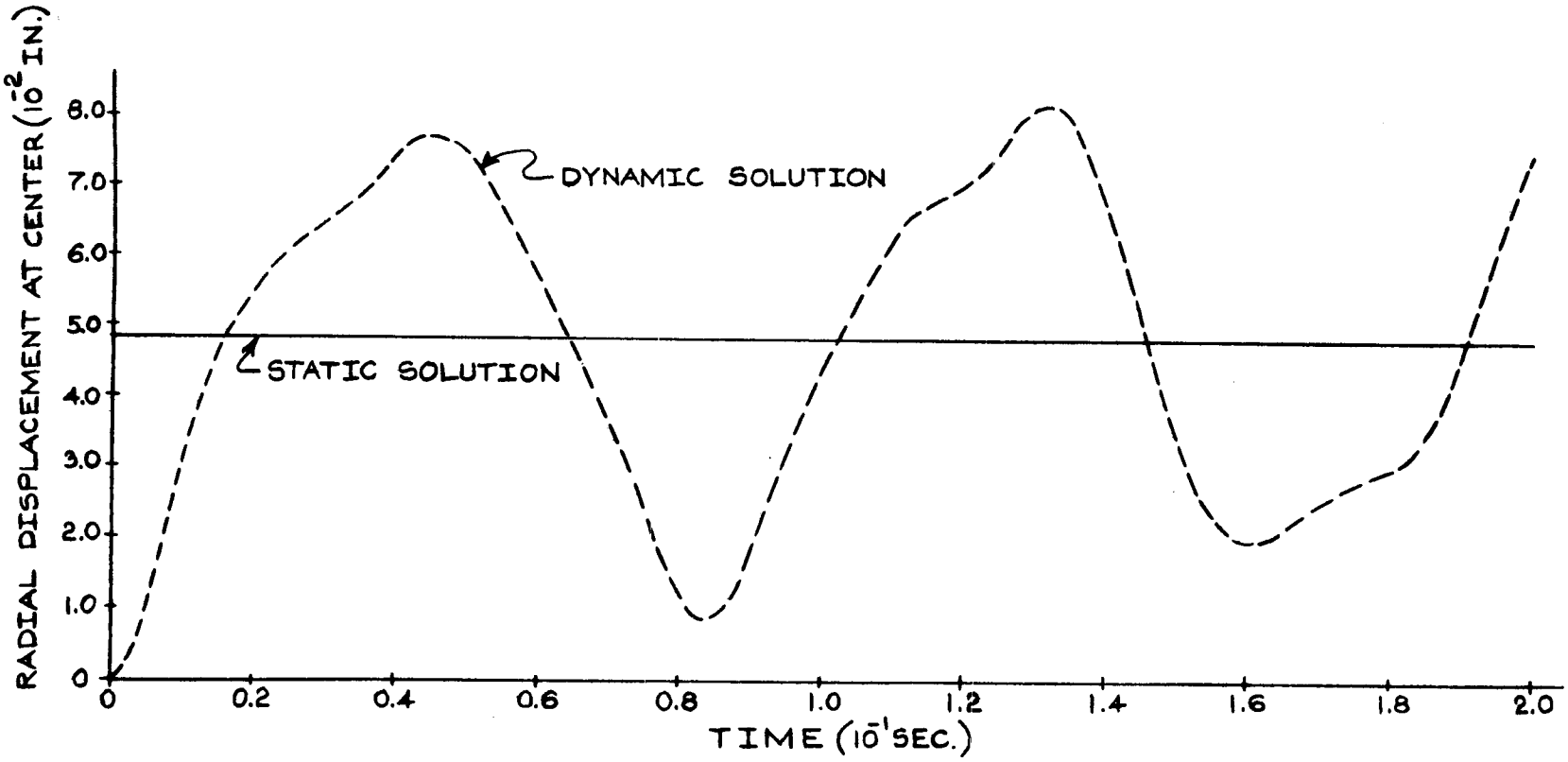

FIG. 32 – RADIAL DISPLACEMENT OF CENTER NODE OF A CIRCULAR CYLINDRICAL SHELL DUE TO A CONSTANT LOAD IMPACT

For the problem of Fig. 30, the shell is completely fixed at its boundaries. With only a quadrant of the shell used in the solution, 181 degrees of freedom were considered. The response curves for the radial deflections of the center node and node number 28 (See Fig. 30.), along with the corresponding static deflections, are shown on Figs. 32 and 33. With a time interval h of 0.10×10^{-4} seconds used for this problem, the central processing time required for the computer was 7 min. 39 sec.

For the problem of Fig. 31, the transverse ends of the shell are supported by diaphragms and the longitudinal edges are hinged. 204 degrees of freedom are considered for a quadrant of this structure. The response curve for the radial deflection of the center node is plotted on Fig. 34 along with the static deflections. The central processing time required by the computer for this solution was 9 min. 23 sec., with a time interval of 0.10×10^{-4} sec. being used.

To draw any conclusions on the dynamic behavior of cylindrical shells, additional problems have to be studied. Since the solution of cylindrical shell problems requires the consideration of a much larger number of degrees of freedom than does the solution of plate problems, the study of moving loads and load-masses requires considerably more computer time and storage capacity for cylindrical shells than for plates.

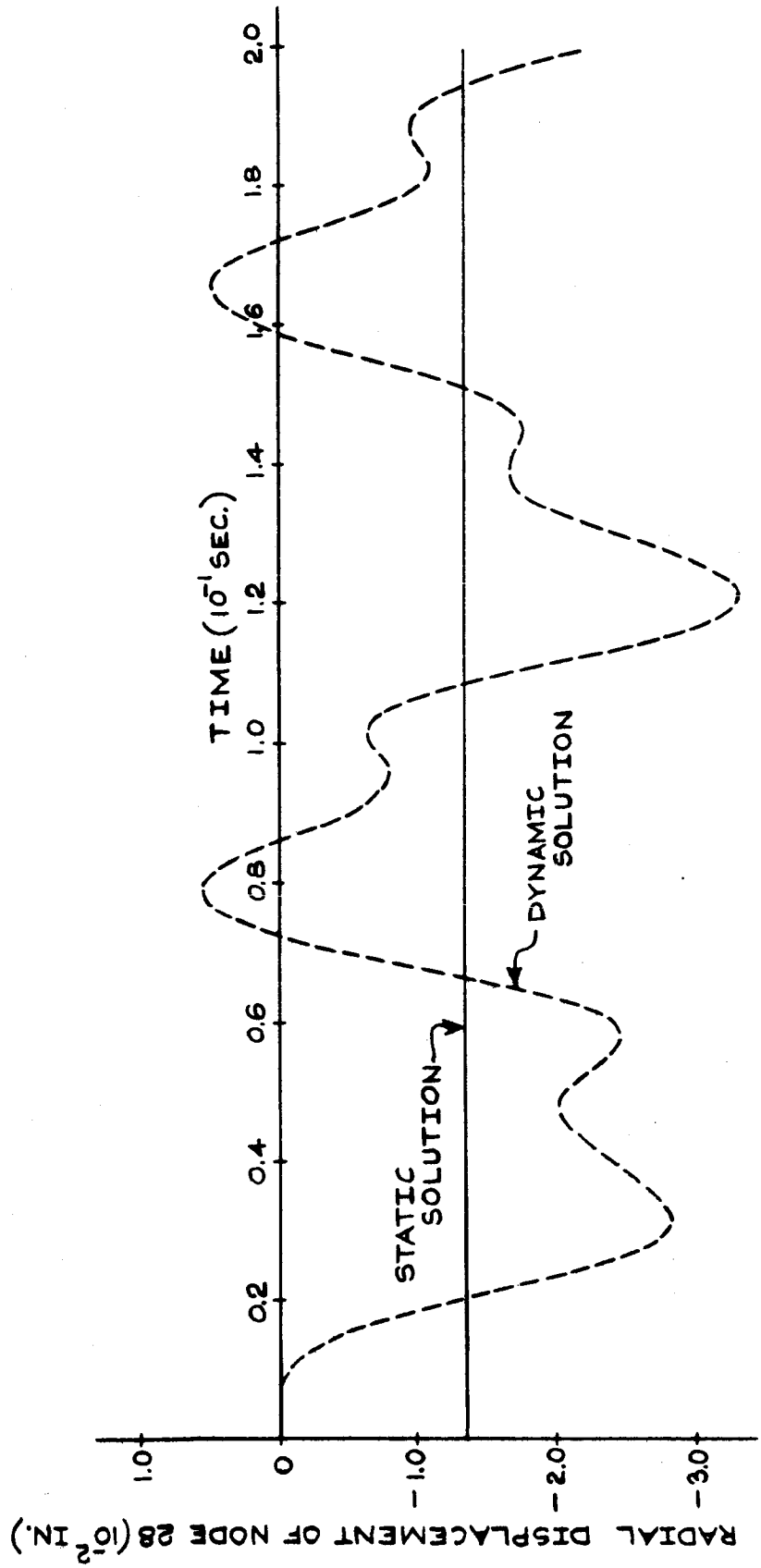

FIG. 33 – RADIAL DISPLACEMENT OF NODE 28 OF CIRCULAR CYLINDRICAL SHELL DUE TO A CONSTANT LOAD IMPACT

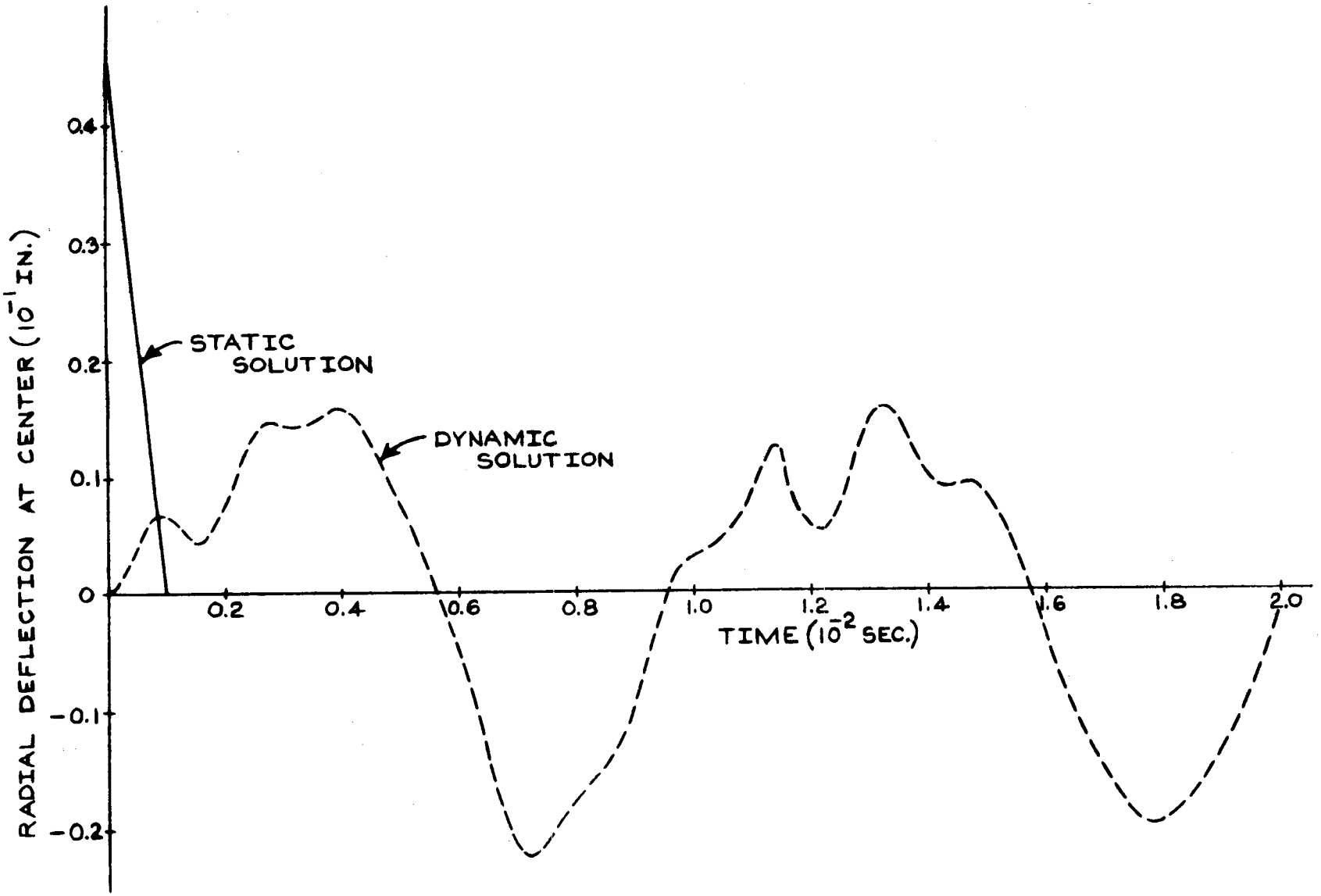

FIG. 34 - RADIAL DISPLACEMENT OF CENTER NODE OF A CIRCULAR CYLINDRICAL SHELL DUE TO A TRIANGULAR IMPACT LOAD

FURTHER APPLICATIONS OF THE METHOD

The method of analysis developed in this research can be modified to analyze various other types of structures.

The extension of the procedure to composite structures is obvious. All that is required is to include the stiffness matrix for each additional structural component in the analysis. Thus, for example, flat slabs supported on columns or plates with stiffening beams can be analyzed. More complex composite systems, as those associated with aircraft, space vehicle, and nautical structures can be analyzed as well. The work of H. Allik[1] on the response of space frames to dynamic loadings is of interest in conjunction with these modifications.

Using triangular elements[6, 7, 8, 27, 28], the procedure presented can be modified to analyze shells and plates of arbitrary shape. Changes have to be made only to account for the different stiffness matrix sizes.

The method of analysis presented can readily be applied to plates and shells of variable thickness. With the thickness varying from point to point in the continuous medium of the structure, an approximate element stiffness matrix can be calculated by using for the element thickness the average of the thicknesses at the nodes of the element[2]. Numerical examples of static problems for plates with variable thickness have been obtained by R. J. Melosh[2] and by O. C. Zienkiewicz and Y. K. Cheung[4]. Melosh[2] has also analyzed for static loading a low aspect ratio wing by considering it as a plate of variable thickness, with spar and rib stiffnesses

included only approximately. In general, these stiffnesses can be included more exactly as indicated by M. J. Turner et al[41]. All of the problems referred to above can be analyzed for dynamic loadings by modifications of the procedure that has been presented.

The procedure that has been presented can also be used for orthotropic plates by substituting the orthotropic plate element stiffness matrix derived by O. C. Zienkiewiecz and Y. K. Cheung[4] for the stiffness matrix that has been used here.

Plates and shells with openings can also be analyzed for dynamic loadings. It is necessary only to omit the element stiffness matrix or matrices corresponding to the physical elements omitted. However, it is expected that in the areas of stress concentration near the opening, poor approximations are obtained with rectangular elements unless a relatively fine grid is used for the whole structure. It is therefore advantageous to use triangular elements for such a problem, so that a relatively fine grid can be used near the opening while a more coarse grid can be adopted for the remainder of the structure.

Recent developments of element stiffness matrices for solids[8, 42, 43] enables the analysis at such structures for dynamic loadings by modifications of the method presented here. The assumed displacement functions used by R. J. Melosh[43] to derive a solid element stiffness matrix can be adopted in conjunction with the necessary modifications of the procedure to replace, for example, the displacement functions A_i (x, y) used here for the plate analysis.

SUMMARY AND CONCLUSIONS

A numerical method has been presented for the analysis of thin rectangular plates and cylindrical shells subjected to moving loadings. Stationary time-varying loads, as well as multiple loads and load-masses moving at constant velocity have been considered in the analysis. Elastic, small deflection theory was used in the formulation of the problem.

For the rectangular plate as well as the cylindrical shell, the continuous medium of an infinite number of degrees of freedom was reduced to a system with a finite number of degrees of freedom by means of a framework analogy. Displacement functions were assumed for the finite elements to obtain equivalent node forces for the applied force and mass loadings. The simultaneous differential equations of motion governing the behavior of the finite element structures were solved by the linear acceleration method of numerical integration. The method of analysis presented is equally valid for arbitrary boundary conditions and for arbitrary interior restraints.

Numerical results have been presented for square and rectangular plates, for continuous plates, and for circular cylindrical shells. Plates subjected to impact loads, moving forces and moving load-masses were included in the numerical studies. For the cylindrical shells, only impact loads were considered. For each of the problems solved, only node displacements were calculated.

The numerical studies indicated that a relatively coarse grid may be used for the finite element model to replace the actual continuous medium of the structure in order to yield acceptable results for the deflections. For the square and rectangular plates considered, a 6x6 grid was sufficient to study the deflections.

The acceptability of a relatively coarse grid for the study of deflections leads to the conclusion that, for the loadings considered, the dynamic response depends predominantly on the lower natural modes of vibration of the system considered.

In the numerical studies, comparisons were made for the effect of time intervals used for integration, grid sizes used for the finite element structure, various velocities of moving loads and load-masses, and paths of the traverse of moving loadings. However, it was seen that numerous additional studies would have to be made to draw general conclusions on the effect of the various parameters on the dynamic behavior of rectangular plates and cylindrical shells.

Modifications of the procedure presented for other types of structures has been discussed.

NOMENCLATURE

a	x-coordinate of forcing function
a_L, a_R	angles defined on Fig. 7
A_i	area of beam i of a framework model element; abbreviation for $A_i(x, y)$
$A_i(x, y)$	displacement function (See Appendix.)
b	y-coordinate of forcing function
$B_i(x, y)$	displacement function (See Appendix.)
cL	length of a typical element in x-direction
$\left[C_i \right]$	geometric transformation matrix for shell element i
d^*_{ij}	element of matrix $\left[d^* \right]$
$\left[d^* \right]$	matrix defined by Eq. (23b) or (44c)
$\left[d^*_r \right]$	element r matrix defined in Eq. (22) or (43)
D_s	number of degrees of freedom of the structure in deflection
$\left[D \right]$	matrix defined by Eq. (24b) or (45b)
$\left[D \right]_{11}$	matrix defined by Eq. (68b)
E	modulus of elasticity of plate material
$\left[E \right]$	matrix defined in Eq. (51a), (55a), (61), or (69a)
F_i	i-th equivalent node force
$\left\{ F_i \right\}$	vector of equivalent node forces for element i

$\{ G \}$	vector defined in Eqs. (51b), (55b), (61), or (69b)
GJ	torsion constant, used with a subscript
h	plate or shell thickness; time increment
I	beam moment of inertia for framework model, used with subscripts or superscripts
k^*_{ij}	element of matrix $[k^*]$
$[k]$	stiffness matrix for the discrete element structure
$[k^*]$	matrix defined by Eq. (23a) or (44b)
$[k_i]$	stiffness matrix for i-th element framework model
$[k^*_r]$	matrix defined in Eq. (22) or (43)
$[K]$	matrix defined in Eq. (24c), (45c), or (60a)
$[K']_{11}$	matrix defined by Eq. (68c)
L	length of element in y-direction
L_x	plate length in X-direction
L_Y	plate length in Y-direction
m^*_{ij}	element of matrix $[m^*]$
$[m]$	mass matrix for the discrete element structure
$[m_i]$	mass matrix for element i
$[m^*]$	matrix defined in Eq. (23c) or (44d)
M	mass of moving load
M_s	number of equivalent node moments from all moving masses

$[M]$ matrix defined by Eq. (24a) or (45a)

$[M]_{11}$ matrix defined by Eq. (68a)

N_s number of degrees of freedom of the structure

P magnitude of forcing function

P_i i-component of forcing function P

q_i i-th node displacement component in system coordinates

$\{q\}$ vector of node displacements in system coordinates

$\{q_i\}$ vector of node displacements of element i in system coordinates

Q_i i-th component of generalized node forces in system coordinates

$\{Q\}$ vector of node forces due to externally applied forces

$\{Q\}_e$ vector of equivalent node forces

$\{Q\}_n$ vector of external loads applied at nodes

$\{Q'\}_1$ vector defined by Eq. (68d)

rL distance between diagonally opposite corners of an element

$\{R\}$ vector of resultant node forces from all external loadings

$\{R\}_{in}$ vector of inertia forces at nodes

$\{R_i\}_{in}$ vector of inertia forces at nodes of element i

S_i i-th component of generalized internal node forces of an element

$\{S_i\}$ vector of internal forces at nodes of element i

t	time coordinate
T_s	shortest natural period of discrete element structure
u_i	i-th node displacement of an element in element coordinates
$\{ u \}$	vector of node displacements in element coordinates
$\{ u_i \}$	vector of node displacements of element i in element coordinates
V_x	velocity of moving forcing function in x-direction
V_y	velocity of moving forcing function in y-direction
$w\ (x, y, t)$	deflection of an element in z-direction under moving mass
$w_o\ (x, y, t)$	virtual deflection of an element in z-direction under moving forcing function
$w_x\ (x, y, t)$	virtual displacement of an element in x-direction at point of application of forcing function
x y z	element coordinates of plate or shell element
XYZ	system coordinates of plate or shell
δu_i	i-th virtual element node displacement
ν	Poisson's ratio of plate material
$[\ ]^{-1}$	denotes inverse of a matrix
$[\ ]^{T}$	denotes transpose of a matrix
$(\dot{\ })$	denotes differentiation with respect to time
$,x$	denotes differentiation with respect to x

REFERENCES

1. Allik, H., "Dynamic Response of Space Frames", Ph. D. Thesis, New York University, 1966.

2. Melosh, R. J., "A Stiffness Matrix for the Analysis of Thin Plates in Bending", Journal of the Aerospace Sciences, v. 28, January 1961, pp. 34-42.

3. Melosh, R. J., "Basis for Derivation of Matrices for the Direct Stiffness Method", AIAA Journal, v. 1, July 1963, pp. 1631-1637.

4. Zienkiewicz, O. C., and Cheung, Y. K., "The Finite Element Method for Analysis of Elastic Isotropic and Orthotropic Slabs", Proceedings of the Institution of Civil Engineers, v. 28, August 1964, pp. 471-488.

5. Zienkiewicz, O. C., "Finite Element Procedures in the Solution of Plate and Shell Problems", Stress Analysis, Edited by O. C. Zienkiewicz and G. S. Holister, John Wiley and Sons, 1965, pp. 120-144.

6. Tocher, J. L., "Analysis of Plate Bending Using Triangular Elements", Ph. D. Thesis, California University (Berkeley), 1962.

7. Przemieniecki, J. S., "Triangular Plate Elements in the Matrix Force Method of Structural Analysis", AIAA Journal, v. 1, August 1963, pp. 1895-1897.

8. Clough, R. W., "The Finite Element Method in Structural Mechanics", Stress Analysis, Edited by O. C. Zienkiewicz and G. S. Holister, John Wiley and Sons, 1965, pp. 85-119.

9. Clough, R. W , and Tocher, J. L., "Finite Element Stiffness Matrices for Analysis of Plate Bending", Proceedings of the Conference on Matrix Methods of Structural Analysis , Wright-Patterson Air Force Base, Ohio, Oct. 26-28, 1965.

10. Pian, T. H. H., "Derivation of Element Stiffness Matrices by Assumed Stress Distributions", AIAA Journal, v. 2, July 1964, pp. 1333-1336.

11. Spierig, S., "Beitrag zur Lösung von Scheiben-, Platten-, und Schalenproblemen mit Hilfe von Gitterrostmodellen", Abhandlungen der Braunschweigischer Wissenschaftlichen Gesellschaft, v. 15, 1963, pp. 133-165.

12. Klein, F., and Wieghardt, K., "Über Spannungsflächen und reziproke Diagramme, mit besonderer Berücksichtigung der Maxwellschen Arbeiten", Archiv der Mathematik und Physik, v. 8, 1904, pp. 1-10 and 95-119.

13. Wieghardt, K., "Über einen Grenzübergang der Elastizitätslehre und seine Anwendung auf die Statik hochgradig unbestimmter Fachwerke", Verhandlungen des Vereins zur Beförderung des Gewerbefleisses, v. 85, 1906, pp. 139-176.

14. Riedel, W., "Beiträge zur Lösung des ebenen Problems eines Elastischen Körpers mittels der Airyschen Spannungsfunktion", Zeitschrift für Angewandte Mathematik und Mechanik, v. 7, 1927, pp. 169-188.

15. Hrennikoff, A. P., "Plane Stress and Bending of Plates by Method of Articulated Framework", Ph. D. Thesis, Massachusetts Institute of Technology, 1940.

16. Hrennikoff, A. P., "Solution of Problems of Elasticity by the Framework Method", Journal of Applied Mechanics, American Society of Mechanical Engineers, v. 63, December 1941, pp. A-169-A-175.

17. Pestel, E., "Investigation of Plate and Shell Models by Matrices," Technische Hochschule Hannover, Report to Office of Aerospace Research, European Office, U.S. Air Force, Brussels, Belgium, 1963.

18. Yettram, A. L., and Husain, H. M., "Grid-Framework Method for Plates in Flexure", Proceedings of the American Society of Civil Engineers, Journal of the Engineering Mechanics Division, v. 91, EM3, June 1965, pp. 53-64.

19. Tocher, J. L., Discussion of "Grid-Framework Method for Plates in Flexure", by A. L. Yettram and H. M. Husain, Proceedings of the American Society of Civil Engineers, Journal of the Engineering Mechanics Division, v. 91, EM 6, December 1965, pp. 190-191.

20. Ang. A. H. S., and Newmark, N. M., "A Numerical Procedure for the Analysis of Continuous Plates", Conference Papers, Second Conference on Electronic Computation, American Society of Civil Engineers, Pittsburgh, Pa., 1960, pp. 379-413.

21. Badir, M., "Bending of Rectangular Plates", Proceedings of the American Society of Civil Engineers, Journal of the Structural Division, v. 87, ST 6, August 1961, pp. 105-134.

22. Lightfoot, E., "A Grid Framework Analogy for Laterally Loaded Plates", International Journal of Mechanical Sciences, v. 6, June 1964, pp. 201-208.

23. Yettram, A. L., and Husain, H. M., "The Representation of a Plate in Flexure by a Grid of Orthogonally Connected Beams", International Journal of Mechanical Sciences, v. 7, April 1965, pp. 243-251.

24. McCormick, C.W., "Plane Stress Analysis", Proceedings of the American Society of Civil Engineers, Journal of the Structural Division, v. 89, ST 4, August 1963, pp. 37-54.

25. Yettram, A. L., and Husain, H. M., "Plane-Framework Methods for Plates in Extension", Proceedings of the American Society of Civil Engineers, Journal of the Engineering Mechanics Division, v. 92, EM 1, February 1966, pp. 157-168.

26. Clough, R.W., "Finite Element Method in Plane Stress Analysis", Proceedings, 2nd ASCE Conference on Electronic Computation, Pittsburgh, Pennsylvania, September 1960, pp. 345-378.

27. Tocher, J. L., and Hartz, B J., "Higher - Order Finite Element for Plane Stress", Proceedings of the American Society of Civil Engineers, Journal of the Engineering Mechanics Division, v. 93, EM 4, August 1967, pp. 149-172.

28. Fraeijs de Veubeke, B., "Displacement and Equilibrium Models in the Finite Element Method", Stress Analysis, Edited by O. C. Zienkiewicz and G. S. Holister, John Wiley and Sons, 1965, pp. 145-197.

29. Benard, E. F., "A Study of the Relationship between Lattice and Continuous Structures", Ph. D. Thesis, University of Illinois, 1965.

30. Hrennikoff, A., and Tezcan, S. S., "Analysis of Cylindrical Shells by the Finite Element Method", Paper presented at the International Symposium on Large Size Shell Structures, Leningrad, U. S. S. R., September 1966.

31. Mohraz, B., and Schnobrich, W. C., "The Analysis of Shallow Shell Structures by a Discrete Element System", Civil Engineering Studies, Structural Research Series No. 304, University of Illinois, March 1966.

32. Pestel, E. C., and Leckie, F. A., Matrix Methods in Elastomechanics, McGraw-Hill Book Co., 1963, pp. 346-352.

33. Pestel, E., "Dynamics of Structures by Transfer Matrices", Technical Report No. 1, Contract AF61(052)-33, Technische Hochschule Hannover, 1959.

34. Pestel, E., "Dynamics of Structures by Transfer Matrices", Final Report, Contract AF61(052)-302, Technische Hochschule Hannover, 1961.

35. Leckie, F.A., "The Application of Transfer Matrices to Plate Vibrations", Ingenieur-Archiv, v. 32, 1963, pp. 100-111.

36. Cappelli, A.P., "Dynamic Response of a Rectangular Plate Subjected to Multiple Moving Mass Loads", Ph. D. Thesis, New York University, 1963.

37. Jones, J.P., and Bhuta, P.G., "Response of Cylindrical Shells to Moving Loads", Journal of Applied Mechanics, Transactions of the ASME, v. 31, Ser. E, No. 1, March 1964, pp. 105-111.

38. Rogers, G.L., Dynamics of Framed Structures, John Wiley and Sons, 1959, pp. 75-79.

39. Timoshenko, S.P., and Woinowsky-Krieger, S., Theory of Plates and Shells, McGraw-Hill Book Co., 1959, pp. 111-112.

40. Young, D., "Clamped Rectangular Plates With a Central Concentrated Load", Journal of Applied Mechanics, American Society of Mechanical Engineers, v. 61, September 1939, pp. A-114 - A-116.

41. Turner, M.J., Clough, R.W., Martin, H.C., and Topp, L.J., "Stiffness and Deflection Analysis of Complex Structures", Journal of Aeronautical Sciences, v. 23, September 1956, pp. 805-823.

42. Clough, R.W., and Rashid, Y., "Finite Element Analysis of Axi-Symmetric Solids", Proceedings of the American Society of Civil Engineers, Journal of the Engineering Mechanics Division, v. 91, EM 1, February 1965, pp. 71-85.

43. Melosh, R.J., "Structural Analysis of Solids", Proceedings of the American Society of Civil Engineers, Journal of the Structural Division, v. 89, ST 4, August 1963, pp. 205-223.

44. Archer, J.S., "Consistent Mass Matrix for Distributed Mass Systems", Proceedings of the American Society of Civil Engineers, Journal of the Structural Division, v. 89, ST 4, August 1963, pp. 161-178.

45. Hurty, W. C., and Rubinstein, M. F., Dynamics of Structures, Prentice-Hall, Inc., 1964, pp. 173-177.

46. Mason, P., "An Introduction to Automated Structural Analysis Methods", Grumman Aircraft Engineering Corporation, June 1965.

VITA

Are Tsirk was born in Tallinn, Estonia, on April 29, 1937. Upon graduation from New York University in 1959 with a Bachelor of Civil Engineering degree, he worked as a structural engineer for Consolidated Edison Company of New York until December, 1960, when he was inducted into military service. After serving in the U.S. Army Corps of Engineers for almost two years, he returned to his former position. In January, 1964, Mr. Tsirk became a structural engineer for the consulting firm of Paul Weidlinger. In 1965 he received a Master of Civil Engineering degree from New York University. While at Paul Weidlinger, he also obtained a New York State Professional Engineers License.

Mr. Tsirk became a Graduate Assistant at New York University in September, 1965. While pursuing his studies, he worked as a Research Assistant under a National Aeronautics and Space Administration grant from February, 1966, until August, 1967.

Mr. Tsirk is an Associate Member of the American Society of Civil Engineers.

APPENDIX

A. Element Stiffness Matrices

The stiffness matrix for the framework model shown in Fig. 3, which has been substituted in the analysis for each typical plate element shown on Fig. 2, is given on the next page. This stiffness matrix is defined by Eq. (1).

The stiffness matrix for a cylindrical shell element can either be assembled from the stiffness matrices of each of the six beams of the framework element shown with its properties on Fig. 8, or it can be assembled by first considering the stiffness matrix for a plate in flexure, shown on p. A2, and for a plate under plane stress. The latter approach is adopted here. Therefore the element stiffness matrix for plane stress has been assembled, and is shown on p. A3. For convenience, the rows and columns of this matrix have been numbered to correspond to the actions indicated on Fig. 5. The stiffness coefficients used in the plane stress stiffness matrix on p. A3 have the following values:

$$p_1 = -(p_4 + p_5 + p_6)$$

$$p_2 = \frac{A_3 E}{L} \quad \frac{c}{r^3}$$

$$p_3 = \frac{6\, EI'_2}{L^2}$$

$$p_4 = -\frac{A_1 E}{cL}$$

$+12E\left(\frac{I_1}{L_1^3}+\frac{I_2}{L_2^3}+\frac{I_3}{L_3^3}\right)$	$+6E\left(\frac{I_2}{L_2^2}+\frac{I_3}{rL_3^2}\right)$	$-6E\left(\frac{I_1}{L_1^2}+\frac{cI_3}{rL_3^2}\right)$	$-\frac{12EI_1}{L_1^3}$	0	$-\frac{6EI_1}{L_1^2}$	$-\frac{12EI_2}{L_2^3}$	$+\frac{6EI_2}{L_2^2}$	0	$-\frac{12EI_3}{L_3^3}$	$+\frac{6EI_3}{rL_3^2}$	$-\frac{6cEI_3}{rL_3^2}$
	$+\frac{4EI_2}{L_2}+\frac{GJ_1}{L_1}+\frac{4EI_3}{r^2L_3}$	$-\frac{4cEI_3}{r^2L_3}$	0	$-\frac{GJ_1}{L_1}$	0	$-\frac{6EI_2}{L_2^2}$	$+\frac{2EI_2}{L_2}$	0	$-\frac{6EI_3}{rL_3^2}$	$+\frac{2EI_3}{r^2L_3}$	$-\frac{2cEI_3}{r^2L_3}$
		$+\frac{GJ_2}{L_2}+\frac{4EI_1}{L_1}+\frac{4c^2EI_3}{r^2L_3}$	$+\frac{6EI_1}{L_1^2}$	0	$+\frac{2EI_1}{L_1}$	0	0	$-\frac{GJ_2}{L_2}$	$+\frac{6cEI_3}{rL_3^2}$	$-\frac{2cEI_3}{r^2L_3}$	$+\frac{2c^2EI_3}{r^2L_3}$
			$+12E\left(\frac{I_1}{L_1^3}+\frac{I_2}{L_2^3}+\frac{I_3}{L_3^3}\right)$	$+6E\left(\frac{I_2}{L_2^2}+\frac{I_3}{rL_3^2}\right)$	$+6E\left(\frac{I_1}{L_1^2}+\frac{cI_3}{rL_3^2}\right)$	$-\frac{12EI_3}{L_3^3}$	$+\frac{6EI_3}{rL_3^2}$	$+\frac{6cEI_3}{rL_3^2}$	$-\frac{12EI_2}{L_2^3}$	$+\frac{6EI_2}{L_2^2}$	0
				$+\frac{4EI_2}{L_2}+\frac{GJ_1}{L_1}+\frac{4EI_3}{r^2L_3}$	$+\frac{4cEI_3}{r^2L_3}$	$-\frac{6EI_3}{rL_3^2}$	$+\frac{2EI_3}{r^2L_3}$	$+\frac{2cEI_3}{r^2L_3}$	$-\frac{6EI_2}{L_2^2}$	$+\frac{2EI_2}{L_2}$	0
					$+\frac{GJ_2}{L_2}+\frac{4EI_1}{L_1}+\frac{4c^2EI_3}{r^2L_3}$	$-\frac{6cEI_3}{rL_3^2}$	$+\frac{2cEI_3}{r^2L_3}$	$+\frac{2c^2EI_3}{r^2L_3}$	0	0	$-\frac{GJ_2}{L_2}$
						$+12E\left(\frac{I_1}{L_1^3}+\frac{I_2}{L_2^3}+\frac{I_3}{L_3^3}\right)$	$-6E\left(\frac{I_2}{L_2^2}+\frac{I_3}{rL_3^2}\right)$	$-6E\left(\frac{I_1}{L_1^2}+\frac{cI_3}{rL_3^2}\right)$	$-\frac{12EI_1}{L_1^3}$	0	$-\frac{6EI_1}{L_1^2}$
							$+\frac{4EI_2}{L_2}+\frac{GJ_1}{L_1}+\frac{4EI_3}{r^2L_3}$	$+\frac{4cEI_3}{r^2L_3}$	0	$-\frac{GJ_1}{L_1}$	0
		SYMMETRICAL						$+\frac{GJ_2}{L_2}+\frac{4EI_1}{L_1}+\frac{4c^2EI_3}{r^2L_3}$	$+\frac{6EI_1}{L_1^2}$	0	$+\frac{2EI_1}{L_1}$
									$+12E\left(\frac{I_1}{L_1^3}+\frac{I_2}{L_2^3}+\frac{I_3}{L_3^3}\right)$	$-6E\left(\frac{I_2}{L_2^2}+\frac{I_3}{rL_3^2}\right)$	$+6E\left(\frac{I_1}{L_1^2}+\frac{cI_2}{rL_3^2}\right)$
										$+\frac{4EI_2}{L_2}+\frac{GJ_1}{L_1}+\frac{4EI_3}{r^2L_3}$	$-\frac{4cEI_3}{r^2L_3}$
											$+\frac{GJ_2}{L_2}+\frac{4EI_1}{L_1}+\frac{4c^2EI_3}{r^2L_3}$

PLATE ELEMENT STIFFNESS MATRIX

	1	2	6	7	8	12	13	14	18	19	20	24
1	p_1											
2	p_2	p_7										
6	p_3	p_8	p_{12}						SYMMETRICAL			
7	p_4	O	O	p_1								
8	O	p_9	$-p_8$	$-p_2$	p_7							
12	O	p_8	p_{13}	p_3	$-p_8$	p_{12}						
13	p_5	O	$-p_3$	p_6	p_2	O	p_1					
14	O	p_{10}	O	p_2	p_{11}	O	$-p_2$	p_7				
18	p_3	O	p_{14}	O	O	O	$-p_3$	p_8	p_{12}			
19	p_6	$-p_2$	O	p_5	O	$-p_3$	p_4	O	O	p_1		
20	$-p_2$	p_{11}	O	O	p_{10}	O	O	p_9	$-p_8$	p_2	p_7	
24	O	O	O	p_3	O	p_{14}	O	p_8	p_{13}	$-p_3$	$-p_8$	p_{12}

ELEMENT STIFFNESS MATRIX FOR PLANE STRESS

$$p_5 = - \frac{12EI_2'}{L^3}$$

$$p_6 = - \frac{A_3E}{L} \frac{c^2}{r^3}$$

$$p_7 = - (p_9 + p_{10} + p_{11})$$

$$p_8 = \frac{6\ EI_1'}{(cL)^2}$$

$$p_9 = - \frac{12\ EI_1'}{(cL)^3}$$

$$p_{10} = - \frac{A_2E}{L}$$

$$p_{11} = - \frac{A_3E}{L} \frac{1}{r^3}$$

$$p_{12} = 2\ (p_{13} + p_{14})$$

$$p_{13} = \frac{2\ EI_1'}{cL}$$

$$p_{14} = \frac{2\ EI_2'}{L}$$

Having the element stiffness matrix for bending out of plane, as shown on p. A2, and the element stiffness matrix for plane stress, as shown on p. A3, the 24x24 cylindrical shell element stiffness matrix is assembled by placing each of the elements of the first two matrices in the appropriate row and column of the shell element stiffness matrix. Thus, for the

plane stress stiffness matrix shown on p. A3, an element in row number i and column number j is placed into the i-th row and j-th column of the shell element stiffness matrix. The elements of the stiffness matrix for out-of-plane bending shown on p. A2 are stored in the shell element stiffness matrix in such a manner that their action numbers as indicated on Fig. 2, used in conjunction with Eq. (1), will correspond to the numbering of the same actions on Fig. 5 which is used in conjunction with Eq. (26) defining the shell element stiffness matrix. Since the foregoing procedure can easily be followed in programming for a computer, it was deemed unnecessary to present here the assembled cylindrical shell element stiffness matrix.

B. Geometric Transformation Matrix for a Shell Element

The 24x24 geometric transformation matrix $[C_i]$ for shell element i, which relates node displacements q_i in the system coordinates to node displacements u_i in the element coordinates, as indicated by Eq. (27), is given by

$$[C_i] = \begin{bmatrix} [L] & & & & & & & \\ & [L] & & & & & & \\ & & [L] & & & & & \\ & & & [L] & & & & \\ & & & & [L'] & & & \\ & & & & & [L'] & & \\ & & & & & & [L'] & \\ & & & & & & & [L'] \end{bmatrix}$$

where all the elements not shown are zero, and where

$$[L] = \begin{bmatrix} 1 & 0 & 0 \\ 0 & \cos a_L & \sin a_L \\ 0 & -\sin a_L & \cos a_L \end{bmatrix}$$

and

$$[L'] = \begin{bmatrix} 1 & 0 & 0 \\ 0 & \cos a_R & -\sin a_R \\ 0 & \sin a_R & \cos a_R \end{bmatrix}$$

where the angles a_L and a_R are shown on Fig. 7. For a circular cylindrical shell a_L is equal to a_R.

C. Plate Element Mass Matrix

An approximate mass matrix for a plate element is obtained by direct lumping of mass parameters at the nodes at the element. The following assumptions are used in this approximation:

1). One quarter of the element mass is assumed to be concentrated at each node of the element.

2). For rotary inertia effect from the element, one quarter of the element is assumed to rotate as a rigid body about each of the nodes of the element, and the angle of rotation is assumed to be equal to that of the corresponding node.

Then the diagonal elements of the plate element mass matrix are:

$$m_1 = m_4 = m_7 = m_{10} = \frac{\mu c L^2}{4}$$

$$m_2 = m_5 = m_8 = m_{11} = \frac{\mu c L^2}{16}\left(\frac{L^2}{4} + \frac{h^2}{3}\right)$$

$$m_3 = m_6 = m_9 = m_{12} = \frac{\mu c L^2}{16}\left(\frac{c^2 L^2}{4} + \frac{h^2}{3}\right)$$

where μ = plate mass per unit area

h = plate thickness

All other elements of the matrix are zero.

Alternately, the mass matrix can be obtained by using the assumed displacement function $A_i(x, y)$ referred to in the derivation of equivalent node forces. It has been shown [44, 45] that the element of the i-th row and j-th column of the resulting plate element mass matrix is

$$m_{ij} = \mu \int_{\frac{-cL}{2}}^{\frac{cL}{2}} \int_{\frac{-L}{2}}^{\frac{L}{2}} A_i(x, y)\, A_j(x, y)\, dxdy \qquad \text{(A1)}$$

D. Cylindrical Shell Element Mass Matrix

As for a plate element, also for a cylindrical shell element an approximate mass matrix is obtained by direct lumping of mass parameters at the nodes of the element. The assumptions used for the plate element mass matrix also hold here. Moreover, it is assumed here that the effect of the rotary inertia associated with the node rotations about the Z-axis, which is normal to the element, is negligible because the rotations referred to are very small. With these assumptions, the diagonal elements of the

24x24 shell element mass matrix are:

$$m_i = \frac{\mu c L^2}{4} \quad \text{where } i = 1, 2, 3, 7, 8, 9, 13, 14, 15, 19, 20, 21$$

$$m_i = \frac{\mu c L^2}{16}\left(\frac{L^2}{4} + \frac{h^2}{3}\right) \text{ where } i = 4, 10, 16, 22$$

$$m_i = \frac{\mu c L^2}{16}\left(\frac{c^2 L^2}{4} + \frac{h^2}{3}\right) \quad \text{where } i = 5, 11, 17, 23$$

$$m_i = O \qquad \text{where } i = 6, 12, 18, 24$$

All other elements of the matrix are zero. It should be noted that when the foregoing mass matrix is transformed into system coordinates, in accordance with Eq. (35), it will no longer be a diagonal matrix.

Alternately, the mass matrix can be obtained by using the assumed displacement functions $A_i(x, y)$ and $B_i(x, y)$. Thus the elements of the i-th row and j-th column of this mass matrix can be calculated as follows:
By Eq. (A1) for i and j = 3, 4, 5, 9, 10, 11, 15, 16, 17, 21, 22, 23, and by

$$m_{ij} = \mu \int_{-\frac{cL}{2}}^{\frac{cL}{2}} \int_{-\frac{L}{2}}^{\frac{L}{2}} B_i(x, y)\, B_j(x, y)\, dxdy \qquad \text{(A2)}$$

for i and j = 1, 2, 7, 8, 13, 14, 19, 20.

All other elements of the matrix are zero.

E. Displacement Functions $A_i(x, y)$

$A_i(x, y)$ is the deflection of the plate element due to a node displacement $u_i = 1$ and $u_j = 0$ for $j \neq i$. (See Fig. 2.) Since no exact functions are available, assumed displacement functions $A_i(x, y)$ are used herein.

Noting that there are 12 degrees of freedom for a discrete plate element, it is assumed that $A_i\ (x, y)$ can be expressed as the following polynomial [1, 4, 5] with 12 undetermined constants

$$A_i\ (x, y) = c_1^i + c_2^i x + c_3^i y + c_4^i x^2 + c_5^i xy + c_6^i y^2 + c_7^i x^3 + c_8^i x^2 y + c_9^i xy^2 + c_{10}^i y^3 + c_{11}^i x^3 y + c_{12}^i xy^3 \qquad \text{(A3)}$$

where $c_1^i,\ c_2^i,\ \ldots,\ c_{12}^i$ are the undetermined constants for $A_i\ (x, y)$. By satisfying the 12 node displacements with Eq. (A3) and its derivatives for the condition that $u_i = 1$ and $u_j = 0$ for $i \neq j$, a set of 12 simultaneous algebraic equations is obtained for the evaluation of $c_1^i,\ c_2^i,\ \ldots.,\ c_{12}^i$, in which x and y in any one equation are evaluated in terms of the coordinates of that node at which the displacement is satisfied by the equation. By repeating this procedure for i = 1, 2, ..., 12, the following expressions for $A_i\ (x, y)$ are determined.

$$A_1\ (x, y) = +\frac{1}{8}\left(2-3\bar{x}-3\bar{y}+4\bar{\bar{x}}\bar{\bar{y}}+\bar{x}^3+\bar{y}^3-\bar{\bar{x}}^3\bar{y}-\bar{\bar{x}}\bar{\bar{y}}^3\right) \qquad \text{(A4)}$$

$$A_2\ (x, y) = +\frac{1}{8}\left(1-\bar{x}-\bar{y}+\bar{\bar{x}}\bar{\bar{y}}-\bar{y}^2+\bar{\bar{x}}\bar{\bar{y}}^2-\bar{y}^3-\bar{\bar{x}}\bar{\bar{y}}^3\right)\frac{L}{2} \qquad \text{(A5)}$$

$$A_3\ (x, y) = -\frac{1}{8}\left(1-\bar{x}-\bar{y}-\bar{x}^2+\bar{\bar{x}}\bar{\bar{y}}+\bar{x}^3+\bar{x}^2\bar{y}-\bar{x}^3\bar{y}\right)\frac{cL}{2} \qquad \text{(A6)}$$

$$A_4\ (x, y) = +\frac{1}{8}\left(2+3\bar{x}-3\bar{y}-4\bar{\bar{x}}\bar{\bar{y}}-\bar{x}^3+\bar{y}^3+\bar{x}^3\bar{y}+\bar{\bar{x}}\bar{\bar{y}}^3\right) \qquad \text{(A7)}$$

$$A_5\ (x, y) = +\frac{1}{8}\left(1+\bar{x}-\bar{y}-\bar{\bar{x}}\bar{\bar{y}}-\bar{y}^2-\bar{\bar{x}}\bar{\bar{y}}^2+\bar{y}^3+\bar{x}\bar{y}^3\right)\frac{L}{2} \qquad \text{(A8)}$$

$$A_6\ (x,y) = -\frac{1}{8}\left(-1-\bar{x}+\bar{y}+\bar{x}^2+\bar{x}\bar{y}+\bar{x}^3-\bar{x}^2\bar{y}-\bar{x}^3\bar{y}\right)\frac{cL}{2} \qquad \text{(A9)}$$

$$A_7\ (x,y) = +\frac{1}{8}\left(2-3\bar{x}+3\bar{y}-4\bar{x}\bar{y}+\bar{x}^3-\bar{y}^3+\bar{x}^3\bar{y}+\bar{x}\bar{y}^3\right) \qquad \text{(A10)}$$

$$A_8\ (x,y) = +\frac{1}{8}\left(-1+\bar{x}-\bar{y}+\bar{x}\bar{y}+\bar{y}^2-\bar{x}\bar{y}^2+\bar{y}^3-\bar{x}\bar{y}^3\right)\frac{L}{2} \qquad \text{(A11)}$$

$$A_9\ (x,y) = -\frac{1}{8}\left(1-\bar{x}+\bar{y}-\bar{x}^2-\bar{x}\bar{y}+\bar{x}^3-\bar{x}^2\bar{y}+\bar{x}^3\bar{y}\right)\frac{cL}{2} \qquad \text{(A12)}$$

$$A_{10}\ (x,y) = +\frac{1}{8}\left(2+3\bar{x}+3\bar{y}+4\bar{x}\bar{y}-\bar{x}^3-\bar{y}^3-\bar{x}^3\bar{y}-\bar{x}\bar{y}^3\right) \qquad \text{(A13)}$$

$$A_{11}\ (x,y) = +\frac{1}{8}\left(-1-\bar{x}-\bar{y}-\bar{x}\bar{y}+\bar{y}^2+\bar{x}\bar{y}^2+\bar{y}^3+\bar{x}\bar{y}^3\right)\frac{L}{2} \qquad \text{(A14)}$$

$$A_{12}\ (x,y) = -\frac{1}{8}\left(-1-\bar{x}-\bar{y}+\bar{x}^2-\bar{x}\bar{y}+\bar{x}^3+\bar{x}^2\bar{y}+\bar{x}^3\bar{y}\right)\frac{cL}{2} \qquad \text{(A15)}$$

where $\bar{x} = \dfrac{2x}{cL}$

$\bar{y} = \dfrac{2y}{L}$

The derivatives of $A_i\ (x,y)$ are

$$\frac{\partial A_i}{\partial x} = A_{i,x}\ (x,y) = \frac{2}{cL}\,A_{i,\bar{x}}$$

$$\frac{\partial A_i}{\partial y} = A_{i,y}\ (x,y) = \frac{2}{L}\,A_{i,\bar{y}}$$

$$\frac{\partial^2 A_i}{\partial x^2} = A_{i,xx}\ (x,y) = \frac{4}{(cL)^2}\,A_{i,\bar{x}\bar{x}}$$

$$\frac{\partial^2 A_i}{\partial x\,\partial y} = A_{i,xy}\ (x,y) = \frac{4}{cL^2}\,A_{i,\bar{x}\bar{y}}$$

$$\frac{\partial^2 A_i}{\partial y^2} = A_{i,yy}(x,y) = \frac{4}{L^2} A_{i,\bar{y}\bar{y}}$$

where the derivatives of $A_i(x,y)$ with respect to $\bar{x}$ and $\bar{y}$ are obtained from Eqs. (A4) thru (A15).

F. Displacement Functions $B_i(x,y)$

$B_i(x,y)$ are defined analogically to $A_i(x,y)$ except that the displacements associated with $B_i(x,y)$ correspond to plane stress condition of a flat shell element. Again, since no exact functions are available for $B_i(x,y)$, these displacements functions will be assumed. Recalling that eight displacements are to be considered here, it is assumed [46] that

$$B_i(x,y) = \frac{1}{E}\left(c_1^i x + c_2^i xy - \nu\left(c_3^i x + \frac{1}{2}c_4^i x^2\right) - \frac{1}{2}c_4^i y^2 + c_6^i y + c_7^i\right) \qquad \text{for } i = 1, 7, 13, 19$$

and

$$B_i(x,y) = \frac{1}{E}\left(-\nu\left(c_1^i y + \frac{1}{2}c_2^i y^2\right) + c_3^i y + c_4^i xy - \frac{1}{2}c_2^i x^2 + 2(1+\nu)c_5^i x - c_6^i x + c_8^i\right) \qquad \text{for } i = 2, 8, 14, 20$$

where $c_1^i, c_2^i, \ldots, c_8^i$ are eight undetermined constants for $B_i(x,y)$. The sign convention and orientation for the displacements referred to above is the same as for u_i indicated on Fig. 5. The procedure for determining the eight constants for each $B_i(x,y)$ is similar to the method of finding the constants for $A_i(x,y)$ explained in the previous section. Since the constants depend on the elastic properties of the shell

material, the assumed displacement functions $B_i(x, y)$ have not been determined explicitly here.